ITTC2024
30TH INTERNATIONAL TOWING TANK CONFERENCE
22–27 SEPTEMBER 2024 | HOBART TASMANIA AUSTRALIA

Report of the Full-Scale Ship Performance Committee

1. INTRODUCTION

1.1 Membership and Meetings

The members of the Full Scale Ship Performance Committee of the 30th ITTC are:

- Hideo Orihara (Chair)
  Japan Marine United Corporation (JMUC), Japan
- Sebastian Bielicki (Secretary)
  Maritime Advanced Research Centre (CTO), Poland
- Se-Myun Oh
  Samsung Heavy Industries (SHI), South Korea
- Gongzhen Xin
  China Ship Scientific Research Centre (CSSRC), China
- Gijs Struijk
  Maritime Research Institute Netherlands (MARIN), The Netherlands
- Giuliano Vernengo
  Università de Genova, Italy
- Stephen Minnich
  Naval Surface Warfare Center, Carderock Division (NSWCCD), United States of America
- Peiyuan Feng
  Marine Design and Research Institute of China (MARIC), China
- Mariko Kuroda
  National Maritime Research Institute (NMRI), Japan
- Seok-Ho Son
  Hyundai Heavy Industries (HHI), South Korea (until Dec. 2022 replaced by Min Woo Kim)
- Min Woo Kim
  Hyundai Heavy Industries (HHI), South Korea (from Jan. 2023)

Thirteen committee meetings have been held during the work period:

- First meeting, 6, December, 2021, Online. All members attended.
- Second meeting, 4, March, 2022, Online. All members except 2 members (Gijs Struijk from MARIN, Seok-Ho Son from HHI) attended.

- Third meeting, 16, May, 2022, On-line. All members except 5 members (Gijs Struijk from MARIN, Giuliano Vernengo from Genova University, Stephen Minnich from NSWCCD, Seok-Ho Son from HHI) attended.

- Fourth meeting, 13, July, 2022, On-line. All members except 3 members (Se-Myun Oh from SHI, Seok-Ho Son from HHI) attended.

- Fifth meeting, 4, November, 2022, On-line. All members except 6 members (Se-Myun Oh from SHI, Gongzheng Xin from CSSRC, Giuliano Vernengo from Genova University, Stephen Minnich from NSWCCD, Seok-Ho Son from HHI) attended.

- Sixth meeting, 8, February, 2023, On-line. All members except 3 members (Giuliano Vernengo from Genova University, Stephen Minnich from NSWCCD) attended.

- Seventh meeting, 28, April, 2023, On-line. All members except 3 members (Se-Myun Oh from SHI, Giuliano Vernengo from Genova University, Stephen Minnich from NSWCCD) attended.

- Eighth meeting, 31 May – 1 July, 2023, SVA Wien, Austria. All members attended.

- Nineth meeting, 13, July, 2023, On-line. All members except 3 members (Gijs Struijk from MARIN, Giuliano Vernengo from Genova University, Stephen Minnich from NSWCCD) attended.

- Tenth meeting, 20, October, 2023, On-line. All members except 5 members (Se-Myun Oh from SHI, Gijs Struijk from MARIN, Giuliano Vernengo from Genova University, Stephen Minnich from NSWCCD, Min-Woo Kim from HHI) attended.

- Eleventh meeting, 12, December, On-line. All members except 2 members (Giuliano Vernengo from Genova University, Gongzheng Xin from CSSRC) attended.

- Twelfth meeting, 15-17, January, 2024, JMUC Yokohama, Japan. All members except 1 member (Giuliano Vernengo from Genova University) attended.

- Thirteenth meeting, 30, April, On-line. All members except 2 members (Giuliano Vernengo from Genova Uni-versity, Gongzheng Xin from CSSRC) attended.

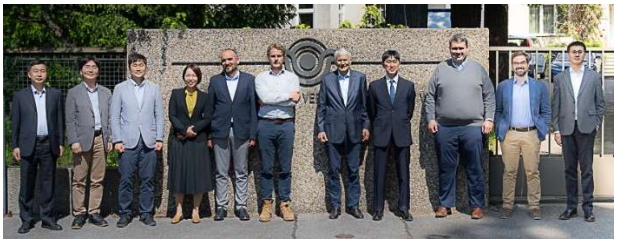

Figure 1: Full Scale Ship Performance committee photo with Prof. Strasser (8th meeting)

The AC representative to IMO Prof. Gerhard Strasser attended all the meetings in order to keep close eye on the progress of the procedures and guidelines and provide feedback from IMO/MEPC meetings.

1.2 Contact with ITTC committees

The 30th Full Scale Ship performance committee has coordinated and exchanged information with the CFD/EFD, Seakeeping, and SC on Wind Powered and Wind Assisted Ships on relevant issues.

1.2.1 Contact Seakeeping committee

The committee has contacted Seakeeping committee on the following aspects: Wind loads on ships which include revision or development of new procedure for wind loads based on Speed/Power trial procedure (R.P. 7.5-04-01-

01.1). Acquisition and analysis of onboard monitoring data.

On the issue of wind loads on ships, this committee agreed to conduct this work in collaboration with Seakeeping committee at the end of February 2023. This committee discussed this issue seriously in the eighth meeting held 31th May to 1st June 2023 and agreed that this committee should prepare the draft of a new stand-alone procedure developed based on Appendix F in 7.5-04-01-01.1 during the present term. On 5th June, AC Chair informed that SC on Wind Powered/Assisted Ships have already prepared a draft of a new stand-alone procedure developed based on Appendix F in 7.5-04-01-01.1. It is also suggested that all Chairs of technical committees concerned should contact the Chair of SC on Wind Powered/Assisted Ships in order to match possible different approaches. In their procedures they then should refer to that ITTC procedures. Responsible member of this committee to this task (S. Bielicki from CTO) contacted the Chair of SC on Wind Powered/Assisted Ships on this issue.

On the issue of acquisition and analysis of onboard monitoring data, This issue was seriously discussed this committee's Ninth meeting in July 2023. It is decided that Chair of this committee will take care of this task since he has wealth of technical experience concerning this issue. On-line meeting on this issue was held on Nov. 2nd, 2023. 3 SKC members (Antonio Souto-Iglesias, Munehiko Minoura and Yulin Pan) and FSSPC Chair attended. Chair of this committee introduced FSSPC's activity on the onboard monitoring issue using the TC's progress report of present term.

1.2.2 Contact SC on Wind Powered/Assisted Ships

The committee has contacted SC on Wind Powered/Assisted Ships on the following aspects: the review of new R.P. 7.5-04-01-02 for conduct and analysis of Speed/Power trials for wind assisted ships powered/assisted ships.

This committee reviewed the new R.P. and the comments was sent to the SC on 12 September 2023. The SC sent the response to this committee's comment on 27 November 2023. In the twelfth (physical) meeting, these responses were discussed, and additional comments were prepared and sent to the Chair of the SC on 13 February 2024.

1.2.3 Contact other committees

The committee has contacted Manoeuvring committee about: Investigate the manoeuvring aspect of design for Smart Ships and Unmanned Surface Vehicles. Identify the need for new or modified procedures of experiments and simulations to evaluate manoeuvring performance.

Concerning the wave correction in Speed/Power trial analysis, at the request of AC Chair, a Windows-Excel format spread sheet for SPAWAVE method with short-term estimation capability has distributed to the FSSPC members for the review of this method.

· AC WG3 Chair (Prof. Y.-H. Kim) have asked this committee to conduct the evaluation of his newly developed combined SNNM-SNU formula for wave correction in Speed/Power trials in the framework of this committee's TOR task 5 B). This formula combines both SNNM for longer wave range and SNU formula for shorter wave range. This evaluation task was conducted using a simplified Windows Excel-format file with GUI provided by Prof. Y.-H. Kim. 4 members of this committee participated. The outcome of this evaluation is described in this final report.

1.3 Contact with AC chairman about IMO and ISO issues

(1) The AC representative to IMO Prof. Gerhard Strasser, attended IMO MEPC 76 - 80 and reported on it during this term. Major outcome/comments related to fluid dynamic issues are as follows:

(2) Major outcome/comments from IMO MEPC 76 meeting:

- 2021 Guidelines on the method of calculation of the attained energy efficiency existing ship index (EEXI) adopted. Amendment to unified interpretation on the dates related to EEDI Phase 2 and 3 for new ships, as provided in Table 1 of MARPOL Annex VI, Chapter 4, Regulation 24.

(3) Major outcome/comments from IMO MEPC 77 meeting:

- Mainly discussion of level of ambition and revision of IMO GHG emission strategy.

(4) Major outcome/comments from IMO MEPC 78 meeting:

- New Guideline for exhaust gas cleaning systems. 2021 Guidance on treatment of innovative energy efficiency technologies for calculation and verification of the attended EEDI and EEXI.
- IMO has received informative submission from ITTC with overview on all procedures that have changed after the 29th ITTC:
  - 7.5-02-02-01 Resistance Tests
  - 7.5-02-02-04 Wave Profile Measurement and Wave Pattern Resistance Analysis
  - 7.5-02-03-01.1 Propulsion/ Bollard Pull Test
  - 7.5-02-03-01.4 1978 ITTC Performance Prediction Method
  - 7.5-02-03-01.7 Performance Prediction Method for Unequally Loaded, Multiple Propeller Vessels
  - 7.5-02-03-02.1 Open Water Test
  - 7.5-04-01-01.1 Preparation and Conduct and Analysis of Speed/Power Trials
  - 7.5-02-07-02.8 Calculation of the Weather Factor f_w for Decrease of Ship Speed in Waves

(5) Major outcome/comments from IMO MEPC 79 meeting:

- Amendments to the 2014 Guidelines on survey and certification of the energy efficiency design index (EEDI) (resolution MEPC.254(67) in Paragraphs 4.3.5, 4.3.6, and 4.3.8 as follows:

  Ship speed should be measured in accordance with ITTC Recommended Procedure 7.5-04-01-01.1 Speed Analysis of Speed/Power Trials (2017, 2021 or 2022 version, as may be applicable at the time of sea trials) or ISO 15016:2015…..
- Discussion on biofuels.

(6) Major outcome/comments from IMO MEPC 80 meeting:

- Interim guidance on the use of biofuels.
- Amendment to the 2021 guidelines on the shaft/engine power limitation system to comply with the EEXI requirements and use of a power reserve (Resolution MEPC.335(76)

(7) Cooperation with ISO.

- The ITTC representative to ISO Prof. Gerhard Strasser attended all 17 virtual meetings and contributed the ITTC achievements for the update of ISO 15016.
- Major outcomes are:
  - STAWAVE 2 was replaced by SNNM method.
  - Raven's method for correction of shallow water replaced Lackenby's method. Higher requirements on instrumentation for environment measurements.

1.4 Tasks

The recommendations for the work of the Full-Scale Ship Performance Committee as given by the 29th ITTC were as follows:

1. Update the state-of-the-art for investigation of full-scale ship performance, emphasizing developments since the 2021 ITTC Conference. The committee report should include sections on:

A) the potential impact of new technological developments on the ITTC

B) new measuring techniques

C) new benchmark data

D) the practical applications of numerical simulation to full-scale ship performance

E) the need for R&D for improving methods of full-scale measurements and numerical modelling.

2. Review ITTC Recommended Procedures relevant to full-scale performance, and

A) identify any requirements for changes in the light of current practice, and, if approved by the Advisory Council, update them,

B) identify the need for new procedures and outline the purpose and contents of these.

3. Address issues related to hull and propeller surface roughness such as:

A) Definition of roughness properties

B) Components of roughness

C) Measurement of roughness

D) Effects of roughness on in-service performance including filtering and analysis methods for evaluating hull and propeller performance separately

E) Roughness usage in performance prediction and cross effects with correlation

4. Provide technical support to ISO and IMO in further development of approaches to in-service performance monitoring (e.g. ISO19030.)

5. Address the following aspects of the analysis of speed/power sea trial results:

A) Initiate and conduct speed trials on commercial ships on deep and shallow water to further validate Raven method.

B) More validation of wave-added resistance method, in particular SNNM, covering all wave encounter angles based on a set of significant ship parameters including the short-term estimation of wave-added resistance in irregular waves.

C) Investigate the influence of drift, rudder action, short wave and wave height on wave added resistance.

D) Investigate the influence of water depth on the hull-propeller interaction (thrust deduction, relative rotative efficiency)

E) Explore and monitor new developments in instrumentation and measurement equipment relevant for sea trials and in service performance assessment (e.g. wind, waves, thrust, speed through water).

6. Develop and keep updated an inventory of the data bases as well as the companies, organisations or any other bodies collecting and processing data on the ship in-service performance of interest to ITTC.

7. Study accuracy of CFD for shallow water applications – cooperate with CFD/EFD Committee.

8. Update the speed/power sea trial procedures 7.5-04-01-01.1 where appropriate, in particular:

A) complement it by a procedure for the correction of yawing (caused by wind) and rudder angle

B) wind averaging method to correctly reflect the wind effect in double run (true wind vector in each run).

9. Support ISO in updating ISO15016 in compliance with 7.5-04-01-01.1

10. Update guideline for determination of model-ship correlation factors, including shallow water and draft dependency (in cooperation with AC Working Group)

11. Update guideline on CFD-based wind coefficient; in particular, re-assess database of wind resistance coefficients and update it according to the new procedure for non dimensionalising.

12. Continue to monitor the development of relevant techniques for ship energy saving and identify the needs to complement the present EEDI framework in response to the adoption of alternative fuels and the receptivity of innovative technologies. Consider, if necessary, a complementary metric to EEDI to represent power savings.

13. Collect full scale data obtained through relevant benchmark tests on the effect of energy saving methods (ESM). Use the full scale data for validating the effect of ESM. Develop a guideline to conduct in-service performance evaluation for ESM. Full-scale data showing the benefits of ALDR (Air Layer Drag Reduction) would be of particular interest.

14. As smart ship technology for cargo and passenger transportation is one of the emerging technologies in maritime industry:

A) Investigate the hydrodynamic aspect of design for Smart Ship and Unmanned Surface Vehicles

B) Explore the suitability of the traditional design spiral for the smart ship and USVs.

C) Identify the need for new or modified procedures of experiments and simulations to evaluate performance in this particular field

2. STATE OF THE ART

2.1 Potential impacts of new technological developments on the ITTC

With the rapid development of artificial intelligence (AI) technologies, the machine learning and big data analysis techniques are getting increasing attentions and have been proven effective for many applications. These techniques are also relevant and useful for the prediction, evaluation and optimization of full-scale ship performance. The most straight-forward and useful application of AI is probably to handle the huge volume of ship's operational data for performance evaluation. Rapidly advancing sensor and telemetry technology onboard ships has provided operators with an extensive database that can be used to improve the assessment of actual ship performance.

Gupta et al. (2022) used machine-learning (ML) methods to estimate the hydrodynamic performance of a ship using the onboard recorded in-service data. Three ML methods, NL-PCR, NL-PLSR and probabilistic ANN, are calibrated using the data from two sister ships. The calibrated models are used to extract the varying trend of the ship's hydrodynamic performance over time and predict the change in performance through several propeller and hull cleaning events. The probabilistic ANN model performs the best, but the results from NL-PCR and NL-PLSR are not far behind, indicating that it may

be possible to use simple methods to solve such problems with the help of domain knowledge.

Gupta et al. (2023) also proposed a streamlined semi-automatic approach to processing the data, which can be used to prepare a dataset for ship performance analysis. Typical data processing steps like interpolating metocean data, deriving additional features, estimating resistance components, data cleaning, and outlier detection are arranged in the best possible manner not only to streamline the data processing but also to obtain reliable results. A semi-automatic implementation of the data processing framework, with limited user intervention, is used to process the datasets and present the example plots for various data processing steps.

Jabary et al. (2023) presented the development of selected data science and ML approaches based on synchronized and integrated operational data available from a Ship Operation Information Model (SOIM). The SOIM is configured in a database management system (DBMS) and considers comprehensive operational data at low/high-frequency of noon reports, AIS, weather, loading conditions and numerous onboard sensors measuring operating and motion parameters. The pre-processed operational data are subjected to correlation analyses in order to identify the main interdependencies between the different operational parameters and thus evaluate the most important factors affecting an operational condition. On the other hand, they are used together with the corresponding design data to implement assessments of ship operational indicators under specific operational conditions.

In recent years, the importance of evaluation of the ship added resistance in waves has increased, both from an economic and environmental protection point of view. A trend can be noted that more and more studies have focused on the modelling and evaluation of wave added resistance using machine learning techniques or based on the big data analysis of actual ship operational data.

Martić et al. (2021) applied an Artificial Neural Network to evaluate the added resistance in different sea states that the ship will encounter during navigation, the model can estimate the added resistance of container ships with sufficient accuracy, based on the ship characteristics, sailing speed, and the sea state.

Taskar and Andersen (2021) used the full-scale data of two ships to compare five different added resistance prediction methods. The effect of using separate wave spectra for wind waves and swell on performance prediction has also been explored. Ships have been simulated in the same weather conditions and propeller speed as in the case of full-scale ships using different methods for added resistance. The performance of these methods has been quantified by comparing speed and power predictions with the full-scale data. It was observed that three out of five methods were able to predict added resistance even in high waves. Even though these methods showed significantly different responses in the frequency domain, its effect on speed and power prediction was minor. Moreover, there was minor improvement in results by using separate wave spectra for wind waves and swell instead of single wave spectrum for combined wind waves and swell.

Mittendorf et al. (2022) implements machine learning methods for the prediction of the added-wave resistance of ships in head to beam wave conditions. The study is focused on nonlinear regression algorithms including Random Forests, Extreme Gradient Boosting Machines and Multilayer Perceptron. The employed dataset is derived from results of three different potential flow methods covering a wide range of operational conditions and 18 hull forms in total. A hyperparameter study based on Bayesian optimization is conducted, and the validation of the final models for three case studies against numerical and experimental data shows satisfactory generalization in case of the neural network. The tree-based ensemble methods, on the other hand, are not able to generalize sufficiently from the given parameter discretization of the underlying dataset.

Kim et al. (2022) proposed a so-called meta model for predicting added resistance in waves by combining two existing methods. The results from the two methods are combined smoothly using a tangent hyperbolic function according to wavelengths and wave headings. The coefficients constituting the function are tuned to minimize mean squared error between predictions and model experiments. Finally, the meta model is verified by full-scale measurements of a general cargo ship and a container ship, and it seems to give good agreement with measurements in all analysis areas, compared to existing semi-empirical methods. Especially, it showed better performance in estimating added wave resistance at high waves, resonance frequencies, arbitrary waves, and low speeds.

Mittendorf et al. (2023) merges telemetry data of more than 200 in-service container vessels with ocean re-analysis data from ERA5. Theoretical estimates relying on spectral calculations of added resistance are made for both long- and short-crested waves and are based on a combination of a parametric expression for the wave spectrum and a semi-empirical formula for the added resistance transfer function. The theoretical estimates are compared to predictions from an indirect calculation of added resistance relying on shaft power measurements and empirical estimates of the remaining resistance components. Overall, the comparison reveals a bias in bow oblique waves and higher sea states of the spectral estimates as well as the large variance of the empirically derived predictions — particularly in beam-to-following waves. One of the study's main findings is that added resistance assessment based on in-service data is complex due to significant associated uncertainties.

Moving on to another machine learning application, short-term temporal predictions of ship responses given the current wave environment and ship state would enable enhanced decision-making onboard and reduce the overall risk during operations for both manned and unmanned vessels. However, the current state-of-the-art in numerical hydrodynamic simulation tools are too computationally expensive to be employed for real-time ship motion forecasting and the computationally efficient tools are too low fidelity to provide accurate responses. In this regard, machine learning techniques have the potential to provide fast and efficient predictions with levels of accuracy closer to the higher-fidelity tools.

Guo et al. (2022) extended a deep learning (DL) model to predict the heave and surge motions of a floating semi-submersible 20 to 50 seconds ahead with good accuracy with the help of the dropout technique.

D'Agostino et al. (2022) investigated the prediction capability of recurrent-type neural networks for real-time short-term prediction (nowcasting) of ship motions in high sea state. The performance of recurrent neural networks, long short-term memory, and gated recurrent units models are assessed and compared. All three methods provide promising and comparable results.

Silva and Maki (2022) developed a methodology with long short-term memory (LSTM) neural networks to represent the motions of a free running David Taylor Model Basin (DTMB) 5415 destroyer operating at 20 knots in Sea State 7 stern-quartering irregular seas. Case studies are performed for both course-keeping and turning circle scenarios. The neural network is able to predict the temporal response of the ship due to unseen waves accurately, which makes this methodology suitable for system identification and real-time ship motion forecasting.

Schirmann et al. (2022) applied ridge regression and neural network models for heave, pitch, and roll prediction using time-and-place specific, multidirectional wave model parameters as input. The performance benefits of providing these predictive models with computationally efficient, physics-based model predictions (PBMPs) of heave, pitch, and roll as additional inputs were examined. Data measured aboard an operational research vessel were used to train and test the data-driven models. The results of

this study showed effective reduction of motion amplitude mean-squared error (MSE) values on multiple test datasets relative to the PBMPs alone. The results also showed that inclusion of PBMPs as input to the data-driven models was typically beneficial in terms of MSE reduction, stressing the importance of retaining physics-based information in data-driven models.

Zhang et al. (2023) presents a novel data-driven methodology to provide multi-step prediction of the ship's roll motion in high sea states. A hybrid neural network is proposed that combines long short-term memory (LSTM) and convolutional neural network (CNN) in parallel. The motivation is to extract the nonlinear dynamics characteristics and the hydrodynamic memory information through the advantage of CNN and LSTM, respectively. Taken a scaled KCS as the study object, the ship motions in sea state 7 irregular long crested waves are simulated and used for the validation. The results show that at least one period of roll motion can be accurately predicted by using the proposed method.

Gao et al. (2023) developed a reliable and efficient tool for real-time and accurate prediction of ship motion. A ship motion attitude prediction model based on the Adaptive Discrete Wavelet Transform Algorithm (ADWT) and the spacetime Residual Recurrent Neural Network (RRNN) with a time-varying structure is proposed. The model performance tests are conducted based on the simulation data of the ship motion of DTMB5415. Compared with other prediction models, the prediction accuracy of the ADWT-RRNN is the highest under all working conditions, its prediction accuracy and stability of it do not fluctuate significantly over a long prediction period. Hence, the more severe the sea states, the more pronounced the performance advantage is over other models.

2.2 New measuring techniques

Full scale ship performance analysis requires a large amount of reliable sea trail data as support. The data of full scale ship sea trail contains not only environmental parameters such as wind, wave and current, but also real ship performance parameters such as speed, main engine power, torque and so on. The methods and ways to obtain these real ship data have been introduced in the past ITTC regulations. With the development of test instruments, sensor technology, data processing and analysing technology, some new technologies for real ship sea trail have been developed and applied continuously.

- Wave

Hyeok-Geun Ki (2015) carried out full scale measurement of 14k TEU containership with the Wave Finder. That is automatic wave data measurement system which records encountered wave data, i.e., wind wave, swell and total wave data including wind data. As described in Fig1, a wave finder antenna and system were installed.

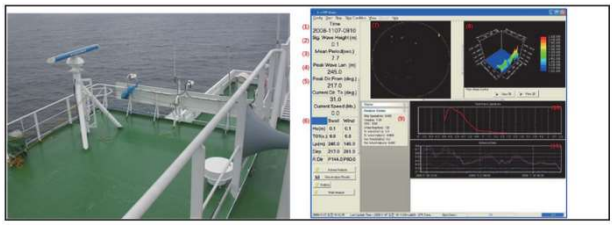

Figure 2 Wave Finder system and antenna

CSSRC developed binocular stereo vision measurement method for the measurement of encounter waves has been reviewed. This method is a type of direct wave measuring methods which is expected to be of higher accuracy compared to indirect wave measuring methods (e.g. wave radar, ship-motion based methods). Accuracy of the method has examined on a stationary offshore structure in China. Onboard tests in ship trials has been considered in China.

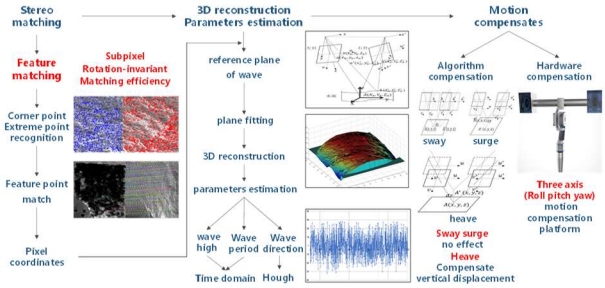

Figure 3 Wave observation technology based on binocular stereo vision.

- Flow field

A scale effect on flow field from model to ship scale has been a big concern for researchers in a ship industry for a long time. Yasuhiko Inukai (2019) presented a new measurement system, Multi-Layered Doppler Sonar (MLDS) was applied in full scale measurement of the flow. MLDS is a Doppler sonar capable of measuring relative water velocity at multiple arbitrary points along ultra-sonic beams. MLDS was installed on a 14,000 TEU container ship and full scale measurement was carried out.

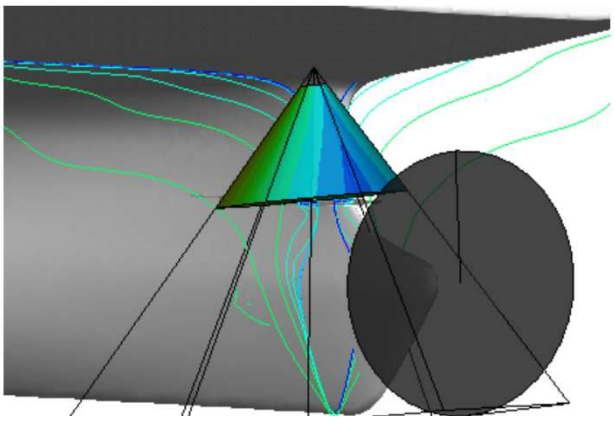

Figure 4 Measuring area by MLDS

Lina Nikolaidou (2021) measured on the characteristics of air lay regimes for a flat plat. Planar PIV was used upstream of the injector in a side-view configuration to characterize the incoming boundary layer. Images of the air layer regimes were acquired with a bottom up view with LaVisions Imager sCMOS CLHS camera. CSSRC (2024) used camara system that mounted on the bottom of ship to observe the shape and distribution of air layer generated by ALS for a “mid-scale” model ship.

- ESD

Pre-swirl ducts (PSDs) have been developed primarily from the viewpoint of improving propulsion efficiency. But little is known on how this affects a vessel’s overall manoeuvring qualities. To study the interaction of the different components of the propulsion system with the PSD, and to assess the maximum loads on the PSD models during manoeuvring. Steven Leonard（2024）carried out manoeuvring tests with a free-running model on a lake. The duct forces were measured throughout. The sensor was integrated into the hull, positioned below the shaft axis. The duct, fins and brackets were manufactured from a single piece and mounted directly on the sensor, having a cylindrical opening for the propeller shaft. The external fairing, in form of the ship contour, covers the sensor and the fins without contact.

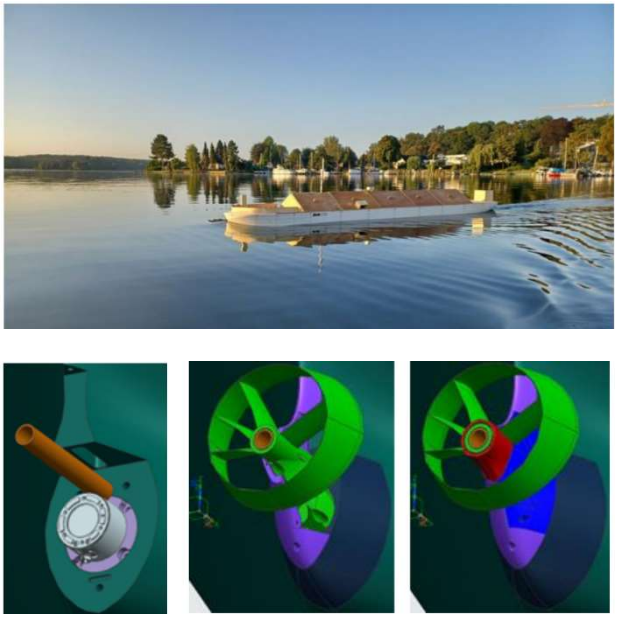

Figure 5 Sensor for measurement of duct forces

- Resistance and propulsion

Youngjun You (2018) propose a new approach to predict and verify the actual RPM and engine power of an LNGC from full-scale measurement data. The sea route, speed over ground

and environmental conditions obtained from the measured data. The results of the simulation are qualitatively reviewed by comparing the calculated time histories of the RPM and the power with the measured RPM and power. Finally, the power increment due to the environmental load is estimated by comparing the predicted power considering the environmental load with the predicted power, not considering the environmental load.

Ulrik D. Nielsen (2019) investigated a semi-empirical model used to estimate added-wave resistance on a ship sailing in waves. The model relies on measurements from a continuous monitoring system, and produces an estimate- the indirect measurement- of added-wave resistance, based on the difference between, on the one side, the measured power and, on the other side, a summation of theoretically calculated resistance contributions but neglecting the component because of seaway. The model has been applied to more than three months of full-scale data recorded on an in-service operating container ship.

Roughness of marine propellers can profoundly affect the efficiency of maritime transportation. Mohamed A. Mosaad（2024）aims to develop a graphical user interface (GUI) program using volumetric image processing (VIP) techniques to predict marine propeller roughness values.

R. Stigter (2024) aimed to investigate the relationship between cavitation inception and microbubble characteristics at full scale. Measurements were conducted on the research vessel Pelagia, operated by the Netherlands Oceanographic Institute (NIOZ), during a 6-day trial from the Bahamas to Curaçao. Cavitation inception and development were measured acoustically, using pressure sensors, and visually, using high and low-speed cameras. The concentration of microbubbles in the proximity of the propeller was monitored using Interferometric Particle Imaging (IPI). Two windows were manufactured in the hull of the ship. One window at portside, just above the propeller, to enable cavitation observations with the high and low-speed cameras. The other window was located at starboard, a few meter upstream from the starboard window. This window was used for the IPI setup, and made it possible to measure the microbubble content upstream of the propeller.

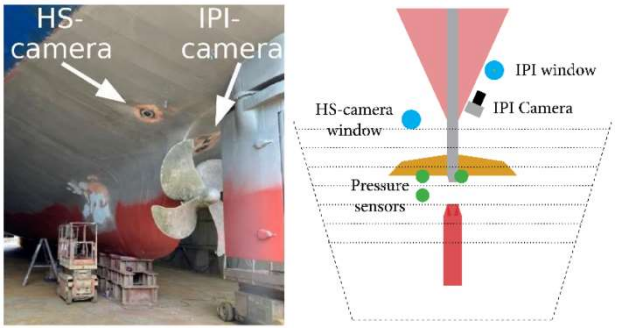

Figure 6 The positions of HScamera window and IPI camera window on the ship

Koruri Tamura (2024) carried out pressure fluctuations around the stern hull of 22,000 DWT chemical tanker were measured during the sea trial using FBG (Fiber Bragg Grating) pressure sensor that can be simply attached to the hull surface without extensive construction work. FBG pressure sensor with a total length of 15 mm, a width of 9 mm and a thickness of 0.7 mm was selected for the purpose of establishing a new method for performing the preparation and measurement efficiently in a short time. This sensor can be directly attached to the hull surface and has the advantage of eliminating the conventional drilling and complicated installation work.

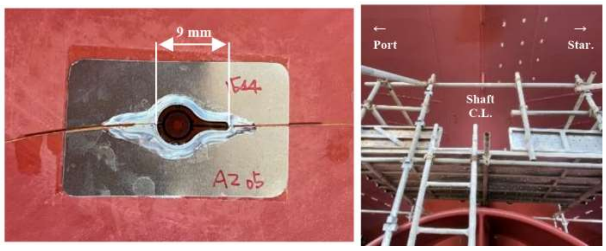

Figure 7 FBG pressure sensor and installed on the stern hull

- Ice environment

Ship operation and ice loading in floe ice fields have received considerable interest during recent years. For the prediction of ship re-

sistance and transit speed in various ice conditions, ship performance in level ice, ridged ice and channel ice are evaluated based on full-scale measurement data of two ships by Fang Li (2018). In their works, Ice thickness in full-scale data was measured using multiple methods to minimize the uncertainty. The thickness of level ice was measured by a stereo camera system. The ridge profile was identified through measurement with an electromagnetic device. Visual observation was conducted for the description of encountered ice conditions. For a better estimation of ship net thrust through propulsive data, the net thrust model is revised in their method to take the effect of power and propeller pitch into consideration. Data acquisition is the most problematic for the investigation of channel ice.

Public data obtained from full-scale measurement covering comprehensively ship performance and ice loads under various ice thicknesses, concentrations and floe sizes are rare. The 2018/19 Antarctic voyage of the Polar Supply and Research Vessel (PSRV) S.A. Agulhas II gathered considerable data of the ship in floe ice fields under various thicknesses, concentrations, and floe sizes. Fang Li (2021) carried out statistical analysis to seek suitable probability distributions which adequately fit the measured ice load and therefore suitable to be used as parent distributions for long-term estimation. The ship is instrumented with shear strain gauges at the starboard side on a total of nine frames, including two at the bow, three at the bow shoulder and four at the stern shoulder. The ice conditions during the voyage are monitored via two sources. The first is visual observation, which are conducted by dedicated ice observers on the bridge, estimating ice concentration, floe size and thickness approximately every minute and summarizing the results in 10-min interval. In addition to that, an ice condition camera is installed on the ship to take photos of the ice condition constantly during the voyage. Hanyang Gong (2022) provides an approach to digitally measuring channel widths from drone videos. Full-scale tests of the Icebreaker (IB) Polaris in the Bay of Bothnia during 2021 were analysed the relation between measured channel widths and icebreaker's operations.

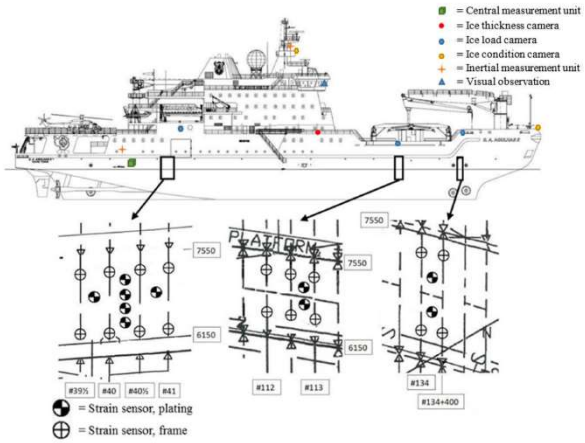

Figure 8 Instrumentation of S.A. Agulhas II.

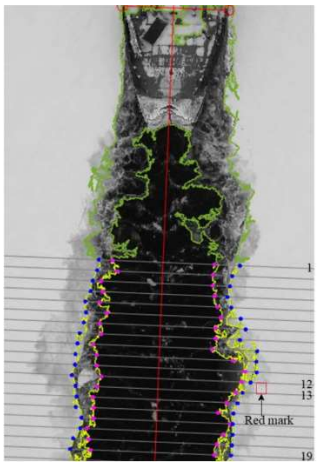

Figure 9 A scheme of the digital channel width measurement approach

2.3 New benchmark data

It is considered that MARIN's JoRes ship-scale test cases data to be published in December 2024 (Ponkratov 2023) are most relevant to meet this TOR task, in particular, due to its coverage of ship types, 3D configurations, ESDs, roughness measurements.

Therefore, it seems to be appropriate for us to recommend ITTC full conference to employ JoRes test cases as benchmark data for full-scale issues in ITTC activity. While the JoRes test

cases will not available to the public by December 2024, it will not cause any trouble since next term activity will starts October 2024.

Survey to ITTC member organizations regarding the provision of their full-scale data to this TOR task was conducted. 1 organization (SVA Potsdam) has contributed full-scale speed/power trails results for 7 ships.

2.4 Practical application of numerical simulation to full-scale ship performance

Possibility of the use of full-scale CFD simulations in ship performance prediction has examined. It is found that the reliability of full-scale CFD simulation results have remined quite low compared to that of model-scale results mainly due to the lack of sufficient full-scale validation data, and that performance prediction based on full-scale CFD simulation results is not practically feasible at present.

3. REVIEW ITTC PROCEDURES

3.1 Requirements for Changes

3.1.1 Overview

The ITTC Recommended Procedure for the Preparation, Conduct and Analysis of Speed/Power Trials (7.5-04-01-01.1) was last updated to Revision 07 in 2022. This version was reviewed to determine whether any updates are required to reflect current practice. An editorial review was conducted first to address various grammatical and formatting issues and to identify any logical gaps in the procedures. The initial result of this effort is a proposed revision to RP 7.5-04-01-01.1. Additionally, a survey was conducted to evaluate the utilization of existing testing and analysis procedures and determine whether there are additional procedures that should be considered for adoption given current practice.

3.1.2 Editorial Review

In addition to basic grammatical and formatting updates, the editorial review identified issues with the 2022 version of RP 7.5-04-01-01.1 regarding missing definitions. These issues are identified here, but potential revisions to address them are recommended as future work of the Full-Scale Ship Performance Committee (FSSPC).

RP 7.5-04-01-01.1 does not provide definitive guidance as to when to transition from the approach phase into the trial run. The procedure recommends monitoring propulsion parameters to determine they have achieved steady state but it does not provide a concise definition of what that condition is. While this ambiguity in the procedure provides the performer flexibility, it also precludes any standardization in this regard and may introduce undesirable error. It is recommended, therefore, that a concise, numeric definition of "steady" be developed and implemented into a future revision of RP 7.5-04-01-01.1.

Next, the concept of the "speed component in the heading direction" is utilized in the process for analysing speed/power (S/P) trial data without a corresponding definition. This terminology implies the scalar projection of the velocity over ground, V_G, in the direction of the ship's heading, ψ. A mathematical definition of this term should be provided in a future revision of RP 7.5-04-01-01.1.

Finally, it is noted that RP 7.5-04-01-01.1 does not provide any treatment as to the estimation of uncertainty from S/P trials data and corresponding analyses. ITTC General Guideline for Uncertainty Analysis in Resistance Tests (7.5-02-02-02) provides a starting point for some of the considerations of S/P trial uncertainty analysis. The corrections involved in the analysis of S/P trial data complicate a full and accurate estimation of the uncertainty due to its propagation through these various calculations. Nonetheless, S/P trial uncertainty estimates have been demonstrated with propagation

through STAWAVE-2 corrections (Seo & Oh, 2021).

3.1.3 Survey

A questionnaire on the usage and sufficiency of RP 7.5-04-01-01.1 with regards to testing and analysis procedures was distributed to member and non-member organizations. A total of 18 responses were received with 11 (61%) indicating that the organization conducts S/P trials and 13 (72%) responding that the organization conducts analyses of S/P trials. The results are discussed here with regards to these two aspects.

Nearly all responses indicated that RP 7.5-04-01-01.1 (or ISO 15016:2015) is currently in practice. Most responses indicated that S/P trials are conducted on displacement monohulls and multihulls as well as high-speed monohulls. Trials on high-speed multihulls and naval or coast guard vessels are less frequent. Other vessel types that respondents indicated include offshore supply vessels, anchor handlers, service operation vessels, fishing boats, research vessels, icebreakers, and submarines.

Regarding the conduct of trials, majorities of responses indicated practice of ITTC recommended limits regarding wind (82%), significant wave height (82%), minimum water depth (73%), current speed change (64%), minimum run length (64%), and maximum steering angle (73%). Negative responses were limited to trials of non-EEDI vessels, use of proprietary limits which are more restrictive than those of RP 7.5-04-01-01.1, or practical limitations of the available test areas. Most respondents indicated that trials are typically aligned to either the wind or waves, whichever has the greater effect (64%). Some organizations are limited by the configuration of the available test areas. The Iterative method is most common amongst respondents (55%), while 18% indicated use the Mean of Means method and a further 18% indicated use of either of those methods.

Only 45% of responses indicated that all recommended primary parameters are measured during trials, with a common exception being bow acceleration. Some respondents indicated that additional parameters are measured beyond those of RP 7.5-04-01-01.1 with common responses including rudder or steering angle and angular rates and displacements. It is recommended that these parameters be considered for inclusion in Table 1 or 2 of RP 7.5-04-01-01.1. Data acquisition capabilities vary widely and are often proprietary in nature. A minority of respondents indicated that wave spectra are sometimes or always measured during trials (36%), but those organizations which measure waves tend to collect the directional spectra instead of the point spectra.

Responses regarding analysis practices indicated more variance relative to recommended procedures. Approximately equal preference was ascribed to each wind resistance correction technique of RP 7.5-04-01-01.1 (wind resistance coefficients derived from model tests, CFD estimates of wind resistance, wind resistance coefficients from standard data sets, and regression formulae). The most common wave resistance correction techniques are STAWAVE-2 and seakeeping model tests (46% each) while STAWAVE-1, SNNM, and the theoretical method are less common at 23-31%. Only 46% of respondents indicated application of shallow water corrections but most negative responses were due to satisfactory water depth at the available test areas. Corrections for water temperature and salinity (58%) and vessel displacement (69%) are in common practice. The analytic tools utilized by respondents were equally divided amongst STAIMO, Class NK PrimeShip-Green/ProSTA, and proprietary tools.

3.1.4 Conclusions

In summary, the survey results indicated that RP 7.5-04-01-01.1 is broadly in practice to guide the conduct of S/P trials amongst respondents. Considering current practice, it is recom-

mended that rudder or steering angle and angular rates and displacements be added to the recommended parameters for measurement during S/P trials. More variability was found in the data analysis techniques and tools employed by respondents. The flexibility afforded by the choice of analytic corrections within RP 7.5-04-01-01.1 is apparently being leveraged. Finally, it is recommended that future revisions to RP 7.5-04-01-01.1 consider the inclusion of definitions of steady approach conditions and the concept of "speed component in the heading direction," and the potential addition of analysis procedures to enable uncertainty estimation for S/P trials.

3.2 Need for new procedures

Air Lubrication technology reduces frictional resistance, comprising more than 60% of total resistance (ITTC, 2017), by introducing air bubbles between the ship's hull and seawater. Between 2010 and 2022, 68 papers have been published on air lubrication technologies, with interest notably increasing after 2018 due to stringent regulations targeting enhanced energy efficiency (EEDI requirements). Figure 10 (Tadris et al., 2023) depicts the distribution of these publications. Several full-scale air lubrication systems are now commercially available and according to ABS (ABS report, 2019) up to 2018 there were 23 ships equipped with ALS. Recently, the MSC ship owner company inquired more than 30 ships equipped in that ship, which will be built in 2022-2024.

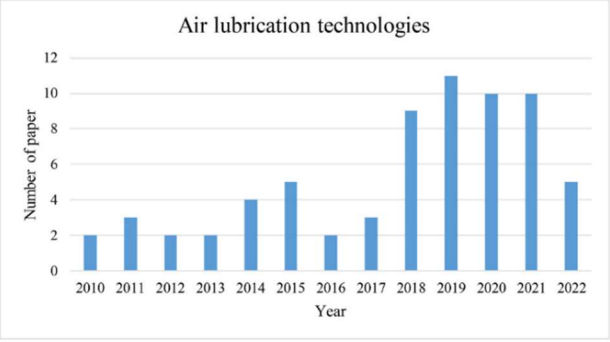

Figure 10 Distribution of air lubrication technologies papers over the years.

Specialist Committee on Energy Saving Methods of 29th ITTC recognized the ALS testing techniques and extrapolation issues, and proposed guideline 7.5-02-02-03 concerning this topic. However, in light of new MEPC.1/Circ.896 guidance, where the reduction rate of ship propulsion power due to ALS is not clearly defined, the update of existing guideline should be considered. Especially for the EEDI draught, for which the reduction rate has status: estimated.

Regarding that fact, in accordance to terms of reference, proposed by FSSP committee the update of existing guideline 7.5-02-02-03 concerning determination of air lubrication system (ALS) scaling issue was proposed. This topic should be considered more precisely due to predicted by increasing share of the air lubrication technology applied in newly designed ships, which follow the IMO regulations towards the green shipping industry.

4. HULL AND PROPELLER SURFACE ROUGHNESS

4.1 General

Effect of hull and propeller surface roughness on ships performance has been thoroughly examined in the previous ITTC activities (e.g. ITTC(2011), ITTC(2014), ITTC(2017), ITTC (2021a)). As described in ITTC(2021a), it is well known that ship's hull and propeller surface roughness have a significant influence on full-scale ship performance. Deterioration in performance can result in more than 10% increase in propulsive power after short time duration after delivery of newly built ships. Principal causes of surface roughness are normally surface coatings and biofoulings. Among them, effect of roughness due to surface coating have examined intensively in recent years compared to that of biofouling. Thus, emphasis has placed on the effect of roughness due to biofouling in the activity of this committee.

In the following roughness related aspects specified as this committee's tasks are described.

4.2 Definition of roughness

Definition of hull and propeller surface roughness is normally made using single roughness parameter height. As a roughness height parameter, Maximum surface roughness parameter *Rz* is employed which is equivalent to BMT roughness parameter in case of 50 mm evaluation length. On the other hand, other roughness shape parameter, in particular, it is well known that roughness wave length has noticeable influence on roughness effect. According to ITTC (2017), roughness effect is reduced when the roughness wave-length is sufficiently longer than the roughness height on coated surfaces. In addition to this, it is also known that the non-uniformity of roughness distribution is not normally considered in the evaluation of roughness effect while the non-uniformity has significant influence. For hydrodynamic evaluation of roughness effect, roughness function is employed. Roughness function ($\Delta U+$) is a downward velocity shift in logarithmic overlap region of the turbulent boundary layer. Roughness function is normally defined as function of roughness Reynolds number ($k+$) evaluated using roughness height parameter (k). Concerning roughness definition, relevant published literatures have investigated in the following.

Demirel et al (2017) evaluated roughness functions for arbitrary barnacle fouling by towing tests of flat plate with artificial roughness with varying height and coverage area. Corresponding roughness length scale k_G is derived so that roughness functions for various roughness conditions are converged to the single functions. k_G is calculated from the polynomial with roughness height (h) and percentage covering area (SC). In the towing tests, actual barnacles of differing sizes were scanned in 3-D in order to generate a CAD model of typical barnacle geometries. Balanus improvisus, an adult juvenile barnacle species, which can grow up to 10 mm in diameter and 5 mm in height (big sized barnacle model) was selected. The digital models of the barnacles were then printed in3-D using 3-D printing technology to generate artificial barnacles. From the towing tank test results the abovementioned single roughness function of k_G for arbitrary barnacle type roughness has derived. By using this roughness function, hydrodynamic evaluation can be conducted by theoretical or numerical calculations.

Song et al (2021a) investigated the effect of heterogeneous hull roughness on ship resistance. Towing tests were conducted in Kelvin Hydrodynamics Lab. at University of Strathclyde with a Wigley model of 3m length in both homogeneous and heterogeneous (1/4, ½ bow/aft rough) conditions. Bow-rough conditions showed larger resistance than aft-rough conditions as expected from the consideration of boundary layer thickness. Using roughness functions derived from the towing tests, new added resistance predations method for homogeneous roughness based on Granville's method is proposed.

Kawashima et al (2019) investigated on the effect of roughness shape parameter of painted surface on frictional resistance by measuring the frictional resistance of flat plates with painted rough surface of different wave length to wave height ratio in towing tests. Surface roughness of painted roughness flat plates are measured with a laser displacement meter, then roughness shape parameters are obtained. By analysing test results and roughness shape parameters, frictional drag coefficient estimation formula for arbitrary wavy rough surface is derived. The estimation formula is derived based on the following assumptions:

- the increase in frictional resistance due to roughness is the sum of the local profile drag of each roughness.

- The frictional resistance of the painted rough surface is the sum of the frictional resistance of the surface and the profile drag of the roughness.

• Resistance increase due to the roughness occurs in the region higher than the thickness of the viscous sublayer, and in the region under the viscous sub-layer there is no increase in resistance.

The derived frictional drag coefficient estimation formula for arbitrary wavy rough surface is defined as a function of following parameters: 1) Total effective front projected area of roughness. 2) flow velocity at the roughness height at the long. centre of plate., 3) average roughness height, 4) average roughness wavelength and 5) experimentally derived coefficient and constants. To show the availability of the newly derived formula, resistance increase ratio for the cases of ks = 150mm with a variety of ship's speeds and lengths were evaluated.

Mieno et al. (2021) investigated added resistance due to roughness of coated surface by rotating cylinder tests. Friction increase rate (*FIR*) due to roughness is examined by means of roughness steepness (*Rc/Rsm, Rc*: average roughness height, *Rsm*: average roughness wave length). By analysing test results and roughness parameters, following features of roughness resistance increase are confirmed:

• Roughness height smaller than a certain level (non-effective thickness $ds \sim k+=2 \sim 4$) do not contribute to resistance increase.

• Simplified projected area of roughness in streamwise direction above ds (*CPA*) calculated with *Rc* and *Rsm* correlate strongly with *FIR* due to roughness is influenced by roughness steepness (*Rc/Rsm*).

From the above results, simple empirical formula for estimating *FIR* for arbitrary wavy rough surface is derived in which *FIR* is calculated with *Rc* and *Rsm*. The range of application is as: Rc/Rsm <1/12(=0.083), this implies that the derived empirical formula is not applicable to sand-grain type steeper roughness.

From the literature survey described above, following findings are obtained concerning the definition of roughness for use in full-scale performance evaluation:

• Formulae proposed by Demirel et al. (2017) for estimating roughness function with corresponding roughness height for arbitrary roughness pattern may be useful for application in CFD and other theoretical calculation.

• Formulae proposed by Kawashima et al. (2019), Mieno et al. (2021) for estimating added resistance due to roughness considering wavelength effects are quite simple and will be applicable in Seed/Power trial in the future after careful verification/ validation for conditions covering wide range of ship types.

• Introduction of the consideration of roughness wave length effects into the present Speed/Power trial analysis in which only roughness height is considered seems to be inevitable since it is shown in the literature that wavelength roughness height to wavelength ratio has significant effects on added resistance due to roughness.

• However, it should be very careful to implement new method/formulae into the ITTC Recommended Procedure (RP) to avoid deterioration of RP's validity and effectiveness, in particular intentional underestimation of roughness effects.

4.3 Components of roughness

As described in 4.1, main components of hull and propeller surface roughness are coating and biofouling. Concerning the biofouling, hydrodynamic drag penalties due to hard macrofouling is better understood than losses due to soft bio fouling. (e.g. slime, macroalgae, tunicates, hydroids) as mentioned in ITTC (2017). Since micro biofouling is most frequently encountered roughness in both speed/power trials and operations, those rough-ness components should be thoroughly addressed in the context of full-scale ship performance issue. Based on these considerations, relevant published literatures have investigated in the following.

Hunsucker et al (2019) studied performance of fouling control coatings by means of hydrodynamic testing. In this study, replicated samples of 5 commercially available coatings (3 fouling release types (FR, silicone based), 2 anti-fouling types (AF, silicone matrix with a biocide(AF1), ablative cooper (AF2))) were deployed at 2 sites (east coast of Florida, USA) for 4 months, then hydrodynamically tested up to a speed of 15m/s to determine the frictional drag increase. After that tests hard fouling adhesion testing was made. Both total coverage of fouling organisms and drag forces were compared before/after hydrodynamic tests. It is found that both coverage of fouling and drag vary significantly among test sites and coating materials. Also noted is that composition of organism's components differs significantly among test sites and that lower fouling with hard structure had a minimum removal at the top speed in hydrodynamic testing.

Yeginbayeva et al (2020) examined combined effects of roughness range of foul-release coating (FRC) and light biofouling (slime). Natural and laboratory biofilms are grown on FRC panels by exposing them in realistic fouling environment. Boundary layer velocity measurement and similarity-law scaling is used to predict the added resistance due to fouling. Following 2 dynamic biofilm growth methods simulating realistic fouling environment are employed:

1) In-field method: panels were placed on the strut arrangement under the moonpool plug of Newcastle University research catamaran vessel operate around port of Blyth (55oN,1oW). Tests were conducted 35% of 6 month period (Mar.-Sep.), research vessel speed 6-20kt. water temperature was 6^{o}C-14^{o}C.

2) Laboratory method: panels were placed in the closed-loop system. Inoculated with the culture extracted from the research vessel. flow speed 0.5m/s for the duration of 1 month and 2 weeks, water temperature was 19^{o}C – 21.5^{o}C.

4 types of coatings were tested in this study. Biofilm coverage area and mean peek-to-valley height (*Rt*) were measured after exposing them in realistic fouling environment. Then, skin friction coefficients is evaluated from moment-um thickness measured in the boundary layer velocity measurement conducted in Emerson Cavitation Tunnel of Newcastle University. Resistance increases for the tested coating ty-pes were compared for the case of KCS container ship using roughness functions evaluated by Granville's similarity-law method. The results showed that resistance increase due to biofilms can be 10% to 20% relative to clean conditions.

From the literature survey described above, following findings are obtained concerning the definition of roughness for use in full-scale performance evaluation:

- Biofouling on hull surface is significant and varied greatly depending on types of coating and environmental conditions encountered.

- Field tests of coating replica will be useful for the examination of anti-fouling performance of coating.

- Light biofouling (slime) has noticeable impact on hydrodynamic resistance with the increase in excess of 10% relative to clean surface condition.

- Coating materials and ambient environmental conditions have significant influence on increase in hydrodynamic resistance. Examination of these issues should be continued and conducted on a variety of ship types.

4.4 Measurement of roughness

Hull roughness impacts fuel consumption significantly. Accurate measurement of this roughness is essential for analysing the speed-power performance of a vessel. Understanding and managing surface roughness optimizes fuel efficiency and enhances overall performance, making it a critical aspect of performance monitoring in operation at sea.

Two different measuring systems, contact and non-contact type, were implemented to compare the results as shown in Figure 1.

- Contact Type - - Non-contract Type –

Figure 11 Hull roughness measurement system

As roughness increases, the difference in measurement results between the two measuring devices increases as shown in Figure 2. Above roughness 500 m, the difference and difference ratio are more than 100 m, 25%.

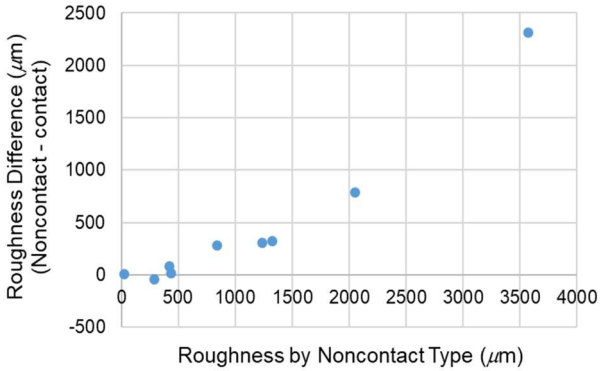

Figure 12 Comparison of roughness measurements

To verify the measurement results, the Laser-Doppler velocimetry (LDV) measurements were performed on a flat plate having roughness elements of various heights in Chungnam National University-Cavitation Tunnel (CNU-CT). Three flat plates with smooth and rough surface were used. The roughness of smooth is $k = 20$ m, and attached sandpapers are $k = 265$ and 1300 m from non-contract measurement system as shown in Figure 13.

Figure 13 Three flat plates with smooth and rough surface

As shown in Figure 14, the velocity profile based on the roughness from non-contract system shows close agreement between the Schlichting equation's predictions and the LDV measurements.

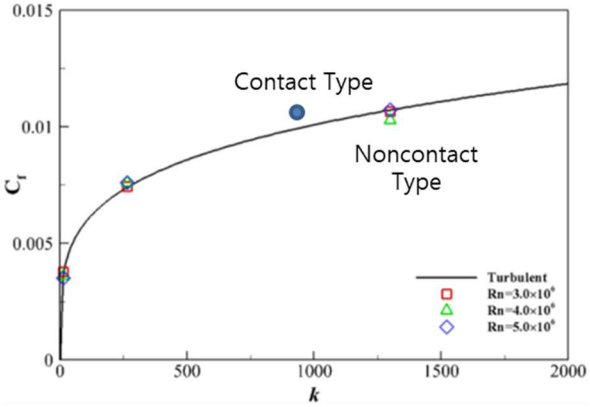

Figure 14 Calculated skin friction coefficient (Cf) along the roughness element, k.

Conclusions. From the LDV measurements of turbulent boundary layer velocity profiles on flat plates with different surface roughness, hull roughness over 500 m recommends to use non-contract type measurement system.

4.5 Effect of roughness on in-service performance

Effect of hull and propeller surface roughness on in-service performance have studied extensively using roughness functions derived from both CFD simulations and model experiments as reported in ITTC (2021) and IMO

(2022). Typical published works are reviewed in the following:

Song et al (2021b) conducted validation of similarity law scaling procedure for roughness effects by tank tests of a flat plate and a ship model in smooth and rough conditions. Roughness functions are derived from the flat plate test results. Total resistance of rough ship is predicted using the similarity-law scaled frictional resistance with 2D and 3D extrapolation method and compared with rough ship model results. It is shown that 3D extrapolation pre-dictions agree well with the measured rough model results.

Song et al (2020) simulated roughness effect of biofouling by URANS calculations for KCS and KVLCC2. Experimentally obtained roughness functions of barnacle fouling were employed in the wall-function of CFD software. The fouling effects on the resistance components, form factors, wake fractions and the flow characteristics were investigated from the simulations.

Song et al (2019) investigated the effects of biofouling on full-scale propeller performance using CFD. Simulations for the full-scale performance of KP505 propeller in open water, including the presence of marine biofouling. Experimentally obtained roughness functions of barnacle fouling (Demirel et al 2017) were employed in the wall-function of CFD. Rough-ness effect of barnacles of varying sizes and coverages on open water performance was predicted for advance coefficients ranging from 0.2 to 0.8.

IMO (2022) compiled and summarized all kinds of results relevant to the effect of biofouling on ship's performance found in the available scientific literature in the form of increase in GHG emissions from ships for different categories of biofouling. It is highlighted in the report that the inherent ability of biofilm sand slime to induce an effective roughness that is well in excess of what its physical appearance would traditionally suggest. For example, a layer of slime as thin as 0.5mm covering up to 50% of a hull surface could trigger an increase of GHG emissions in the range of 25 to 30%, depending on ship characteristics, its speed and other prevailing conditions. For more severe biofouling conditions, such as a light layer of small calcareous growth (barnacles or tubeworms), an average-length container ship could see an in-crease in GHG emissions of up to 60%, dependent on ship characteristics and speed. For the medium calcareous fouling surfaces, the in-crease in GHG emissions could be as high as 90%.

As described above, full-scale performance deterioration due to roughened hull and propeller surfaces have studied extensively using roughness functions derived from both CFD simulations and model experiments. However, as mentioned in IMO (2022), How-ever, estimating their impact of biofouling is not straightforward from such findings in the literature, as quantification is done using different ship performance parameters such as in-creased frictional resistance, effective power or shaft power. These parameters are not easy to understand from the perspective of non-specialists in ship hydrodynamics. In addition, validation of the predictions is decisively scare due to the non-availability of appropriate full-scale data. Therefore, rigorous validations of the full-scale predictions are indispensable for the development of practically reliable procedure for evaluating roughness effects on in-service performance.

4.6 Roughness usage in full-scale performance prediction

Roughness relates to fouling and aging effects on the full-scale performance prediction. In order to evaluate performance with these effects, ship performance throughout lifecycle in operation should be considered. Then, the evaluation of life cycle fuel consumption is considered as shown in Figure 15 (Sogihara, 2019).

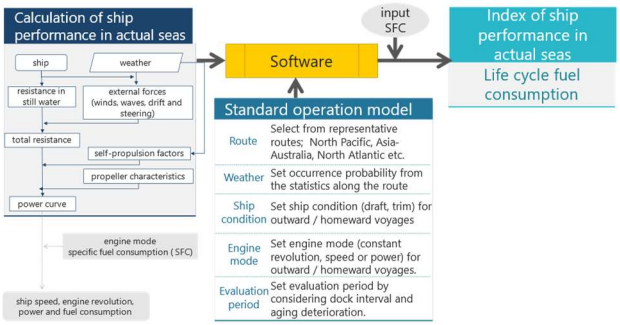

Figure 15 Concept of life cycle fuel consumption.

According to the concept shown in Figure 15, the life cycle fuel consumption is evaluated by combining the prediction of ship performance in actual seas (speed-power curve), which is estimated by following the flowchart shown in Figure 16 (Tsujimoto, 2018), and the standard operational model. (Kuroda, 2022)

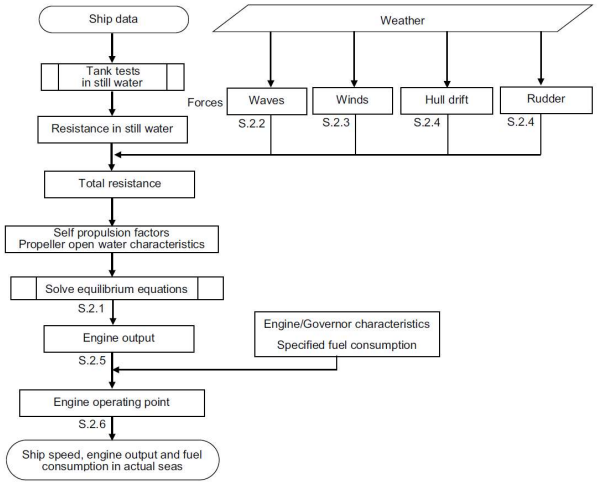

Figure 16 Flowchart for prediction of ship performance in actual seas.

In standard operational model, deterioration due to fouling and aging can be expressed as changes in hull resistance, propeller thrust and propeller torque as shown in following formulae. Here R_t is the hull resistance, T_p is the propeller thrust, Q_p is the propeller torque, t is the elapsed time, R_{t0}, T_{p0}, Q_{p0} are values at newly-built, p_{as} and p_{fs} are the deterioration ratios per year on hull resistance due to aging and fouling respectively, p_{fp} is the deterioration ratio per year on propeller efficiency, t_{ch} and t_{cp} are timings of cleaning for hull and propeller respectively.

$$R_t(t) = R_{t0}\{1 + p_{as}t + p_{fs}(t - t_{ch})\} \quad (1)$$

$$T_p(t) = (1 - a)T_{p0} \quad (2)$$

$$Q_p(t) = (1 + a)Q_{p0} \quad (3)$$

$$a = \frac{p_{fp}(t - t_{cp})}{2 - p_{fp}(t - t_{cp})} \quad (4)$$

Aging deterioration pas and fouling deterioration p_{fs} for hull resistance are expressed with the roughness parameter as shown in the following equation based on the Himeno's equation for the resistance coefficient due to roughness. (Himeno, 1983) Here, R_n is the Reynolds number, C_{T0} is the total hull resistance coeffeient, L is the ship length, and k_A is the apparent roughness height.

$$\left.\begin{matrix} p_{as} \\ p_{fs} \end{matrix}\right\} = \frac{1.8 \times 10^{-5} R_n^{0.55}}{C_{T0} L} \frac{dk_A}{dt} \quad (5)$$

Fouling deterioration pfs was set from the investigation results by Schultz(2007), and the life cycle fuel consumption is evaluated for the Cape-size bulker as shown in Figure 17. (Sogihara, 2022) Here p_{fs} was set as 2%(high-quality), 6.5%(middle), 11.0%(low quality) depending on quality of paint type, and pas was set as 0.3% based on the survey by Schultz(2007).

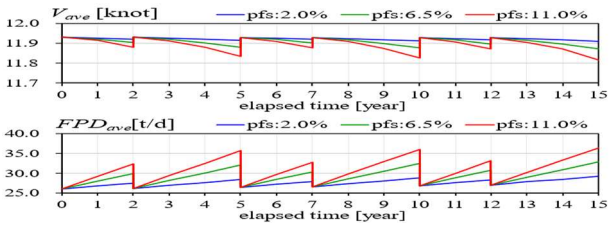

(a) Time variation of fuel consumption per day

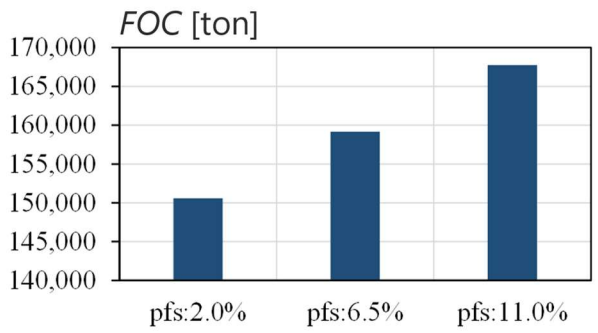

(b) Total fuel consumption in life cycle (15 years)

Figure 17 Results of fuel consumption

Performance prediction with roughness can be carried out with the relation between Roughness parameter and hull resistance. The aging effects can be considered with the change in resistance due to hull surface condition. Using the presented calculation model, aging effects on hull and propeller as well as fouling effect on hull can also be reflected in the performance prediction.

If analysed results for fouling and aging effects by onboard monitoring data for full-scale ships is obtained, a more realistic evaluation can be conducted.

5. SHALLOW WATER CORRECTION

5.1 General

The results of speed power trials are aimed to represent ideal conditions, including unrestricted deep water. In reality, the choice for practical trial locations may result in depths at which the ship's propulsion is influenced. In such case, a shallow water correction method is warranted to correct for these effects. Last term, a new shallow water correction method was introduced: the "Raven method". From that term, the need for further validation work was indicated. Within the current term, Raven's full report on the correction method was published and shared to the public. The committee reviewed the full report.

The 30th ITTC assigned the FSSPC with the following tasks:

Initiate and conduct speed trials on commercial ships on deep and shallow water to further validate Raven method)

Investigate the influence of water depth on the hull-propeller interaction (thrust deduction, relative rotative efficiency)

5.2 Validation

The committee members were invited to contribute to the validation of the method by conducting full-scale trials in shallow (and deep) waters. An emphasis was put on other parties than the developer of the method (MARIN), which has already provided validation within its publications. Organising such dedicated systematic trials on commercially operated ships has proven difficult, and no new results from trials were delivered or collected.

Propulsion factors

From literature review, including Raven's full report, it was concluded that the total propulsion efficiency is expected to remain relatively unaffected within the application range of the correction method. Raven's study on different ships showed the thrust deduction factor t increases for decreasing depth, but only for very shallow water (outside the method's application range). No clear trend was found within the application range. The wake fraction is more sensitive to shallow water effects within the application range, with (1-w) decreasing for decreasing depth. However, no usable approximation for all ship types is found yet. The changes in thrust deduction and wake fraction combined lead to a rise in hull efficiency. On the other hand, the propeller open water efficiency is expected to drop due to the increased resistance, (and thus higher propeller loading) and a reduced inflow speed (due to the increase of the

wake fraction). This counteracts the rise in hull efficiency, leading to a small overall change in propulsive efficiency η_D .

Based on several test cases, it was concluded by Raven that assuming an unchanged propulsive efficiency η_D showed better merit. For the relative rotative efficiency no clear indication is found on the effect of shallow water. While large changes to the wake field may occur at very shallow water, the effect within the trial application range is expected to be minor.

5.3 Conclusion

For the last two terms, validation efforts by conducting dedicated series of trials have proven difficult to realize.

After review, is concluded appropriate to keep considering the propulsion effects unchanged within the application range of the shallow water correction method.

Based on the presently available validation results, it is recommended to keep the Raven method as the shallow water correction method in ITTC 2024 Procedure 7.5-04-01-01.1.

It is recommended to continue monitoring the research efforts in this field in the future.

6. WAVE CORRECTIONS

The mean value of wave added resistance in irregular waves is the end result to be actually used for the S/P trial analysis. Therefore, more validation of wave-added resistance methods, in particular SNNM, covering all wave encounter angles are carried out targeting the short-term estimation of wave-added resistance in irregular waves.

Additionally, following the request of AC, validation of the SNNM-SNU and SPAWAVE methods is conducted with the participation of 3 members of this committee. The wave added resistance responses in regular waves are validated against model test results.

6.1 Validation of SNNM method for the evaluation of wave added resistance in irregular waves

Validation setup. Validation of wave added resistance in irregular waves is not as straightforward as that in regular waves. To properly validate methods for the evaluation of mean wave added resistance in irregular waves, it is necessary to carefully setup the validation procedures.

The first and foremost issue is to determine the benchmark data. One obvious option is to use the model test result in irregular waves. However, it is unanimously agreed by this committee that such model results are scarce and the uncertainty of such tests can be very high. Therefore, it is deemed rational to apply the spectral analysis technique to the Quadratic Transfer Functions (QTFs) obtained from seakeeping model test, and use the short-term prediction result of mean wave added resistance as the benchmark. Moreover, due to limited available data, the evaluation is considered only for long-crest irregular waves, as according to equation (1).

$$R_{mean} = 2 \times \sum_{\omega_{min}}^{\omega_{max}} QTF(\omega) \cdot S_{\eta}(\omega) \cdot \Delta\omega \qquad (6)$$

The parameters in equation (1) will influence the end result of mean wave added resistance, which are listed and explained as follows:

- $QTF(\omega)$: quadratic transfer function of wave added resistance in regular waves corresponding to wave frequency ω;
- $S_{\eta}(\omega)$: wave energy spectrum;
- $\omega_{\min}$: lower limit of wave frequency for integration;
- $\omega_{\max}$: upper limit of wave frequency for integration;

- $\Delta\omega$: wave frequency interval for integration.

Considering that only a limited number of wave frequencies can be obtained through seakeeping model test, interpolation and extrapolation are necessary.

Three interpolation methods are compared, i.e., linear, spline, and a function approximation method provided by CTO Fowles and Cassiday (1986). Based on the model test result of a 20000TEU container vessel, these methods are compared as shown in Figure 1~3. As can be noticed, the spline and the function approximation methods may sometimes produce unrealistic wiggles. Therefore, linear interpolation of the QTF is preferred for robustness, and is adopted for the validation.

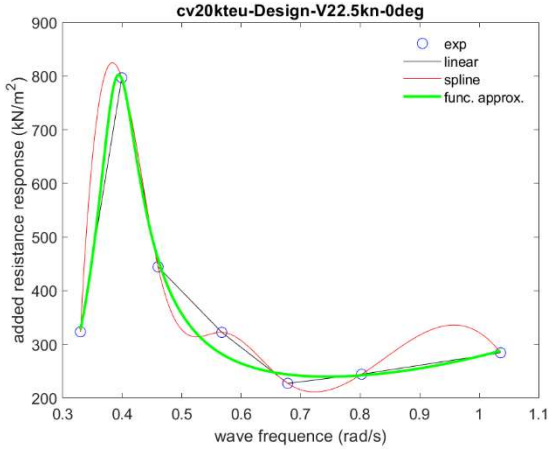

Figure 18 Comparison of interpolation methods (head wave case).

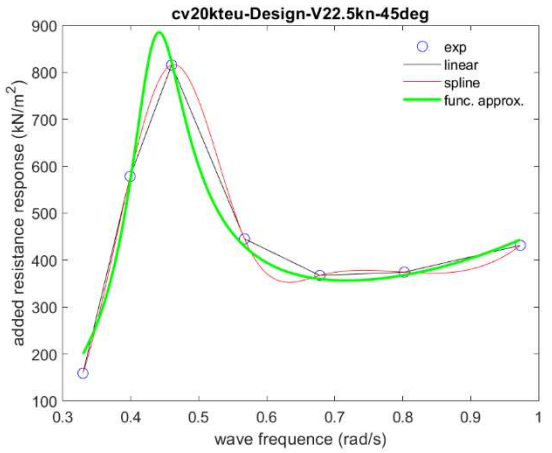

Figure 19 Comparison of interpolation methods (bow oblique wave case).

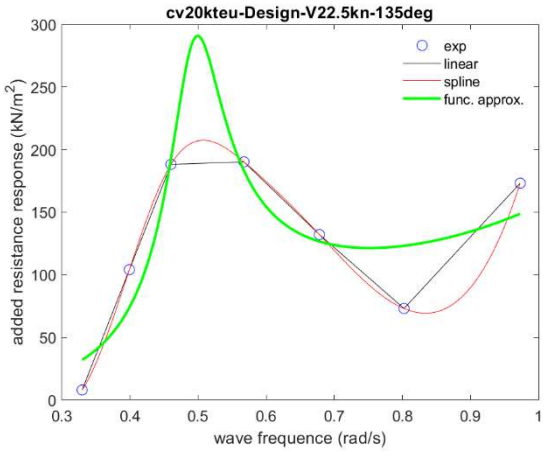

Figure 20 Comparison of interpolation methods (stern quartering wave case).

Extrapolation of the QTF in the long-wave (low wave frequency) range is manageable since it is both theoretically and experimentally proved that the wave added resistance responses will approach zero with the increase of wave length. In line with the linear interpolation method adopted for the validation, the QTF is considered to be linearly decrease to zero in the long-wave range, from the end data point to the upper limit.

Extrapolation of the QTF in the short-wave (high wave frequency) range is much more controversial, because there is no consensus on the trend of wave added resistance responses in the short-wave range. This is further due to the limited testing capacities and high uncertainties associated with the wave added resistance tests in short waves. To circumvent the problem, it is required that the model test data to be used as benchmark must contain at least one data point tested in the short regular waves, whose wave length to ship length ratio (λ/L) is smaller or equal to 0.5. If this requirement is met, then the QTF is extrapolated as constant in the short-wave range; otherwise, the set of model test data is discarded.

Moreover, it is also required that the set of model test data must contain at least 5 data

points covering the range of λ/L from 0.5~2.0, with the peak response included to properly reflect the shape of the response spectrum.

Figure 21 is a demonstration of the treatment of the QTF for spectral analysis.

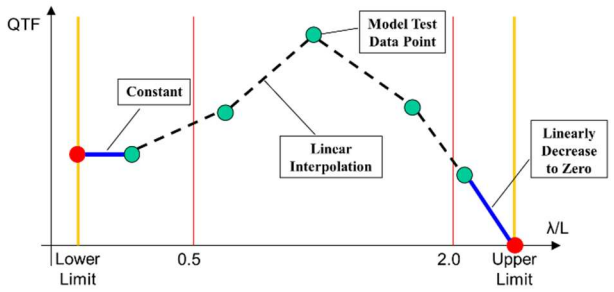

Figure 21 Treatment of QTF for spectral analysis.

Subsequently, the ITTC wave spectrum according to equation (2) is adopted for the validation, in consistent with the ITTC R.P. and the ISO15016 standard.

$$S_\eta(\omega) = 173\frac{H_S^2}{T_{01}^4\omega^5}\exp\left(-\frac{691}{T_{01}^4\omega^4}\right) \qquad (7)$$

In equation (2), H_S is the significant wave height; T_{01} is related to the peak wave period T_P, i.e., T_{01}=0.773T_P.

In order to more comprehensively validate the performance of SNNM method in various sea conditions, four sea states are considered. Each sea state is the combination of one wave height with four likely wave peak periods, as listed in Table 1.

Table 1 Sea conditions for the validation

Sea State	SS2	SS3	SS4	SS5
H_S (m)	0.5	1.0	2.0	3.0
T_P (s)	6,7,8,9	7,8,9,10	8,9,10,11	9,10,11,12

Last but not least, computational-wise, the evaluation of equation (1) presents no challenge at all, so for our purpose, $\omega_{\min}$ is set to be 0.01rad/s, $\omega_{\max}$ is set to be 10rad/s, and $\Delta\omega$ is set to be 0.001rad/s to guarantee adequate spectrum coverage and integration accuracy.

Validation database. The same database adopted by the 29th ITTC Specialist Committee on Ships in Operation at Sea (SOS) is used for the current validation, containing the necessary input parameters of the sample ships for SNNM calculations and the seakeeping model test result of wave added resistance QTFs in regulars under various loading conditions, ship speeds and wave headings.

The sets of QTFs available from the database are checked according to the requirements specified in the validation setup section. Some cases are excluded either due to too few data points, or lack of certain input parameters. For cases involve repeated tests, the mean values are used for the spectral analysis.

In result, a total of 23 ships are included for the validation as listed in Table 2. The composition of ship types is shown in Figure 5.

Table 2 Validation database

No.	Ship	Organization	Condition	Vs (kn)	Heading (deg)
1	bulker	CSSRC	ballast	9	0, 45, 90, 135, 180
			scantling	9	0, 45, 90, 135, 180
			ballast	13	0, 45, 135, 180
			scantling	13	0, 45, 135, 180
			ballast	15	0, 45, 135, 180
			scantling	15	0, 45
2	KCS	CTO	design	12	180
			design	20	180
		MARIC	design	24	0, 45
3	cruise	HSVA	design	13	0
4	cruise		design	17	0
5	cruise		design	15	0, 30, 60, 90, 120
			design	21	0, 30, 60, 90, 120, 150, 180
6	cruise		design	15	0, 30, 60
			design	21	0, 30, 60
7	bulker	MARIC	design	13	0, 30, 60, 90, 120, 150, 180
8	bulker		design	10	0, 45, 90, 135, 180
9	KVLCC2		design	12	180
			design	15	0
10			design	14	0, 45, 90

	LNG C		design	20	0, 45, 90
11	S175		design	12	0, 30, 60, 90, 120, 150, 180
			design	20	0, 30, 60, 90, 120, 150, 180
12	bulker		design	8	0, 30, 150
13	tanker		design	10	0, 30, 60
			design	14	0, 30, 60
14	cruise	MARIN	design	12	0, 45, 90, 135, 180
15	ropax		design	22	0
			design	20	0
16	ropax		design	23	0, 45, 120
17	contai ner		design	22	0, 45
			design	12	0
18	bulker	NMRI	ballast	17	0, 40
			laden	15	0, 40, 60
19	contai ner		laden	21	0, 20, 40
20	pcc		laden	17	0, 60
			laden	21	0, 40
21	tanker		laden	18	0, 45
22	tanker	SAMSU NG	laden	10	0, 30, 60, 90, 120, 150, 180
			laden	15	0, 30, 60, 90, 120, 150, 180
23	LNG C		laden	13	0
			laden	20	0

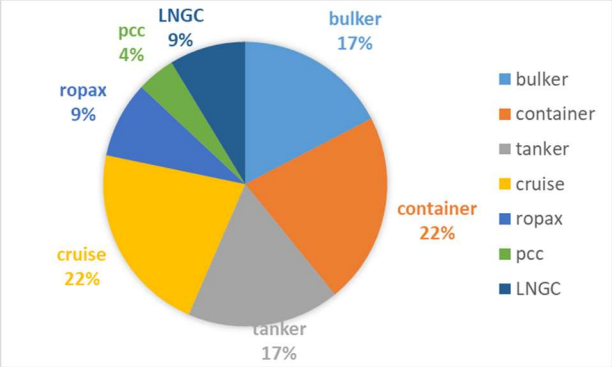

Figure 22 Composition of ship types.

Validation result. The spectral analysis of the QTFs under the sea conditions listed in Table 1 result to a total of 2144 data points. Calculations based on the SNNM method under the same conditions are performed.

The validation results are plotted in Figures 6~10, with data binned for various wave heading ranges. The correlation factors R between the benchmark and the SNNM method are listed in Table 3. The performance of SNNM is excellent in head to beam waves, but deteriorate in beam to following waves where the mean wave added resistances are small.

Table 3 Correlation factor

Wave heading range	Correlation factor
All wave headings	0.919
Head wave only	0.972
Head to bow oblique waves	0.946
Head to beam waves	0.931
Beam to following waves	0.713

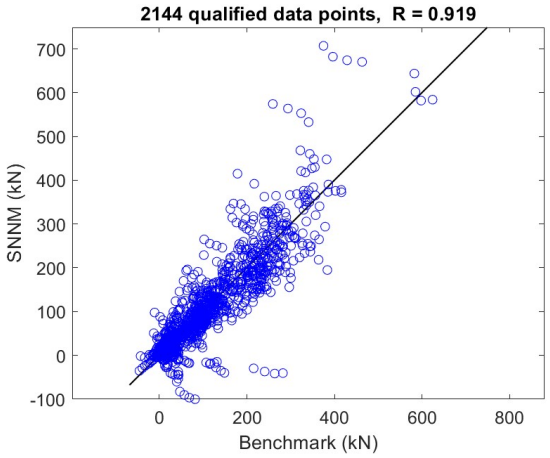

Figure 23 Validation result (all wave headings).

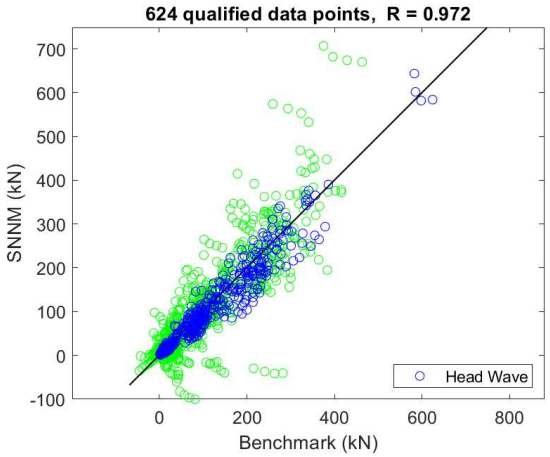

Figure 24 Validation result (head wave only)

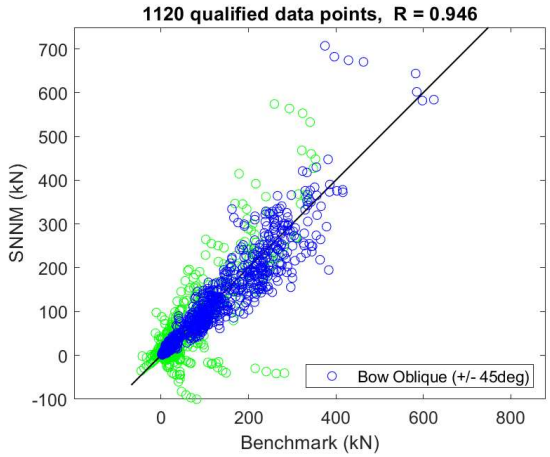

Figure 25 Validation result (head to bow oblique waves).

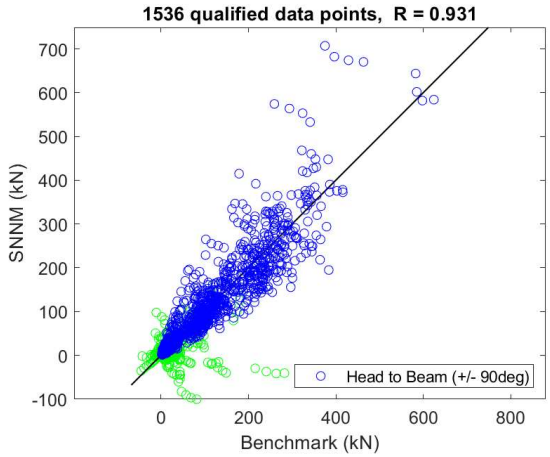

Figure 26 Validation result (head to beam waves).

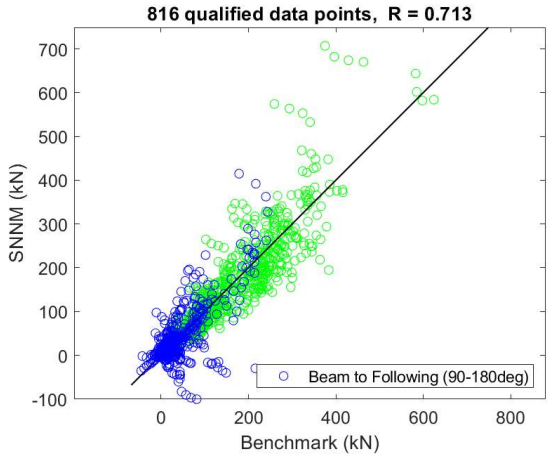

Figure 27 Validation result (beam to following waves).

6.2 Validation of various methods for the evaluation of wave added resistance in irregular waves using devoted dataset

Due to the lack of input parameters of the sample ships, the validation of methods other than the SNNM method is not feasible using the database in Section 6.1. For this reason, NMRI provided an in-house database and this committee performed the evaluation of wave added resistance in irregular waves based on 4 methods: STAWAVE-1, SNNM, NMRI and simple-NMRI (Kuroda, 2023). Among the methods, simple-NMRI is the latest and is introduced as follows.

Simple-NMRI method was proposed in order to solve the issue on the current simplified method: STAWAVE-1, that is, the effect of ship speed on added resistance in waves is not taken into account in STAWAVE-1. Because the speed trials are conducted at the different ship speed, the lack of the consideration of the ship speed is the critical matter and should be improved.

The update of the simplified method was considered based on the concepts for a simplified method:

- Easiness: calculate with a calculator,

- Simplicity: calculate with a small number of ship dimension,

and also based on the concepts for STAWAVE-1:

- Considering the component of the added resistance due to wave reflection in head waves which is primary in the short-waves,

- The same input as STAWAVE-1.

Simple-NMRI method applies the parameter expressing the effect of speed based on the NMRI method (theoretical method) in order to solve the problem for the current simplified

method that the ship speed is not taken into account.

The outline of the method is described by the following formula. The details of the method and the validation results can be referred to the paper (Kuroda, 2023).

$$R_{AWL} = \frac{1}{16}\rho g H_S^2 B \frac{1.3(B/2)^2}{L_{BWL}^2 + (B/2)^2}(1 + C_{Ue}F_r) \quad (8)$$

$$C_{Ue} = \begin{cases} 10 & \text{for } \frac{L_{BWL}}{B} \le 1.22 \\ 68 - 310\frac{1.3(B/2)^2}{L_{BWL}^2 + (B/2)^2} & \text{for } \frac{L_{BWL}}{B} > 1.22 \end{cases} \quad (9)$$

Where, R_{AWL} is the added resistance in long-crested irregular waves, ρ is the fluid density, g is the gravitational acceleration, H_S is the significant wave height, B is the ship breadth and L_{BWL} is the distance of the bow to 95% of the maximum breadth of the waterline, Fr is the Froude number.

Validation setup. The treatment of the QTFs obtained by seakeeping model test is the same as that elaborated in Section 3.1.

As for the wave conditions, the ITTC wave spectrum is also used, but only the significant wave height of 1m is considered, along with the wave peak periods varying from 6s to 12s at an interval of 1s.

Validation database. The sample ships included in the database provided by NMRI are listed in Table 4. Seakeeping model test results of the head wave case alone are considered for the validation.

Table 4 Validation database

No.	Ship	Condition	Vs (kn)
1	container	laden	21, 26
2	PCC	laden	16.8, 20.9
3	PXBC	laden	12.1, 14.9
4	VLCC	laden	13.3
5	JBC	laden	14.5
6	DTC	laden	16, 18
7	chemical tanker	laden	12.7
8	domestic cargo ship	laden	8.9

Validation result. The validation results are shown in Figure 28÷Figure 39. The correlation factors of the 4 methods against the benchmark are listed in Table 5. All methods have achieved a R value larger than 0.8. For the given data set, NMRI method is the most competitive.

Table 5 Correlation factor

Method	Correlation factor
STAWAVE-1	0.822
SNNM	0.887
NMRI	0.982
Simple-NMRI	0.897

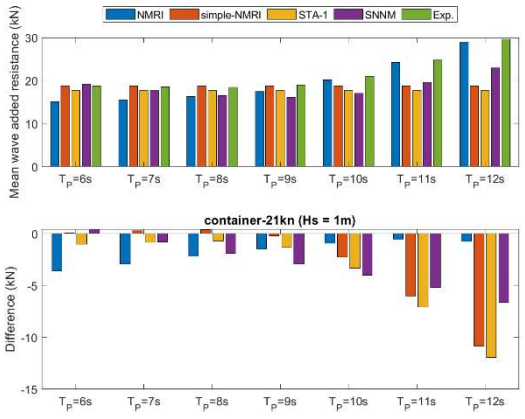

Figure 28 Validation result (container, 21kn).

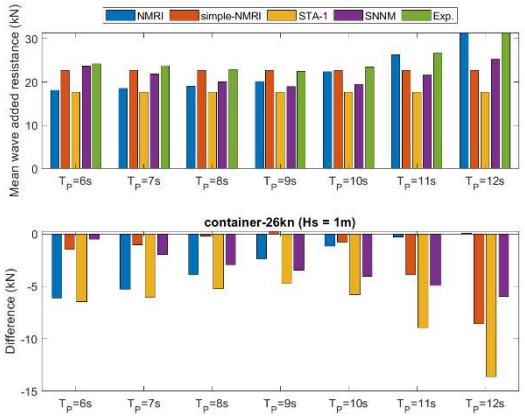

Figure 29 Validation result (container, 26kn)

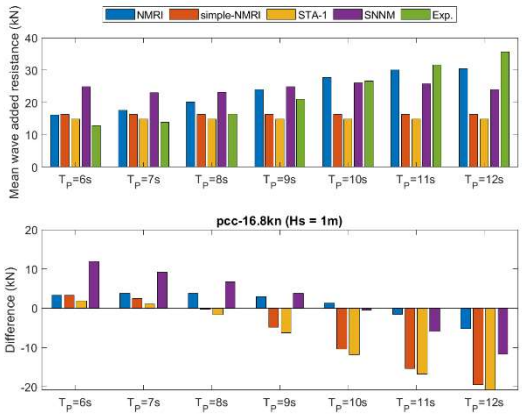

Figure 30 Validation result (PCC, 16.8kn).

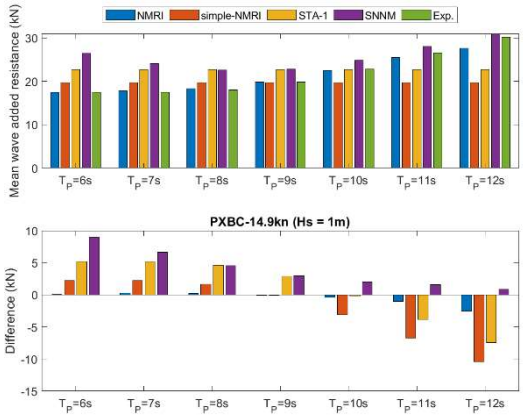

Figure 33 Validation result (PXBC, 14.9kn).

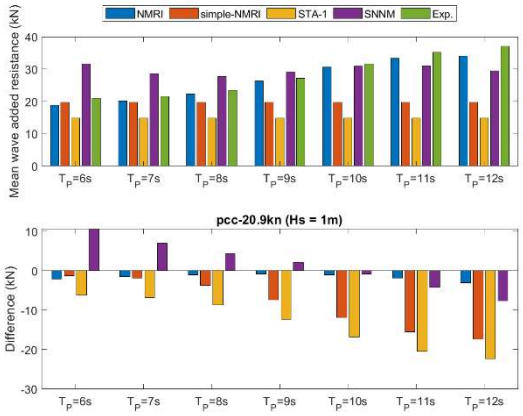

Figure 31 Validation result (PCC, 20.9kn).

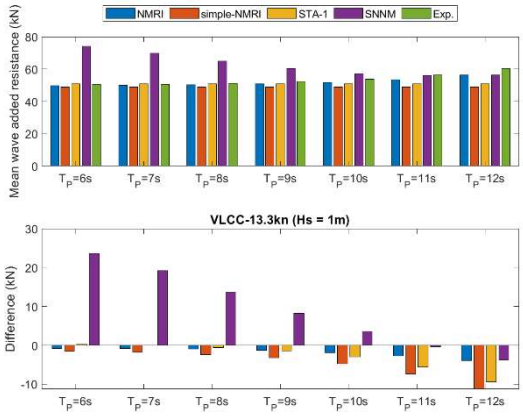

Figure 34 Validation result (VLCC, 13.3kn).

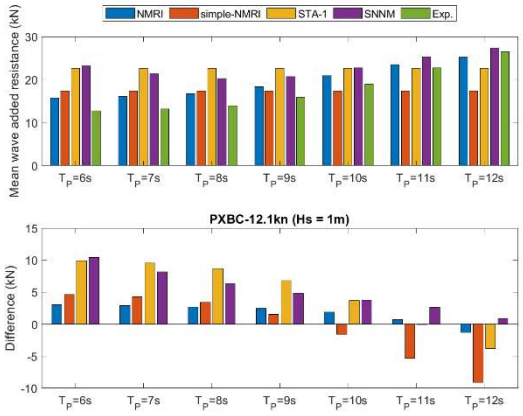

Figure 32 Validation result (PXBC, 12.1kn).

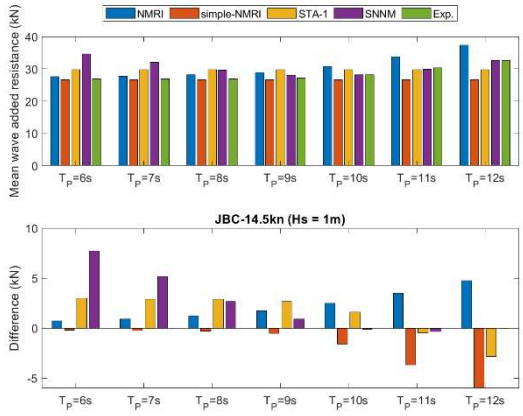

Figure 35 Validation result (JBC, 14.5kn).

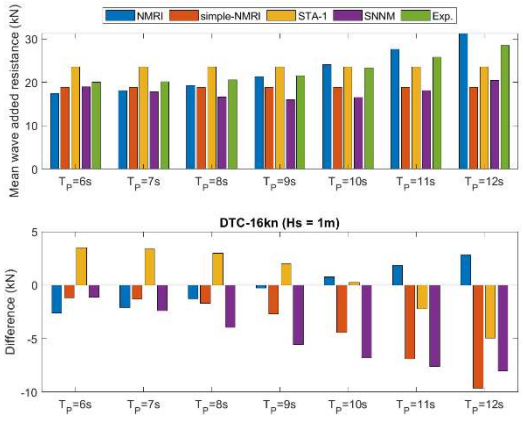

Figure 36. Validation result (DTC, 16kn).

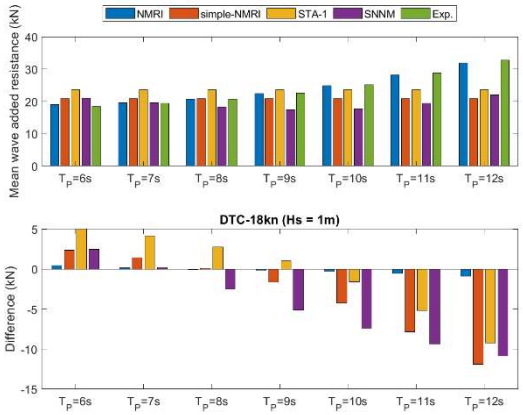

Figure 37 Validation result (DTC, 18kn).

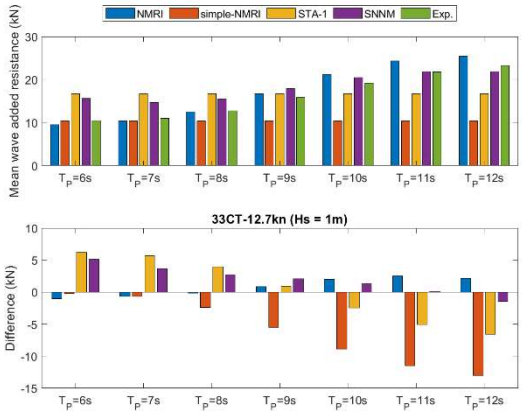

Figure 38. Validation result (chemical tanker, 12.7kn).

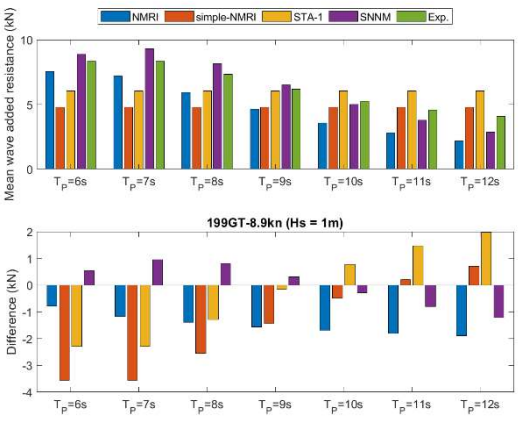

Figure 39 Validation result (domestic cargo ship, 8.9kn).

6.3 Comparison of calculated added waves resistance obtained from various methods in regular and irregular waves

To examine the capability of calculation methods for added wave resistance, comparisons have been made in terms of evaluation of added wave resistance in both regular and irregular waves. 3 methods including SNNM, SPAWAVE (Grin, 2022) and SNU methods (Lee & Kim, 2023) are used in this study.

The following 4 ship models are employed:

Model 1: Oil tanker
Model 2: Bulk carrier
Model 3: Ore carrier
Model 4: Container carrier

Added wave resistances in regular waves are calculated for the 4 ship models in fully loaded condition and compared with experimental data in Figure 40～Figure 43. 7 wave direction cases from head (180deg.) to following (0 deg.) with an interval of 30 degrees are examined. Added wave resistance is reduced to non-denationalized form (K_{AW}) with the square of double wave amplitude. It is noted that K_{AW} is equivalent to QTF for added wave resistance:

$$K_{AW} = \frac{R_{AW}}{4\rho g \zeta_a^2 (B^2/L)} \tag{10}$$

Where, R_{AW} is the added resistance in waves, ρ is the fluid density, g is the gravitational acceleration, ζ_a is the wave amplitude, B is the ship breadth and L is the ship length.

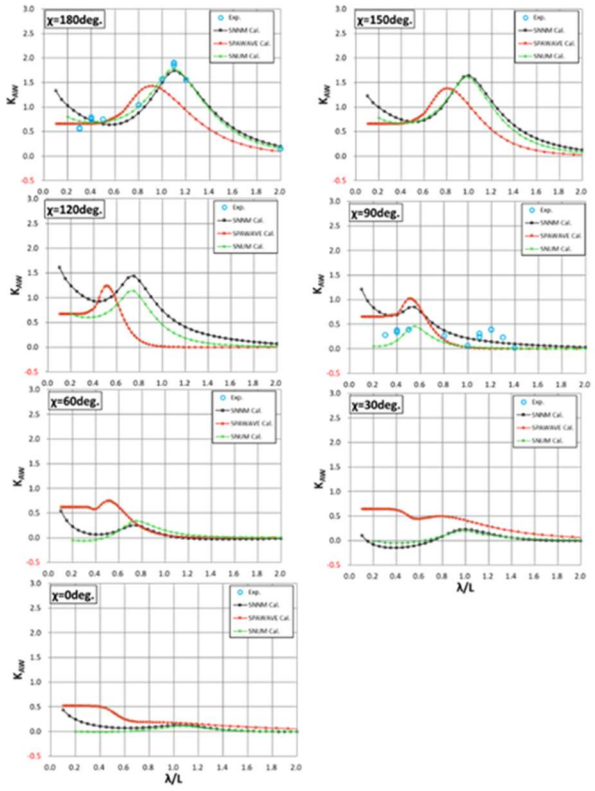

Figure 40 Comparison of added resistance in regular waves (Model 1 oil tanker).

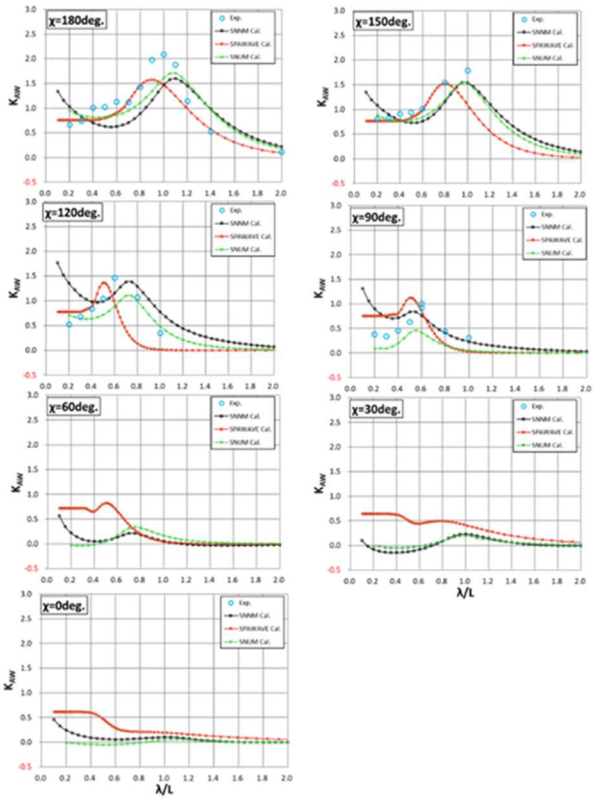

Figure 41 Comparison of added resistance in regular waves (Model 2 bulk carrier).

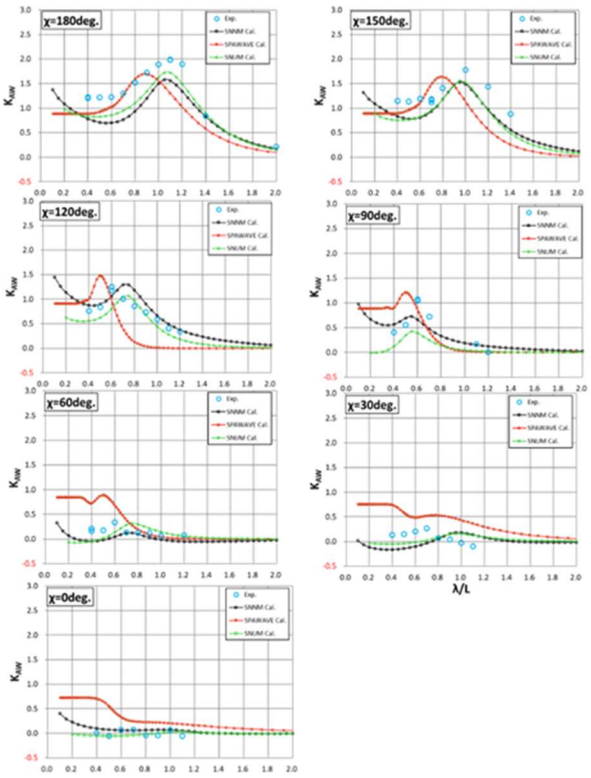

Figure 42 Comparison of added resistance in regular waves (Model 3 ore carrier)

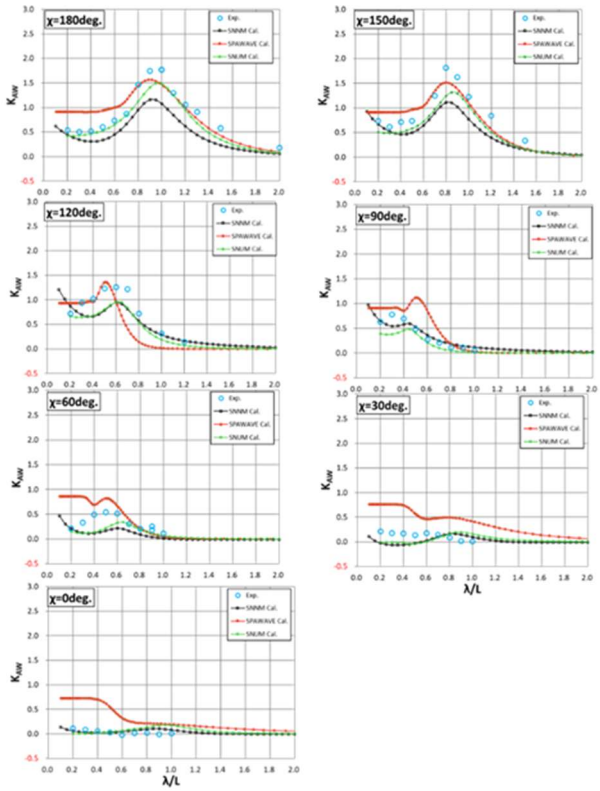

Figure 43 Comparison of added resistance in regular waves (Model 4 container carrier).

From the comparison of added wave resistances in regular waves, the following features can be observed among the calculation methods:

a) SNU method shows similar behaviour as SNNM method except for in shorter waves.

b) SPAWAVE method calculations are generally higher than the other 2 methods in shorter waves in beam to following directions.

c) SPAWAVE method tends to predict peak of added resistance in shorter waves than the other 2 methods.

Added wave resistances in long-crested irregular waves are calculated for the 4 ship models using QTFs shown in Figure 44÷Figure 47. In the calculation ITTC (1964) wave spectrum is employed. Mean Wave Period (Tm) range corresponding to BF scales from 1 to 12 (1.2s to 15.0s) are considered. Calculated data are compared with experimental ones in Figure 44÷Figure 47 at 7 wave direction cases from head (180deg.) to following (0 deg.) with an interval of 30 degrees. Mean added wave resistance in irregular waves are evaluated in the form normalized with the square of significant wave height.

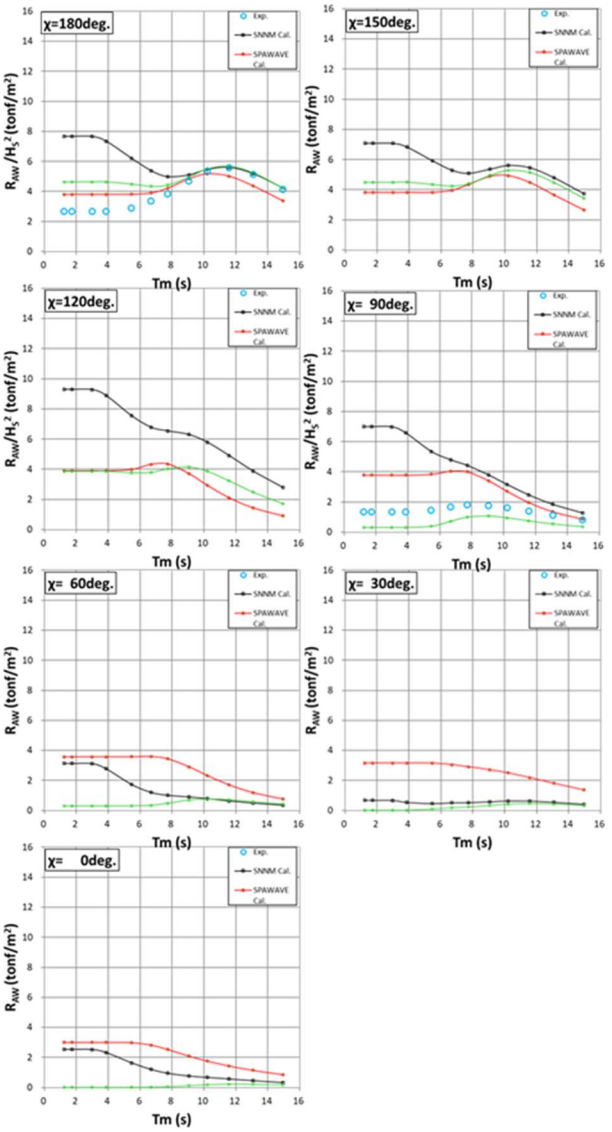

Figure 44 Comparison of added resistance in irregular waves (Model 1 oil tanker)

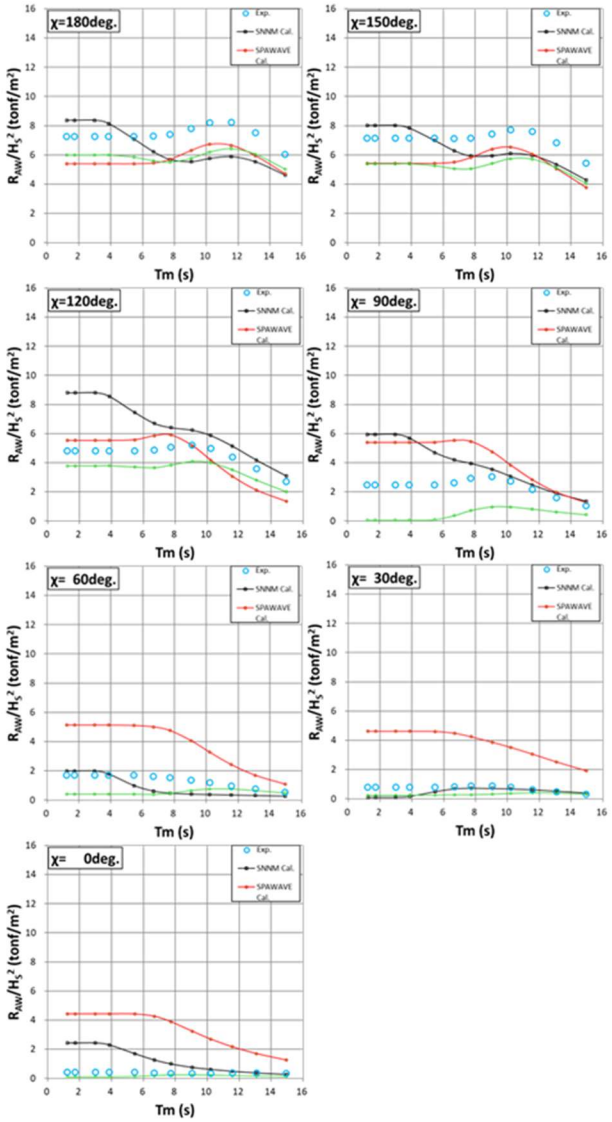

Figure 45 Comparison of added resistance in irregular waves (Model 2 bulk carrier).

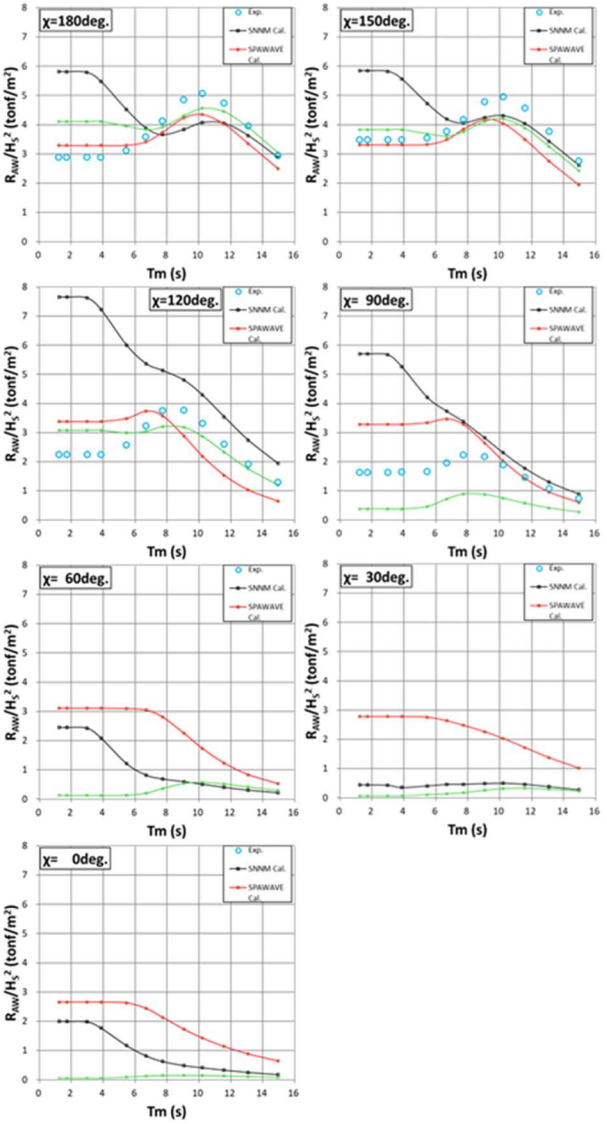

Figure 46 Comparison of added resistance in irregular waves (Model 3 ore carrier).

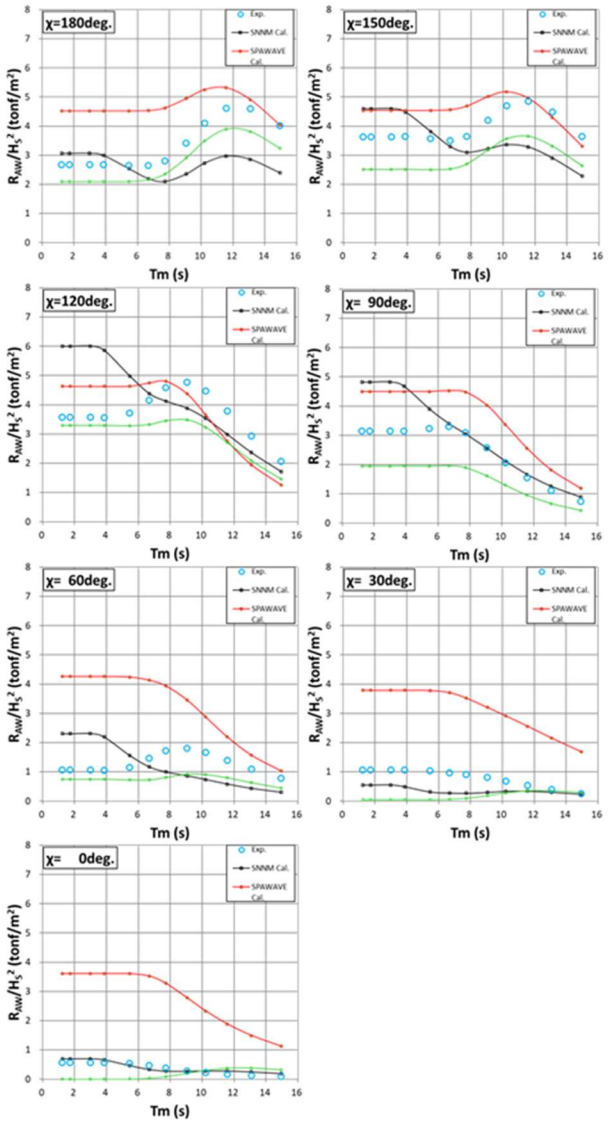

Figure 47 Comparison of added resistance in irregular waves (Model 4 container carrier).

As clearly shown in the comparisons above, there are significant variations among calculated added wave resistances, in particular, at shorter waves periods. Also noted is that agreement with the experimental data is not satisfactory. No general trends can be drawn from this comparison in terms of the capability of the calculation methods evaluated in this study. That is, difference between particular calculation methods and experimental data is quite variable depending on model cases. Since accuracy in calculated wave added resistance in shorter wave periods is indispensable to enhance the accuracy of Speed/Power trial results, further examination and refinement of methods for the capability of wave added resistance may be needed.

6.4 Validation of SNNM-SNU method

For SNNM-SNU method, the simplified method has been developed for the practicability, and it is denoted as SNNM-SNUs method (Lee & Kim, 2023). Here, SNNM-SNU method is used for the validation.

The published experimental data (Yokota and Kuroda et al. 2021, Yokota and Tsujimoto et al. 2021, Sasaki et al. 2009, Tsujimoto et al. 2018, Tsujimoto 2012, Tsujimoto et al. 2023) are used for the validation, which is data of the same ships shown in Table 4 in Section 6.2.

The validation results are shown in Figure 48. Here, K_{AW} is the coefficient of the added resistance in regular waves.

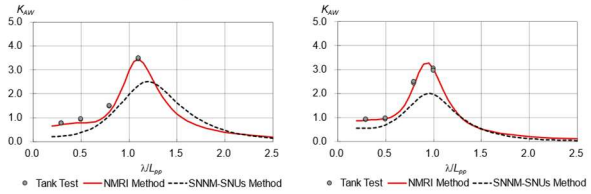

(a) container, 26kn(left: head waves, right bow waves(40 deg.)).

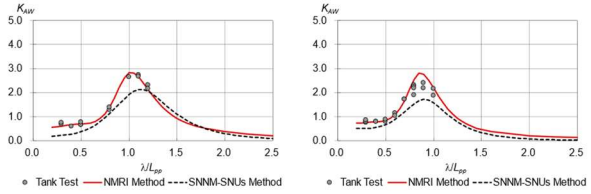

(b) container, 21kn(left: head waves, right bow waves(40 deg.)).

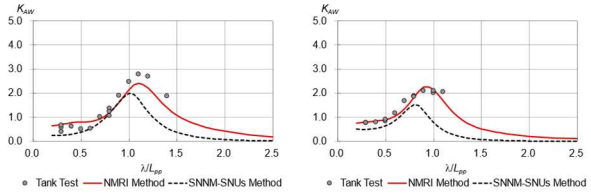

(c) PCC, 20.9kn (left: head waves, right bow waves(40 deg.)).

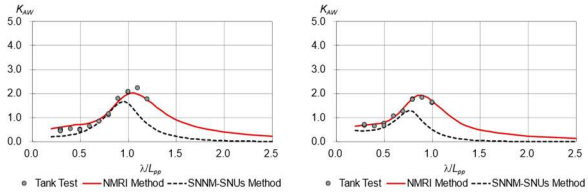

(d) PCC, 16.8kn (left: head waves, right bow waves(40 deg.)).

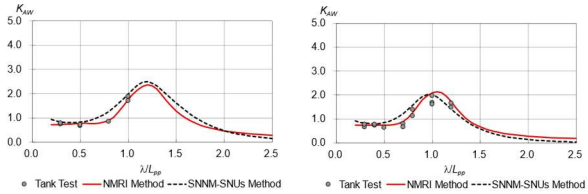

(e) PXBC, 14.9kn (left: head waves, right bow waves(40 deg.)).

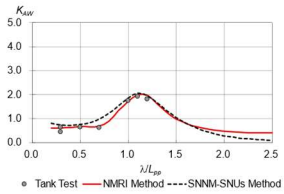

(f) PXBC, 12.1kn (head waves).

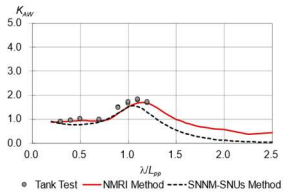

(g) VLCC, 13.3kn (head waves).

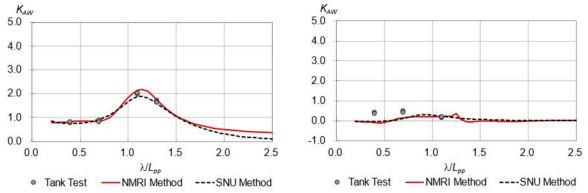

(h) JBC, 14.5kn (left: head waves, right: quartering waves(135 deg.)).

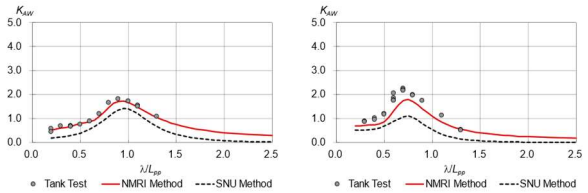

(left: head waves, right: bow waves(45 deg.))

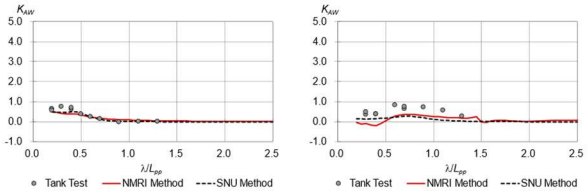

(left: beam waves, right: quartering waves(135 deg.))

(i) DTC, 18kn.

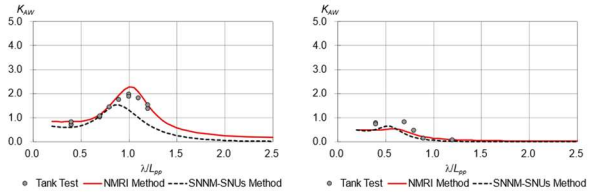

(left: bow waves(45 deg.), right: beam waves)

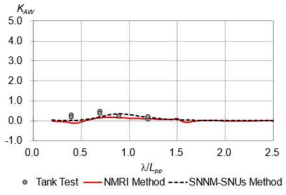

(quartering waves(135 deg.))

(j) chemical tanker, 12.7kn.

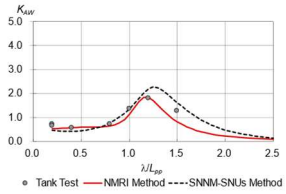

(k) domestic cargo, 8.9kn.

Figure 48 Validation result in regular waves for SNNM-SNUs

From the comparison between SNNM-SNUs method and tank test results, the followings are findings.

For fine ships: container ships and PCC, calculated results underestimate tank test results. For blunt ships: bulk carriers, tankers and general cargo, relation between calculated results and tank test results are different in each ship. These discrepancies have been found both in short waves where the contribution by SNUs is larger and in longer waves where the contribution by SNNM is larger. The cause is the effect of ship hull forms that cannot be

considered just by representative ship parameters since calculated results by NMRI method are in good agreement with tank test results.

As the conclusions, there is no advantage to apply the SNNM-SNUs method as the recommended method since calculation accuracy of SNNM-SNUs is inferior to that of NMRI method.

6.5 Added resistance in short waves

The added resistance in short wave be-comes more important for the larger ship. However, due to the difficulties of generating very short waves in experimental tank, it is also difficult to validate the estimation method.

Here are shown the experimental results for very short waves in Actual Sea Model Ba-sin in NMRI and those from referred paper for the post-Panamax container ship (DTC) (Yokota, 2020).

Figure 49 shows the frequency response of the added resistance in regular waves and three types of interpolations. Case1 is the constant from λ/L =0.2 of EXP.1 (NMRI), case2 is monotonically increasing from λ/L=0.2 of EXP.2 (SHOPERA) and case3 is constant from λ/L =0.2 of EXP.2. Figure 50 shows the added resistance in long-crested irregular waves for three cases. It was found that the three types have difference only in very short waves for the frequency response, but when converted at irregular waves, there is a large difference. For example, at T=6.7s, the wave correction by case2 will be four times larger than that by case 1. It may lead unreasonable high-performance ship as a result of speed trial.

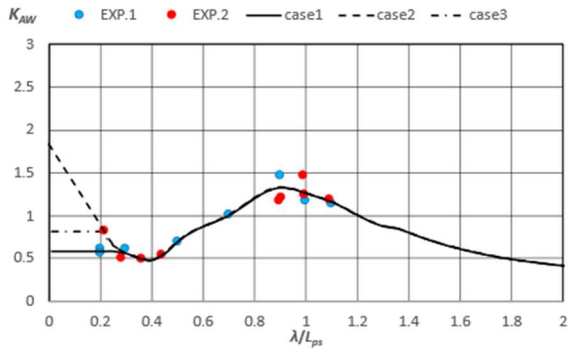

Figure 49 Three types of frequency response interpolated from experimental values.

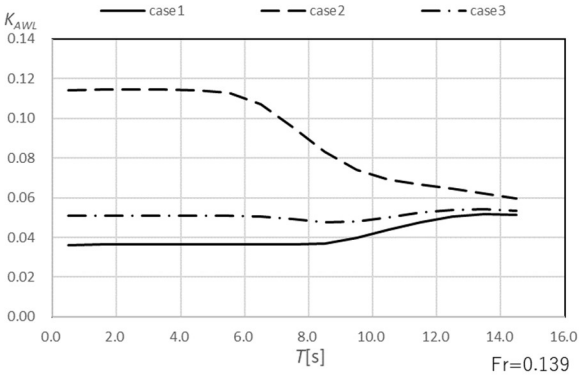

Figure 50 Added resistance in long-crested irregular waves (Fr 0.139).

The effect of the tendency of added resistance in very short waves is remarkable in irregular waves.

The effects of differences in test results in very short waves cannot be ignored, and highly accurate measurements are required.

For the validation in very short waves, quality assured data should be used and accumulated.

Until sufficient validation would be completed, it is recommended that the added resistance in short waves is treated as a constant value for the analysis of speed trial.

6.6 Wave height effect on the added resistance in waves

The added resistance in waves is expressed as proportional to the square of the wave height,

and linear superposition with the wave spectrum is conventionally used for the evaluation in irregular waves. It has been reported that uncertainty of tank test is larger in smaller waves, and the added resistance divided by the square of wave height becomes small due to nonlinear effects in larger waves (e.g. Nakamura, 1975). However, the wave height effect has difficulty to treat on the linear superposition for the conventional spectrum method.

Figure 51 shows an example for the comparison between test results in long-crested irregular waves and predicted results with the wave frequency spectrum and the response function. (Yasukawa, 2020) It was found that the difference of added resistance in irregular waves was shown at the wave height of 5m.

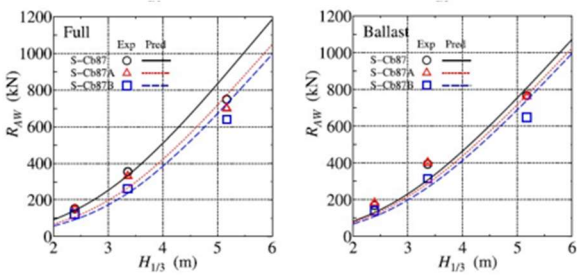

Figure 51 Comparison between test results in long-crested irregular waves and spectrum prediction.

On the other hand, In the guideline by ClassNK (Nippon Kaiji Kyokai, 2010), 3m is recommended for the experiment. Here, it is noted that for smaller ships, the wave height can be set to small: Length/100 in order to avoid nonlinear effects, and for larger ships, the wave height can be set to large: Length/100 in order to avoid large uncertainly.

The wave height effect is difficult to be included currently. Considering the wave height at the actual speed trial, the wave height effect can be negligible.

7. WIND CORRECTION

In full-scale ship performance evaluations by sea trials, the added resistance by wind has a significant impact. Considering this importance, accurate determination of wind speed and direction is essential. Ideally, undisturbed incident wind should be measured for accurate ship performance evaluation. However, the wind measurement method using an anemometer is susceptible to interference from the ship's structure. To address this, the Wind Averaging Method (WAM) was introduced, but its accuracy and potential side effects have not been thoroughly validated in actual sea environments. In this study, we examined the limitations of WAM in actual sea trial conditions and explored alternative approaches.

7.1 Problem of Wind Averaging Method in Actual Sea Trial Environments

Table 6 Power correction error due to WAM when wind velocity changes during double run

Incident true wind velocity	Wind velocity variation during double run					
	0%	+5%	+10%	+15%	+20%	+25%
10 m/s	0.0%	0.5%	0.9%	1.4%	1.8%	2.3%
8 m/s	0.0%	0.4%	0.8%	1.2%	1.6%	2.0%
6 m/s	0.0%	0.3%	0.7%	1.0%	1.3%	1.7%
4 m/s	0.0%	0.2%	0.5%	0.7%	1.0%	1.2%

Table 7 Power correction error due to WAM when wind direction changes during double run

Incident true wind velocity	Wind direction variation during double run				
	0°	+10 °	+20 °	+30 °	+40 °
10 m/s	0.0%	0.6%	1.9%	4.1%	6.5%
8 m/s	0.0%	0.3%	0.9%	2.2%	3.9%
6 m/s	0.0%	0.1%	0.5%	1.2%	2.2%
4 m/s	0.0%	0.1%	0.3%	0.7%	1.2%

It was confirmed that WAM can cause errors on ship's speed-powering performance evaluation in an environment where the wind changes during double run. Under the assumption that the wind measurement is accurate, if the incident true wind velocity and direction change during double run, the WAM itself generates error as shown in Table 6 and Table 7. The cases in which the error caused by the WAM due to the wind variation exceeds 0.5% and 1.0% of the total propulsion power are marked in orange and red respectively. For

instance, errors due to WAM when over 1 m/s or 20 degrees change in actual true wind could significantly impact (over 1% in power) on performance evaluation.

In actual sea trial environments where wind speed and direction easily fluctuate, the WAM is likely to introduce significant errors during sea trials. Table 8 is the calculation results of the probability that the wind is stable (wind speed variation below 1 m/s and wind direction variation below 20 degrees) for 2 hours by analyses five years of data from the Korea Meteorological Administration (KMA)'s marine weather buoy located in the three sea areas surrounding the Korean Peninsula. The probability that such stable conditions occur is only 32% per year on average, with a particularly low probability during winter (around 12%). These findings highlight that WAM has a high possibility of causing performance evaluation errors exceeding 1% in typical sea trial situations. Therefore, the accurate wind measurement is crucial rather than compensating for disturbed wind using WAM.

Table 8 the probability of stable wind in Korean offshore

Location of buoy (Korea)		East sea (Ulsan)	West sea (Mokpo)	South sea (Jeju)	monthly average
Month	1	12%	33%	47%	31%
	2	12%	35%	31%	26%
	3	32%	40%	30%	34%
	4	24%	28%	44%	32%
	5	31%	32%	40%	34%
	6	37%	25%	24%	29%
	7	54%	36%	39%	43%
	8	48%	34%	41%	41%
	9	26%	41%	24%	30%
	10	25%	41%	28%	31%
	11	22%	37%	33%	31%
	12	12%	34%	25%	24%
average		28%	35%	34%	**32%**

7.2 Methods for Accurate Onboard Wind Speed Measurement

Two methods were investigated for accurate onboard wind speed measurement: LiDAR-based remote sensing and Computational Fluid Dynamics (CFD) simulations to determine optimal anemometer placement.

7.2.1 Remote wind measurement by using LiDAR

LiDAR appears to be a promising instrument that can remotely measure wind flow accurately, but its high cost and the need for continuous maintenance and large equipment for installation limit practical use. Additionally, its onboard installation may introduce the errors due to ship motion and vibrations, requiring further research for sea trial applications.

7.2.2 Validation of CFD-Identified Anemometer Locations

To address the practical limitations of LiDAR and avoid errors associated with WAM, Computational Fluid Dynamics (CFD) was employed to calculate the airflow around a ship and determine suitable locations for anemometer installation.

To establish criteria for identifying appropriate positions, we investigated errors of ship's performance estimation due to amount of wind distortion in 15K TEU container carriers where wind resistance is relatively significant. We aimed for power estimation errors due to wind distortion within 2%. As shown in Table 9 and Table 10, when wind disturbance by wind speed were within 10% and direction were within 10 degrees compared to inflow wind, the performance estimation error remained within 2%.

Table 9 Estimated propulsion power error due to 10% of wind velocity error in container carrier

Inflow wind velocity (m/s)	Inflow wind direction (deg.)						
	0	30	60	90	120	150	180
4	0.5%	0.5%	0.3%	0.0%	-0.2%	-0.2%	-0.2%
6	0.9%	0.9%	0.5%	0.1%	-0.1%	-0.3%	-0.2%
8	1.3%	1.3%	0.7%	0.3%	0.0%	-0.2%	-0.2%
10	1.8%	1.8%	1.0%	0.5%	0.0%	-0.1%	-0.1%

Table 10 Estimated propulsion power error due to 10 deg. of wind direction error in container carrier

Inflow wind velocity (m/s)	Inflow wind direction (deg.)						
	0	30	60	90	120	150	180
4	0.2%	-0.3%	-0.7%	-0.7%	-0.5%	-0.3%	0.2%
6	0.4%	-0.5%	-1.2%	-1.1%	-0.7%	-0.3%	0.2%
8	0.6%	-1.0%	-1.7%	-1.3%	-0.9%	-0.4%	0.1%
10	0.8%	-1.5%	-2.0%	-1.6%	-1.1%	-0.4%	0.1%

The CFD conditions used to calculate the airflow around the ship are summarized in Table 11 and Table 12. Calculations were performed for three ship types (LNG carriers, LPG carriers, and tankers). Incident wind is considered as relative wind to simulate the actual sea trial situation.

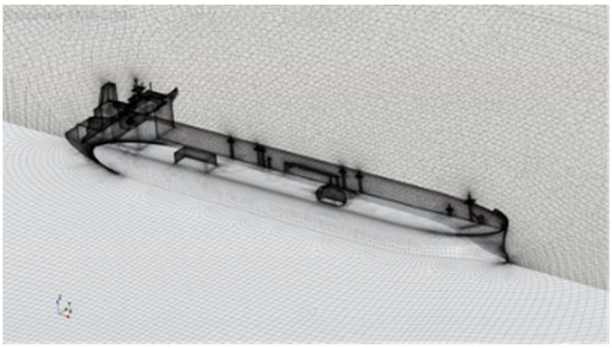

Figure 52 Example of CFD grid (LPG carrier)

Table 11 CFD calculation conditions

CFD Code/version	OpenFOAM v10
Solver	PimpleFoam
Fluid	Air, constant density
No. of cells	15~20 millions

Table 12 Incident wind condition for CFD calcualtion (V: velocity, D: direciton)

Ship type	LNGC		VLCC		LPGC		Container C.	
Ship V_{Ref}	18.0 knots		15.0 knots		16.0 knots		22.0 knots	
Wind V_{inflow}	8 m/s		8 m/s		8 m/s		8 m/s	
Inflow direction (deg.)	V	D	V	D	V	D	V	D
0	17.3	0	15.7	0	16.2	0	19.3	0
30	16.7	13.9	15.2	15.3	15.7	14.8	18.7	12.4
60	15	27.6	13.6	30.6	14.1	29.5	16.8	24.3
90	12.2	40.8	11.1	46	11.5	44.2	13.9	35.3
120	8.7	52.8	7.9	61.8	8.1	58.6	10.1	43.4
150	4.6	59.8	4.1	78.9	4.2	72	5.9	42.3
180	1.3	0	0.3	180	0.2	0	3.3	0

As shown in Figure 53 to Figure 58, the possibility of finding an appropriate location by CFD was confirmed. There were some anemometer positions where the disturbance of wind velocity and wind direction was calculated within 10% or 10 degrees respectively in cases of LNG carrier and tanker. However, for LPG carrier case, appropriate positions could not be determined by using CFD simulations. Therefore, some supplementary methods such as LiDAR or additional WAM usage may be necessary in this case. (These results are not representative of specific ship types because they are ones of example vessels)

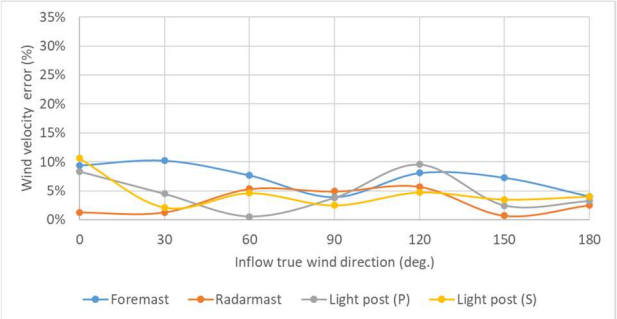

Figure 53 Wind velocity disturbance rate calculated by CFD for a LNG carrier

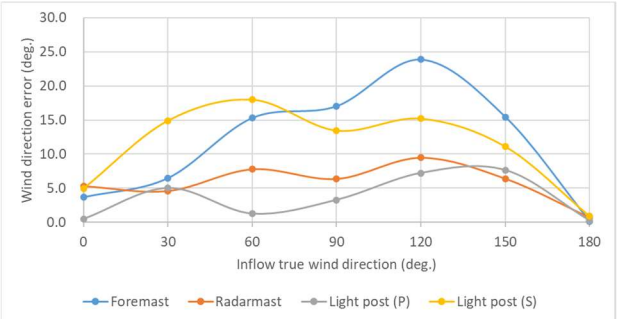

Figure 54 Wind direction disturbance calculated by CFD for a LNG carrier

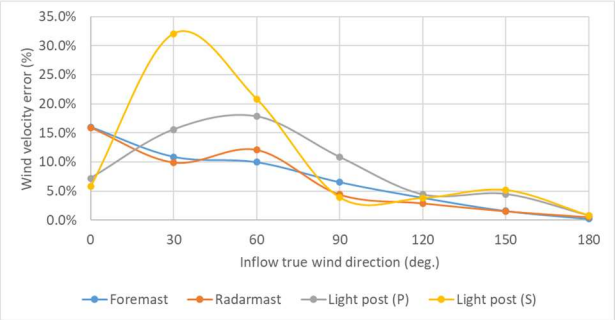

Figure 55 Wind velocity disturbance rate calculated by CFD for a LPG carrier

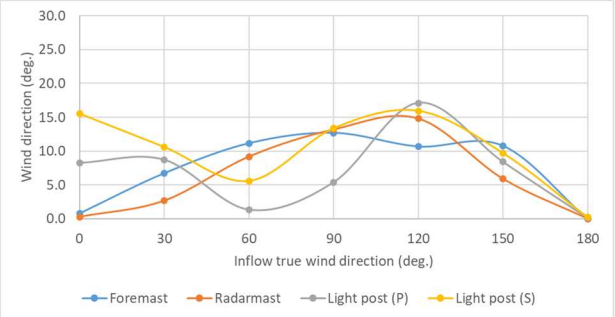

Figure 56 Wind direction disturbance calculated by CFD for a LPG carrier

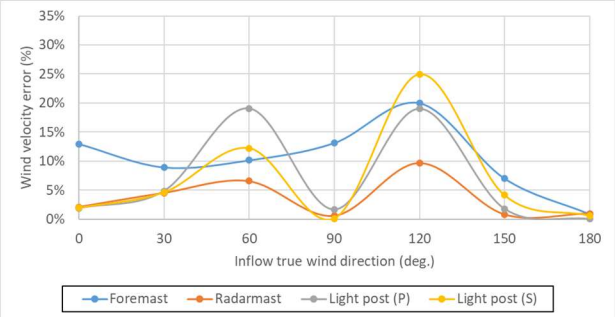

Figure 57 Wind velocity disturbance rate calculated by CFD for a Tanker

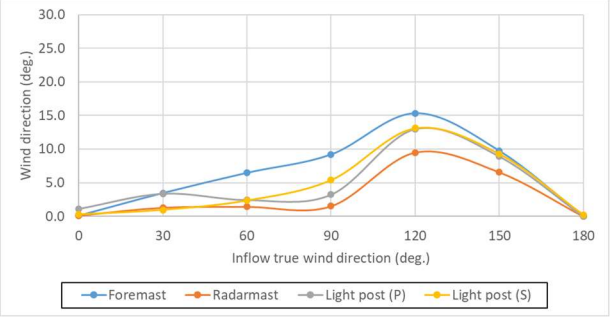

Figure 58 Wind direction disturbance calculated by CFD for a Tanker

Some anemometer positions where is evaluated by CFD were validated through onboard measurements during sea trials. The wind disturbance rate of radar mast, signal light post, and foremast was evaluated by CFD calculation, and measurements were performed at each location during speed trial of a LPG carrier and a container carrier. the wind measurement results obtained from anemometers at each location were compared to undisturbed wind measured by LiDAR. The comparison results were observed when the wind was stable and when the wind change was severe during sea trial.

As shown in Table 13, Figure 59, and Figure 60 below, it was confirmed that in a situation where the wind is stable during the speed trial of a LPG carrier, the measurement at Foremast where determined to be the best position by CFD can derive a more accurate wind than the case where measured wind is corrected by WAM at the onboard anemometer position (Signal post) where is being more disturbance.

Table 13 Absolute error rate at each anemometer position compared to Lidar measurement during speed trial

Run No.	Signal post (Onboard)	Radar mast	Foremast	WAM (Signal post)
1-1	16.3%	17.3%	7.8%	8.2%
1-2	2.0%	3.4%	0.6%	5.8%
2-1	27.5%	14.8%	12.7%	15.5%
2-2	0.4%	1.5%	3.0%	11.2%
3-1	17.1%	17.3%	9.3%	13.3%
3-2	0.2%	1.1%	2.1%	3.3%
Average	10.3%	8.3%	5.3%	8.9%
CFD results	9.9%	8.8%	2.3%	

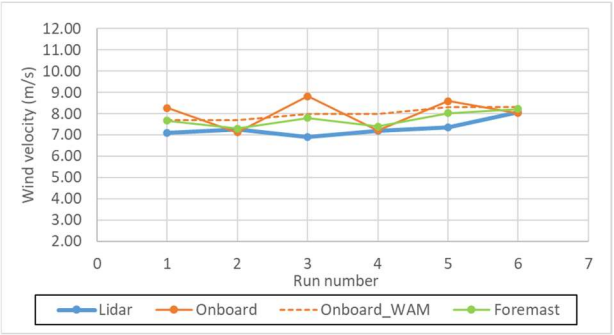

Figure 59 Wind velocity measurement results at each anemometer position during speed trial of a LPG carrier in stable wind

Figure 60 Wind direction measurement results at each anemometer position during speed trial of a LPG carrier in stable wind

As shown in Figure 61 and Figure 62, it was confirmed that even in the situation where the wind changes during speed trial, the measurement at Foremast, which was judged to be an appropriate position through CFD, can derive a more accurate wind than the case where measured wind is corrected by WAM at the onboard anemometer position (Radar mast) where is being more disturbance. In particular, when the wind dramatically changes during speed trial, the wind speed and wind direction corrected by WAM cannot even keep up with the actual wind trend measured by Lidar.

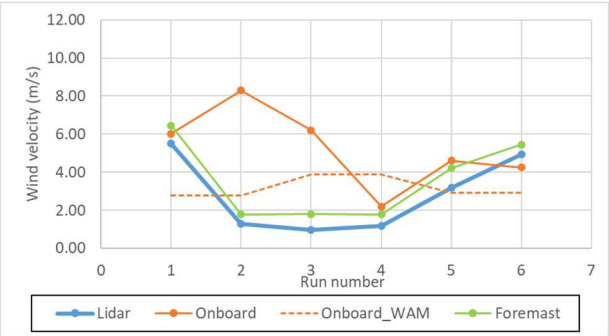

Figure 61 Wind velocity measurement results at each anemometer position during speed trial of a container carrier in unstable wind

Figure 62 Wind direction measurement results at each anemometer position during speed trial of a container carrier in unstable wind

7.3 Conclusions

In the process of ship's performance evaluation, WAM could generate significant errors frequently, so it is important to make the accurate measurement rather than correcting the wind after disturbed measurement.

It was confirmed that remote wind measurement using LiDAR or the searching for an appropriate location for anemometer installation by CFD calculation were helpful for accurate wind measurement. LiDAR is a promising remote sensing technique for wind measurement but is necessary to have more practicality for sea trial. Also, the effects of ship motion or vibration on wind measurement by LiDAR should be assessed. It was confirmed that wind measurement with determination of appropriate anemometer location by using CFD calculation was effective to measure wind accurately and practically. It will be reviewed more to prepare standardized procedures.

It was confirmed that errors generated by WAM were increased when the wind velocity and direction change more during speed trial. Therefore, WAM should be applied only in an environment where the wind blows uniformly during double run in the speed trial.

8. YAW AND RUDDER ANGLE CORRECTIONS

8.1 Influence of yaw angle

As the influence of yaw angle, the effect due to drift is examined. First, the effect of the drift angle on the added resistance in waves can be considered as the change of inflow velocity as shown by the following equation.

$$\Delta R_{wave}(V,\beta) = \Delta R_{wave}(V\cos\beta) \qquad (11)$$

Additionally, the resistance due to drift is considered. Examples for experimental results of longitudinal force for wide range of the drift angle and for estimated results of speed-power curves are shown in Figure 63 and Figure 64 for a large container ship. (Kuroda, 2021) Here X_D' is the coefficient of longitudinal force due to drift expressed as the following equation, and X_D is the longitudinal force due to drift, ρ is the fluid density, L is the ship length, d is the draft and V is the ship speed.

$$X'_D = \frac{X_D}{0.5\rho L d V^2} \qquad (12)$$

In Figure 63, two types of estimation are also shown. The one by Kijima(1990) shows opposite tendency in small drift angle, and the other by Kijima's equation with lift-induced drug (Sogihara, 2010) shows a large discrepancy in large drift angle. From Figure 64, it is found that this discrepancy results in the effect on the power at low speed since the drift angle at low speed is larger than that at usual operational speed near design speed.

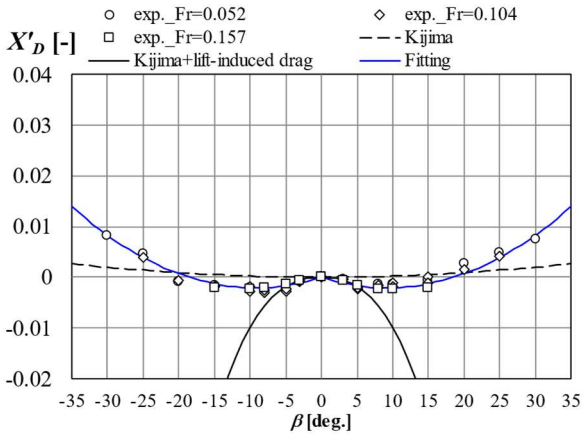

Figure 63 Longitudinal force due to drift for a large container ship.

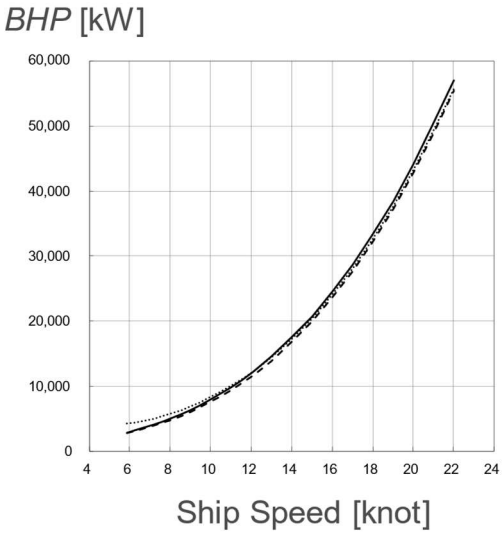

Figure 64 Speed power curve for a large container ship (Oblique weather conditions of Beaufort scale 6)

It was found that the resistance due to drift angle is larger at lower speed than the designed speed, and existing model may lead inaccurate estimation of power curve. However, the resistance due to drift is small at designed speed, and influence to speed trial analysis is limited. Therefore, on this stage, additional correction by the resistance due to drift is not needed.

8.2 Influence of rudder angle

In ITTC Recommended Procedures and Guidelines 7.5-04 01-01.1, conditions of speed

trial are prescribed. According to the description, the rudder angles are assumed to be minimal (less than 5 degrees) in the speed trial. Therefore, the effect of rudder angle is expected to be limited.

For the quantitative investigation, contribution of rudder action to resistance components is investigated. (Kuroda, 2022, Sakurada, 2023) Here, hydrodynamic forces due to steering are estimated by following regression formulae. Parameters in the equations can be estimated by model tests or regression formulae by Kijima et al. (1990) They are the same expression as ISO15016(2002).

$$\Delta R'_{rud} = (1 - t_R) F_N{}' \sin\delta \qquad (13)$$

$$F'_N = \frac{A_R}{Ld} f_\alpha U'^2_R \sin\alpha_R \qquad (14)$$

$$f_\alpha = \frac{6.13\lambda_R}{2.25 + \lambda_R} \qquad (15)$$

Where, t_R is the steering resistance deduction fraction, A_R is the projected rudder area, δ is the Rudder angle f_α is the rudder lift gradient coefficient, $U_R{}'$ is the non-dimensional resultant inflow velocity to the rudder, α_R is the effective inflow angle to the rudder, and λ_R is the aspect ratio of rudder.

As examples for calculated results, resistance components for PCC are shown in Figure 65. It indicates that the effect of steering is smaller than that of winds, waves and drift for lower speed and for designed speed.

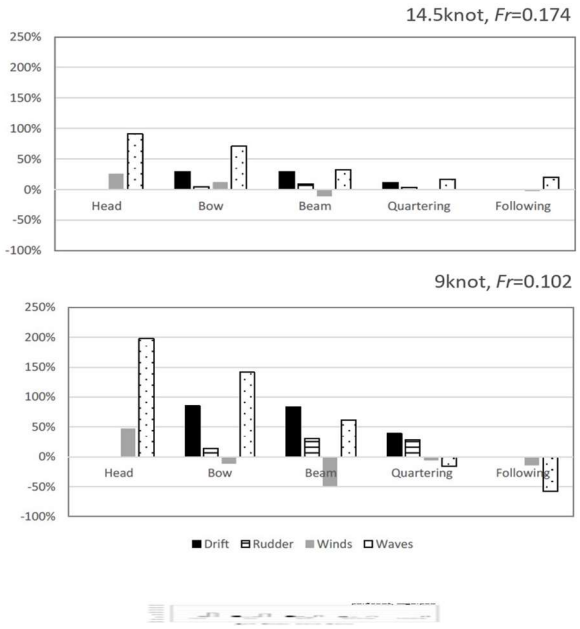

Figure 65 Resistance components for PCC (upper: 14.5 knot, lower: 9 knot)

The expression of the effect of rudder angle as the inclusion in the resistance due to drift has been proposed and is shown by the following empirical formulae.(eq.(16)-(18)) The formulae calculate the resistance due to drift by side wind. However, there are several issues such that the effect of waves is not considered, and that coefficients are not verified for the application.

$$R_{Drift} = \frac{\rho}{2} V^2 \left(L^2 \left(0.00022 \frac{V}{u} + 0.00466 \left(\frac{V}{u}\right)^2 \right) + 0.5 S_{App} 0.0041 \delta_R \right) \qquad (16)$$

$$Y_{Rudder} = 0.0372 \frac{\rho}{2} V^2 S_{App} \qquad (17)$$

$$N_{Rudder} = 0.0372 \frac{L}{2} \frac{\rho}{2} V^2 S_{App} \qquad (18)$$

Where, R_{Drift} is the resistance due to drift by the side wind, V/u is the ratio lateral/ longitudinal speed, S_{App} is the area of rudder, δ_R is the rudder angle, Y_{Rudder} is the rudder side force and N_{Rudder} is the rudder yawing moment.

As a conclusion, since the speed trials are assumed to be conducted in head winds and waves or following winds and waves as far as possible, and the rudder angles are assumed to be minimal (less than 5 degrees), the effect of steering is limited. Therefore, on this stage, additional correction by the resistance due to steering for correction is not needed.

8.3 Summary

Through investigations based on case studies with estimation and experimental results, it is concluded that additional corrections by the resistance due to drift and steering are not needed on this stage.

9. NEW DEVELOPMENTS IN INSTRUMENTATION AND MEASUREMENT EQUIPMENT RELEVANT FOR SEA TRIALS AND IN-SERVICE PERFORMANCE ASSESSMENT

Both the speed trials and in service performance, accurate measurement of environmental conditions and ship operational data such as wind, waves, and propeller thrust is crucial. These factors significantly impact the ship's performance and efficiency. Therefore, accurate and reliable on-board measurement of the wind and propeller thrust are essential for the evaluation of the ship’s speed power performance.

The full-scale measurements of the propeller thrust, torque, and revolution for a series of crude oil tankers were conducted during the speed trials. Two different measuring systems, strain gauge and optical type, were implemented to compare the performance of sensors as shown in Figure 66.

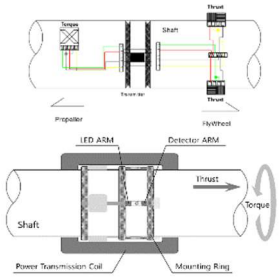

– strain gauges – – optical –

Figure 66 Schematic representation of strain gauges and optical measurement system

To verify the results of thrust measurement using electrical and optical sensors, the relation of revolution, torque and thrust are compared with model test results (Figure 67 and 68).

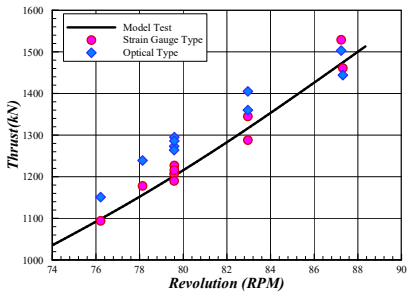

Figure 67 Comparison of thrust between speed trials and prediction results based on model test of crude oil tanker

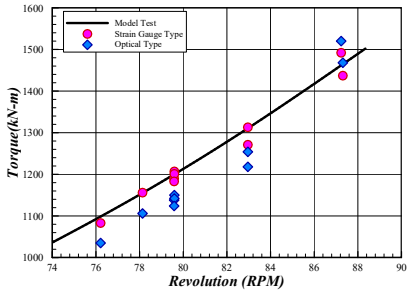

Figure 68 Comparison of torque between speed trials and prediction results based on model test of crude oil tanker

As an important index that decides the accuracy of the thrust measurement, the relation between propeller thrust and torque was investigated as shown in Figure 69.

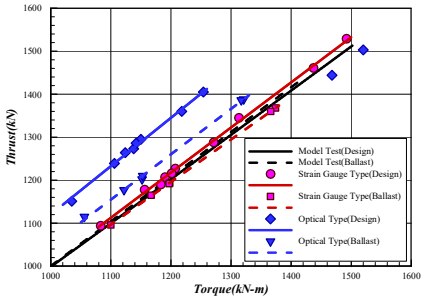

Figure 69 Comparison of thrust - torque of crude oil tankers

The results of thrust measurement at the same torque show approximately 10% difference from the model test results, mainly due to the stability of the zero value, which is found as a problem to be solved for the stable and reliable measurement of thrust.

The characteristics of wind speed and direction by LiDAR have been investigated for RV vessel, LNG carriers, and large container (Figure 70). As shown in Figure 71, true wind speed and direction based on the wind LiDAR measurements and empirical wind profiles were compared.

Figure 70 Wind LiDAR

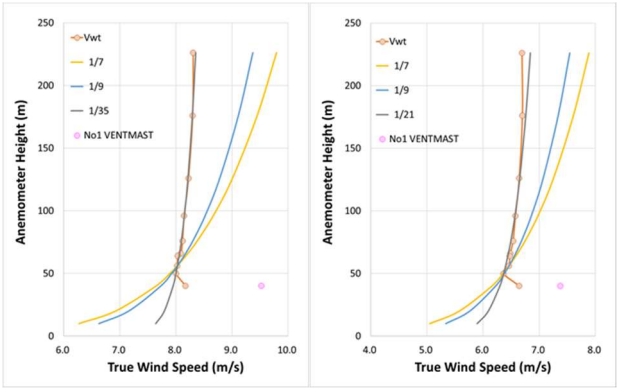

Figure 71 Comparison of Wind Profile for LNG Carrier

Conclusions. For explore and monitor new developments in instrumentation and measurement equipment relevant for sea trials and in-service performance assessment, propeller thrust measurement system and wind LiDAR have been investigated. The experience with the strain gauge and optical sensor shows that extensive effort is required to realize precise thrust measurement. For the further study, the long term stability of the thrust measurement needed. The wind LiDAR offers the advantage of high precision in measuring wind direction and speed under various environmental conditions. The discrepancies between traditional Wind Profiles and LiDAR measurement results have been investigated. Further research is needed to determine the cause of differences. .

10. UPDATE AN INVENTORY OF DATA BASES ON IN-SERVICE PERFORMANCE

It is considered that MARIN's JoRes ship-scale test cases data to be published in December 2024 (Ponkratov 2023) are most relevant to meet this TOR task, in particular, due to its coverage of features relevant to in-service performance issues, e.g., ship types, 3D configurations, ESDs, roughness measurements.

Therefore, it seems to be appropriate for us to recommend ITTC full conference to include JoRes test cases in data base for full-scale issues in ITTC activity. While the JoRes test cases will not available to the public by December 2024, it

will not cause any trouble since next term activity will starts October 2024.

Survey to ITTC member organizations regarding the provision of their full-scale data to this TOR task was conducted. 1 organization (SVA Potsdam) has contributed full-scale speed/power trails results for 7 ships.

11. ACCURACY OF CFD FOR SHALLOW WATER APPLICATIONS

Accuracy of CFD for shallow water applications mainly concerning the shallow-water effect on propulsive performance has examined by the literature survey. Unfortunately, due to the scarcity of the published works, sufficient examination of the issue has not been conducted. In the following, results of literature survey conducted in this committee which are relevant to effect of shallow-water on self-propulsion factors are described.

Wang et al (2016) conducted the numerical prediction of ship self-propulsion in different shallow water conditions: H/T=2.0 and H/T=1.2(H : depth of water, T : draft of ship). The KRISO Container Ship (KCS) model is used in the simulations. Numerical computations are carried out by using a solver named naoe-FOAM-SJTU which is developed on the open source platform OpenFOAM and mainly composed of a dynamic overset grid module and a full 6DoF motion module with a hierarchy of bodies. A proportional-integral (PI) controller is applied to adjust the rotational speed of the propeller to achieve the desired ship speed. The simulated results, i.e. the rate of revolution of propeller n, propulsion coefficients, are compared to the experimental data provided by Flanders Hydraulics Research (FHR) in SIMMAN 2014. Good agreements between simulation results and experiment are demonstrated. It is concluded that the present approach is applicable for self-propulsive prediction in shallow water.

Cai et al. (2022) investigated the shallow-water effects on self-propulsion factors by numerical simulations. In this study, ship self-propulsion simulations were conducted by using STAR-CCM+, with both discretized propeller model and body force model. KVLCC2 hull form is employed. The results of the body force method show good agreement with the discretized propeller method in different water depths. In addition, it was shown that water depth influences the thrust deduction fraction and the wake fraction significantly. It is concluded that the calculation results can provide a basis for the optimization of ship with low speed and large block coefficient as well as for the propeller optimization in shallow water.

From the survey results described above, usefulness of CFD for the study of shallow-water effect on self-propulsion factors can be confirmed. However, validation of the CFD has not sufficient for the application to the evaluation of full-scale ship performance yet. Further validations, in particular, comparison with full-scale data may be indispensable and should be continued in the following ITTC terms.

12. TECHNICAL SUPPORT TO ISO AND IMO CONCERNING IN-SERVICE PERFORMANCE MONITORING

For this task, the initial intention of this committee's activity was directed to the contribution to the revision of ISO19030 for the measurement of changes in hull and propeller performance and defines a set of performance indicators for hull and propeller maintenance, repair and retrofit activities.

While ISO19030 has widely employed for the evaluation of in-service performance mainly in terms of performance of hull-surface coating system, its procedure seems to be not adequate from the ship hydrodynamic point of view and further modification may be necessary to be used as a technically reliable measure for in-service performance evaluation. Our main concern

in the existing ISO19030 is in the lack of consideration of wave effect in analysing the on-board performance data, that is no correction for wave effect are applied, when reducing to the performance indicator. Due to the lack of the wave correction, the derived performance indicator which nominally intended to indicate the deterioration due to hull and propeller surface fouling is contaminated with the effect of wave during in-service navigation. Thus, this committee intended to contribute in the revision of ISO19030 by providing technical support concerning of introduction of wave correction procedure in on-board performance data analysis.

Despite above mentioned intention of this committee to provide technical support to the revision for enhancing accuracy of ISO19030, unfortunately from our point of view, the review for revision of ISO19030-2016 conducted in 2021 resulted in a major vote to leave ISO 19030:2016 unchanged. Thus, a new edition of ISO 19030 may not be published until 2029.

There is no activity in both ISO and IMO relevant to in-service performance monitoring during the present ITTC term. No activity in technical support to ISO and IMO concerning in-service activity.

13. SURPORT ISO IN UPDATING ISO15016 IN COMPLIANCE WITH RP7.5-04-01-01.1

This committee has closely followed the activities of ISO/TC 8/SC 6/WG 17 (WG for short hereafter) for revising ISO15016.

The 1st DIS voting of the ISO15016 revision was conducted from 25 September to 18 December 2023. In the voting, 72% of the participating members approved the DIS. However, 32% of all members disapproved the DIS, so the DIS was not approved. Technical comments submitted at DIS voting were reviewed, which included two specific proposals for amendment. One is that only the 3D ultrasonic anemometer system is allowed for wind measurement, and the other is that wave added resistance transfer functions derived from model tests/SNNM can only be used in combination with the in-situ measured wave spectrum. These two issues were eventually resolved and the 2nd DIS was approved.

This committee's members participating in the WG as experts tried strenuously to achieve harmonization of the revised ISO15016 with ITTC R.P. 7.5-04-01-01.1. However, full harmonization has not been achieved so far.

Besides several minor differences between the two documents, the most outstanding difference lies in the permissible methods for the evaluation of resistance increase due to waves, as shown in Table 14.

Table 14 Permissible wave correction methods

Method	ITTC R.P. 7.5-04-01-01.1	ISO15016 2nd DIS
Seakeeping model test	√	√
STAWAVE-1	√	√
STAWAVE-2	√	×
SNNM	√	√
NMRI	√	×

According to ITTC R.P. 7.5-04-01-01.1, five methods can be used for the evaluation of wave added resistance, including seakeeping model test, STAWAVE-1 (simplified correction method for ships with limited heave and pitch during the speed runs), STAWAVE-2 (empirical correction method with frequency response function for ships with heave and pitch during the speed runs), SNNM (semi-empirical method for predicting the added resistance of a ship advancing in waves of arbitrary directions) and NMRI (theoretical method with simplified tank tests in short waves or empirical formula). However, the STAWAVE-2 and the NMRI methods are not included in the 2nd DIS of ISO15016. Further work for harmonization should be continued.

14. UPDATE GUIDELINE FOR DETERMINATION OF MODEL- SHIP CORRELATION FACTORS

AC Working Group has been in principally responsible for this task and preparing the update. After receiving the report of AC Working Group, the Committee requested a proposal to forming a new guideline on model-ship parameters for full-scale power predictions. But their proposal was late for due date of last R&P submission, therefore, the Committee had no choice but to decide to postpone the preparation work for the new guideline to the next ITTC term. Since then, AC Working Group has drafted their own R&P and is currently in the process of collecting opinions from ITTC member organizations.

The main contents of the draft R&P for evaluating power ratio between drafts proposed by AC Working Group are as follows:

After the towing tank test of a given case, the facility predicts the extrapolated full-scale speed-power curves for trial and stipulated draught (EEDI draught and/or con-tract draught). The predicted power ratios are derived as

$$\Delta P_{PR} = P_{stipulated}/P_{trial} \tag{19}$$

To verify that the predicted power relations are reasonable, the model scale measurements and a few ship parameters are entered into a web-based software that AC Working Group has prepared. The output from the webpage is the Guideline power ratio:

$$\Delta P_{GL} = P_{stipulated}/P_{trial} \tag{20}$$

The fraction between the predicted and the guideline power ratios is derived as:

$$D = \Delta P_{GL}/\Delta P_{PR} - 1 \tag{21}$$

D expressed in % is the deviation when predicting the loaded draught curve, after that the trial model test curve would be shifted to the speed trial results.

The requirements of accepted test are:

- 10-15 cases are submitted to the Sample Collection (no more, no less)
- The median D of the Sample Collection should be within ±3%
- The absolute value of D should be within 5% for 90% of the cases in the Sample Collection
- The absolute value of D should be within 10% for 100% of the cases in the Sample Collection

15. UPDATE GUIDELINE ON CFD-BASED WIND COEFFICIENT

The update of the guideline on CFD-based wind coefficients was done by rearranging and simplifying the formulae for height average wind speeds V_{A1} and V_{A2}. The expanded new formulae are as follows:

$$V_{A1}^2 = \frac{V_{ref}^2}{2\alpha+1} \cdot \left(\frac{H_{BR}}{z_{ref}}\right)^{2\alpha} \tag{22}$$

$$V_{A2}^2 = \frac{V_{ref}^2}{2\alpha+1} \cdot \left(\frac{H_L}{z_{ref}}\right)^{2\alpha} \tag{23}$$

Above formulae were derived assuming the wind profile given by formulae:

$$V(z) = V_{ref} \cdot \left(\frac{z}{z_{ref}}\right)^{\alpha} \tag{24}$$

where:

α – wind profile exponent; 1/9 at the sea level
V_{ref} – reference velocity at reference level z_{ref}
z_{ref} – height of reference wind velocity; typically 10 m
The problem revolves around the dependence of wind resistance coefficients on the wind profile. The existing guidelines and databases do not adequately define the wind profile.

Taking the above into consideration, it is recommended to update the guideline on CFD-

based wind coefficients by recalculating the existing database of wind resistance. The updated database should be used to provide a more accurate representation of wind resistance, taking into account the variations in wind profiles.

16. DEVELOPMENT OF RELEVANT TECHNIQUES FOR ENERGY SAVING AND THE NEEDS TO COMPLEMENT THE PRESENT EEDI FRAMEWORK

The shift towards low-carbon and zero-carbon fuels necessitates a reassessment of the EEDI framework to ensure it remains relevant and effective in promoting energy efficiency. Additionally, the integration of cutting-edge technologies in maritime design and operation requires new methods for evaluating their impact on energy efficiency. In cases where the EEDI alone may not adequately capture power savings, additional metrics may be needed to provide a more comprehensive assessment of energy efficiency improvements.

The IMO circular MEPC.1 / Circ.896 (14 Dec 2021) outlines methods for the calculation and verification of the attained EEDI, in line with various regulations of Annex VI to MARPOL. It addresses the combination of propulsion power (P_P) and reference speed (V_{ref}), integrating speed-power curves to reflect their combined effects. Additionally, it accounts for technologies that generate electricity (P_{AEff}), reducing the need for propulsion power.

According to the IMO circular the power reduction includes several categories. Category (A) involves adjusting the power curve by changing either P_P or V_{ref}. Category (B) focuses on reducing propulsion power at V_{ref} without generating electricity. Within this category, technologies usable anytime have an availability factor (f_{eff}) of 1.0 (category B-1), while those used under limited conditions have f_{eff} less than 1.0 (category B-2). Category (C) includes generating electricity to reduce propulsion power at V_{ref}. Technologies effective all the time have f_{eff} equal to 1.0 (category C-1), whereas those dependent on ambient conditions have f_{eff} less than 1.0 (category C-2).

Power reduction might be categorized into those that affect main engine power (A and B) and those that influence auxiliary power (C). Technologies that reduce friction, optimize hull and propeller design, or utilize energy-saving devices (ESDs) fall under Type (A). Hull air lubrication systems that can be switched on or off are categorized as Type (B-1). Wind assistance technologies like sails, Flettner rotors, and kites are classified as Type (B-2). Waste heat recovery systems that function continuously are categorized as Type (C-1), while photovoltaic cells that depend on environmental conditions fall under Type (C-2).

The air lubrication system (ALS) is becoming more popular in recent days; however, implementation in EEDI calculation needs a deeper look into the metrics used for sea-trial-derived power curve corrections. The auxiliary power requirement includes the energy consumed by running the air lubrication system itself. Performance measurement involves both calculated and measured data from full load and sea trials, both with ALS on and off. The total power reduction is given by formula:

$$P_{eff} = P_{effAL} - P_{AEeffAL}\frac{C_{FAE}}{C_{FME}}\frac{SF_{AE}}{SFC_{ME}} \qquad (25)$$

where:

P_{effAL} – propulsion power reduction due to air lubrication

$P_{AEeffAL}$ – auxiliary power of running air lubrication

Further the power reduction due to air lubrication system is derived is calculated by:

$$P_{effAL(T)} = ADR_T \times P_P \qquad (26)$$

where index (T) means draught, which might be trials draught, design or full load. It is obvious that during sea-trials the actual reduction

rate (*ADR*) is derived directly from evaluated power curves (see Figure 72), however calculation of ADR for other draughts is based only on estimations. Thus there are several key challenges in the integration of ALS technology. Firstly, there is a lack of clear guidelines on how to estimate reduction rates using model tests, computational fluid dynamics (CFD), or empirical formulas. Secondly, there are no standardized procedures or recommendations for conducting sea trials with ALS. Additionally, there is no definitive evidence showing the proportional relationships between full load and sea trials load reduction rate scaling. Lastly, there is insufficient information on how sea state and weather conditions impact ALS performance.

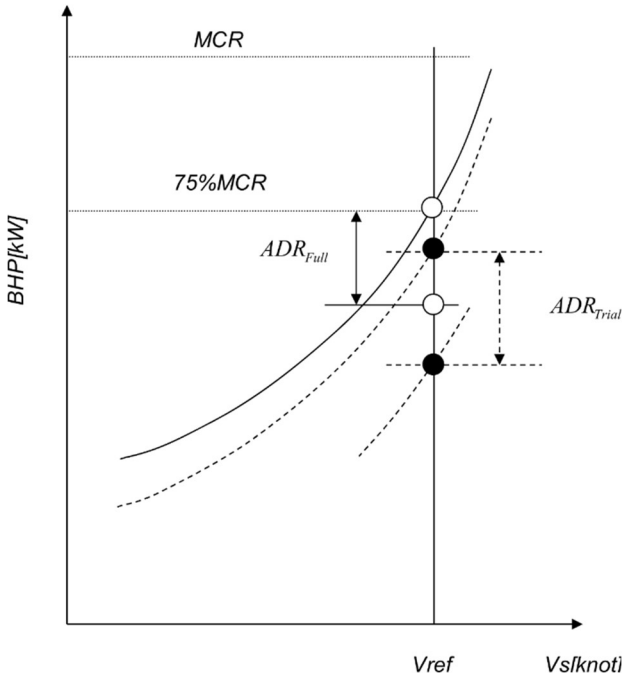

Figure 72 Definition of ADR from sea trials

Several areas need further research and standardization to improve the capability and reliability of ALS technologies. Clear estimation methods should be established to standardize ADR derivation for draughts other than those applied during sea trials. Standard procedures and recommendations for conducting sea trials with ALS need to be developed. Correlation studies are necessary to establish proportional relationships between different load conditions and reduction rates. Finally, investigating the influence of weather conditions on the performance of ALS and other innovative technologies is crucial.

17. FULL SCALE DATA ON THE EFFECT OF ENERGY SAVING METHODS

17.1 Overview

In the current context of carbon peak and carbon neutrality, the energy-saving and emission-reduction technologies that the ship industry is focusing on. Extensive theoretical research and practical ship applications have proven that these technologies are the potentially effective techniques for reducing the EEDI and EEXI of ships.

In order to improve the energy efficiency of operating ships, systematic energy efficiency solutions are often used today. These include the optimization of hull lines for actual sea conditions, the use of high-efficiency propellers, the selection of optimal hydrodynamic energy-saving devices (Pre-ESDs: PSV, WID, PSS; Post-ESDs: PBCF, Rudder Bulb, Rudder Fins and so on), and the adoption of revolutionary and innovative energy-saving technologies (ALDR, Wind Rotor, Wind Sail). There are multiple methods to evaluate the energy saving effect after the application of these technologies. Numerical simulations are usually used at the design stage to optimize the solution and forecast the energy saving effect. Laboratory model tests can also be used to assess the energy savings and to predict the energy efficiency level of the full scale ship. Both numerical simulations and model tests generally consider the relative comparison between applying energy-saving technologies and not using energy-saving technologies in still water. However, the real sea state environment, including wind, waves, and currents, will have an impact on the final energy efficiency, and there is also a scale effect between the model scale and the full scale, and all these factors need to be supported by sufficient sea

trail data of full scale ship. Especially, the statistical data of long-term operation is more meaningful for evaluating the energy-saving effect after applying energy-saving technologies. Therefore, full scale data are very important for the prediction and evaluation of energy saving effect.

Table 15 Combination of energy saving technologies

OBJECT	TARGET	TECHNOLOGIES
HULL	DRAG REDUCTION	Hull lines optimization under still water and sea condition
		Trim optimization
		Upper building optimization for low wind resistance
		Surface drag reduction such as micro-bubble, low drag coat, etc.
ENGINE	EMISSION REDUCTIOIN	Power limitation
		Optimum working condition
		Low carbon fuel or no carbon fuel
PROPELLER	EFFICIENCY IMPROVING	Optimum match among stern, main engine and propeller
		Suitable Propulsion type
		High efficiency propeller
	ENERGY SAVING	Pre-ESDs (PSV, WID, PSS...)
		Post-ESDs (PBCF, Rudder Bulb, Rudder Fins...)

17.2 Hydrodynamic Energy Saving Technologies

Some energy-saving technologies whose basic principles are closely related to hydrodynamics, usually we call them hydrodynamic energy-saving technologies. The energy saving device pre-shroud-vanes (PSV or PSD) in front of the propeller, the high-efficiency propeller (HEP), and hub vortex absorbed fins (HVAF or PBCF) behind the propeller, etc. are all in this category. Different energy saving devices produce different energy saving benefits.

- **Pre-ESDs: PSV**

-Producing added thrust by accelerated ducts;
-Producing favourable pre-swirled inflow into propeller by inside vane and reducing rotational losses of slipstream;
-Helping to improve propeller efficiency by establishing a more uniform inflow into the propeller;
-Energy saving about 3%~8%;

- **Propeller Optimization: HEP**

-Optimum diameter for higher efficiency;
-Skewed blade for lower induced vibration;
-Using new profile for higher efficiency, better cavitation performance;
-Optimum radial pitch for higher efficiency, better cavitation performance;
-Specific skew at tip to vortex cavitation suppression;
-Wake adapted for optimum match with Hull;
-Theoretical design to Balance optimization on efficiency-vibration-cavitation;
-Energy saving about 3%~5%;

- **Post-ESDs: HVAF**

-Energy saving by installing behind propeller instead of Propeller Cap, to reduce the energy losses of hub vortex;
-Energy saving about 2%~5%;

17.3 Analysis Method Based on Sailing Records

Forecasting and evaluating the effect of energy saving methods can be done through model tests, including resistance and self-propulsion tests in towing tank, propeller hydrodynamic tests in cavitation tunnel, etc. These methods are used to compare with each other the propulsive efficiency of the whole ship with and without energy-saving devices, so as to forecast the performance of the full-scale ship and obtain the EEDI or EEXI index.

Another method is to obtain data such as loading capacity, speed, main engine power, fuel consumption and so on through the full scale ship sea trial or long-term monitoring. By comparing and analyzing the changes of these data with and without ESD with the same type of ships or sister ships, we can obtain the full scale energy saving effect.

However, full scale ship data are different from laboratory data, uncertain and subject to greater environmental interference. More systematic data are mainly analyzed and processed. For example, when utilizing full scale ship fuel consumption data for analysis, the effect of different loadings must be corrected.

The analysis is based on Admiralty Coefficient – C_m, i.e.,

$$C_m = \frac{\triangle^{2/3} \cdot V^3}{P_m} \quad (27)$$

Where, $\triangle$ is the displacement; V is the vessel speed; and P_m is the power of main engine.

Herein, the displacement and the power of main engine can be represented by the load capacity and the fuel oil consumption, respectively.

$$F.O.C_{\Delta correction} = \left(\frac{\Delta_{correction}}{\Delta_{actual}}\right)^{\frac{2}{3}} \times F.O.C_{actual} \quad (28)$$

$$F.O.C_{Vcorrection} = \left(\frac{V_{correctio}}{V_{actu}}\right)^{3} \times F.O.C_{\Delta correction} \quad (29)$$

Where,

$F.O.C_{\triangle correction}$: the fuel oil consumption after displacement correction;

$F.O.C_{actual}$: the fuel oil consumption before displacement correction;

$F.O.C_{Vcorrection}$: the fuel oil consumption after ship speed correction;

$\triangle_{correction}$: the displacement at the load condition after displacement correction;

$\triangle_{actual}$: the displacement at the load condition before displacement correction;

$V_{correction}$: the ship speed at the load condition after speed correction.

V_{actual}: the ship speed at the load condition before speed correction;

Based on this analysis method, the fuel oil consumption can be transformed into the same condition including the same vessel speed and same load capacity. Thus, the energy saving effect can be calculated by

$$EnergysavingEffect = \left(1 - \frac{F.O.C_{after}}{F.O.C_{befor}}\right) \times 100\% \quad (30)$$

Where,

$F.O.C_{after}$: the corrected fuel oil consumption after energy efficiency upgrade;

$F.O.C_{before}$: the corrected fuel oil consumption before energy efficiency upgrade.

According to the experiences, the data (with steaming time $\geqslant$16 hours, the laden condition (drafts) close, and the rotation of ME close also before and after Energy Efficiency Upgrade are chosen as the sample data to analysis.

The actual fuel consumption depends not only on the technical status of the ship, but also on the sea condition (Removing the influence of sea state $\geqslant$5) as well as hull fouling conditions (Basically the same). In order to even the influence of these conditions, it is necessary to collect more sailing data to get more accurate energy saving effect.

17.4 Some Full Scale Date about Energy Saving Effect of ESDs

In order to analyse the full-scale ship energy saving effect of ESDS, CSSRC collected some model test and full scale sail trail data through CMES-Tech (CSSC Shanghai Marine Energy Saving Technology Co., Ltd) to help the full

scale analysis of the energy saving effect from 2021 to 2024.

- **HVAF or PBCF**

HVAF is a simple and commonly used energy saving device. Usually, the energy saving effect measured in the model test in the laboratory is only about 2%, while a large number of real ship application results show that the energy saving effect of the full scale is larger than that of the model scale. There were collected five cases full scale data about using HVAF (PBCF), and these cases can be compared with sister ships sea trail results. Some case has model test result.

Table 16 Full scale data with HVAF

No.	Ship	Sister Ship
Case1	27000DWT MPC	1
Case2	57000DWT B.C	1
Case3	75200DWT B.C	1
Case4	114,500DWT B.C	5
Case5	180,000DWT B.C	Long period record

Two 27000DWT MPC vessels, one is "PING AN" without HVAF and the other is "XIN FU" with HVAF, were carried out sea trail in Class 1 and Class 2 sea state respectively. Normally, the measured speeds under class 1~2 sea state can be uncorrected, and the ballast condition of these two ships is close to each other during the sea trial. The measurement and recording of the main engine shaft power during the sea trial can be used to derive the speed-power-revolution relationship of each ship. Comparative analysis of the data of the trial voyage of two vessels can be used to evaluate the energy-saving effect of HVAF. The result indicate that it can obtain about 4%~5% energy saving of HVAF.

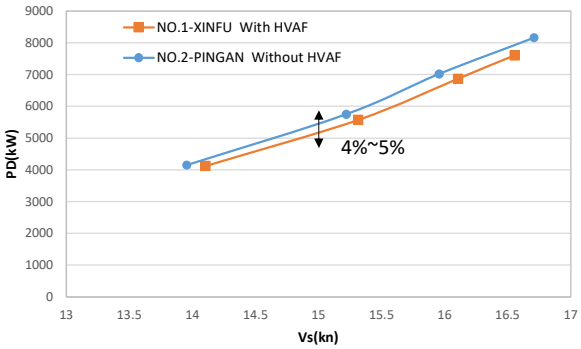

Figure 73 Energy saving effect of 27000DWT MPC with HVAF

Two sister vessels of 57000DWT bulk carrier, N276 is installed with conventional cap and N373 is installed with HVAF. N373 is moored in the harbour for a long time before the sea trial, and the hull has a lightly fouled. When analysing the data of the sea trail, if it directly compares the speed and power, the speed increased by 0.08 knots with HVAF under the same power, and consumed 167kW less power under the same speed. The energy saving effect is abt. 2.4%. If roughness correction is applied to the N373 vessel, the energy saving effect can be increased to 5%.

Table 17 Roughness effect for energy saving of HVAF

Design Draught	N276 Without HVAF	N373 With HVAF	△	Energy Save(%)	Corrected Roughness effect
7308kW	14.64kn	14.72kn	0.08kn	--	--
14.46kn	6927kW	6760kW	167kW	2.40%	~5%

HVAF for a 114,500DWT bulk carrier was designed and has been installed onto ship numbered as HN1164, and the sea trial was carried. According to the model test results, it can be seen that the efficiency of propeller with HVAF increased about 2.7% at design point ($J_0 \approx 0.43$), and the ship speed can be increased about 0.14kn at different drafts. Since there are five sea trial reports for five delivered sister ships of HN1164, the energy saving effect of HVAF can be analyzed based on the comparison between HN1164 and its sister ships. The sea trial drafts

and environmental conditions of these ships are shown in Tab 18 and 19.

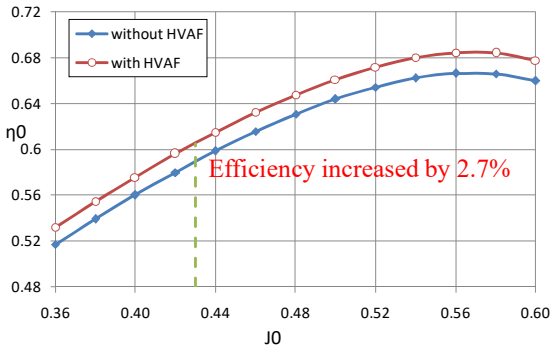

Figure 74 Open water efficiency of model test result with and without HVAF

Table 18 The sea trial drafts of HN1164 and its sister ships

Hull No.	Sea Trial Drafts			
	T_F (m)	T_M (m)	T_A (m)	Corresponding Disp. (tons)
HN1155	7.80	8.900	9.650	73959.30
HN1156	7.91	8.820	9.740	73975.20
HN1157	7.93	8.850	9.400	73674.06
HN1158	8.08	8.965	9.600	74877.80
HN1163	7.76	P 8.85/S 8.71	9.670	74634.00
HN1164	7.77	P 9.05/S 9.11	9.960	75583.80

Table 19 The environmental conditions of HN1164 and its sister ships

Hull No	Environmental Conditions				
	Geo-graphic Position	Wind Force	Wind Direc-tion	Sea Condi-tion	Depth
HN1155	East China Sea	4-5 Bft	NE	Douglas 3/4	Around 70m
HN1156	East China Sea	5 Bft	NW	Douglas 4	Around 70m
HN1157	East China Sea	3 Bft	SE	Douglas 2	Around 70m
HN1158	East China Sea	4 Bft	N	Douglas 3	Around 70m
HN1163	East China Sea	4-5 Bft	NE	Douglas 3	Around 70m
HN1164	East China Sea	2 Bft	SW	Douglas 1	Around 70m

With the correction of the wind, wave, tide, shallow water and still air condition of model test, the corrected results can be obtained as listed in Tab 20 without HVAF. From the results, it can be found that the displacement of each ship is different from the design condition. Thus, it is necessary to correct the displacement effect for each ship. According to ITTC Procedures and ISO 15016, the displacement effect can be corrected by Admiralty Coefficient Method. It is easy to find that the ship speed of each ship is quite different from each other, the difference between the highest one and the lowest one is about 0.456 knots. The averaged results of ship speed is 15.488 knots at service point.

Table 20 Ship speed of 114,500DWT bulk carrier without HVAF at service point

CSR with Sea Margin: P_D=MCR*0.85*0.985/1.15=11518kW						
Hull No.	T_F(m)	T_M(m)	T_A(m)	Displace-ment(t)	Vs (kn)	N(rpm)
Model Test	7.742	8.823	9.903	73716.36	15.080	98.27
HN1155	7.80	8.90	9.65	73959.30	15.670	98.58
HN1156	7.91	8.82	9.74	73975.20	15.214	99.73
HN1157	7.93	8.85	9.40	73674.06	15.678	100.58
HN1158	8.08	8.97	9.60	74877.80	15.349	99.45
HN1163	7.76	8.80	9.67	74634.00	15.411	99.44
Average	----	----	----	----	15.464	----

Table 21 Ship speed of 114,500DWT bulk carrier without HVAF after corrected for displacement

Hull No.	Model Test	HN1155	HN1156	HN1157	HN1158	HN1163	Average (Sea trials)
Vs (kn)	15.080	15.681	15.226	15.676	15.402	15.452	15.488

The HN1164 has been installed HVAF, and the sea trials has been carried. Passed through the wind and wave analysis, tide analysis and still air correction, the ship speed at service point before and after corrected displacement is shown in Tab 22. By analyzing the results, the ship speed with and without HVAF can be obtained. As for without correcting of displacement, the ship speed without HVAF is about 15.46kn, while it is about 15.60kn with HVAF. As for with correcting of displacement, the ship

speed with and without HVAF is 15.69kn and 15.49kn, respectively. Consequently, the ship speed has been increased 0.14kn and 0.20kn before and after displacement correction, respectively. As a result, it can be concluded that energy saving effect of HVAF based on sea trial results is about 3% to 5%, better than the model test results.

Table 22 Ship speed of HN1164 with HVAF after corrected for displacement

CSR with Sea Margin: P_D=MCR*0.85*0.985/1.15=11518kW						
Hull No.	T_F(m)	T_M(m)	T_A(m)	Displacement(t)	Vs (kn)	N(rpm)
HN1164	7.700	9.100	9.960	75583.80	15.60	101.05
Displacement Correction						
HN1164	7.742	8.823	9.903	73716.36	15.69	----

Table 23 Ship speed prediction under heavy ballast draft before displacement correction

Vs(kn)	P_S (η_S=0.985) Unit: kW							EN-ERGY SAV-ING
	Without PBCF						With PBCF	
	HN1155	HN1156	HN1157	HN1158	HN1163	AVER-AGE	HN1164	
14.5	8904.1	9779.6	8544.3	9682.0	9606.9	9303.4	8897.1	4.37%
15.0	10081.0	11091.9	9785.8	10870.5	10760.3	10517.9	10136.7	3.62%
15.5	11269.4	12467.4	11179.1	12068.2	11895.4	11775.9	11444.6	2.81%

Table 24 Ship speed prediction under heavy ballast draft after displacement correction

Vs(kn)	P_S (η_S=0.985) Unit: kW							EN-ERGY SAV-ING
	Without PBCF						With PBCF	
	HN1155	HN1156	HN1157	HN1158	HN1163	AVER-AGE	HN1164	
14.5	8879.3	9750.9	8548.6	9567.2	9512.4	9251.7	8710.7	5.85%
15.0	10055.2	11060.5	9790.8	10743.9	10667.9	10463.7	9922.3	5.17%
15.5	11242.1	12433.6	11184.9	11943.6	11795.6	11720.0	11222.4	4.24%

The shipowner of 180,000DWT bulk carrier "DA YUAN" provided the data of full scale ship operation in one year period. Based on these data with and without HVAF, the energy saving can be analysed. Statistical analysis was performed by excluding data from days of sailing in rough sea conditions. Based on full scale operation record data, the HVAF can save fuel consumption about 10% both loaded and unloaded conditions.

Table 25 The record results in no load condition

Project	criterion: all record data		criterion: only include the data of MOD SEA and SLT SEA	
	Without HVAF	With HVAF	Without HVAF	With HVAF
Day.	86	54	56	36
Total voyage (mile)	23321	14736	15313	10456
Total time（h）	1919.5	1203.1	1248	841
Average speed (kn)	12.15	12.25	12.27	12.43
Total Fuel consumption（t）	2724.3	1579.5	1754.2	1117.9
24 hour AV. Fuel consumption（t/d）	34.06	31.51	33.7	31.902

Table 26 Comparison with 12kn Fuel consumption average

Project	criterion: all record data		criterion: only include the data of MOD SEA and SLT SEA	
	Without HVAF	With HVAF	Without HVAF	With HVAF
Average speed (kn)	12.15	12.25	12.27	12.43
24 hour AV. Fuel consumption（t/d）	34.06	31.51	33.7	31.902
At 12 kn speed condition 24 hour AV. Fuel consumption（t/d）	32.53	29.19	31.03	28.00
Energy saving (%)	10.26%		9.78%	

- **PSV or PSD**

PSV is increasingly used in many hydrodynamic energy saving devices. Its energy-saving effect is also very significant. It can be used alone or together with HVAP, rudder bulb (RB) and high-efficiency propeller, etc., thus pursuing higher energy-saving effects. There are some full scale data of cases with PSV.

Table 27 Full scale data with PSV

No.	Ship		ESDs
Case1	1100TEU	1	PSV
Case2	298,000DWT VLCC	1	PSV
Case3	325K DWT VLOC	1	PSV+HVAF

Case4	210K B.C	1	PSV+HVAF
Case5	57000DWT B.C	6	PSV+HVAF
Case6	175K B.C	1	PSV+HVAF
Case7	180,000DWT B.C	1	PSV+HVAF+ LR Coating
Case8	230,000DWT Ore CARRIER	1	PSV+HVAF+ RB+PM

Both the 1,100 TEU and 298,000 DWT VLCC are fitted with PSV energy saving devices. Forecasts of laboratory model test results show that the energy-saving effect of PSV on container ships is only about 3%, while PSV on VLCC can reach 5% to 7%. There are 11 voyages number and 22 groups data without PSV, and 9 voyages number and 18 groups data with PSV. According to the full scale voyage data of 1,100 TEU, the fuel consumption is decreased 1.4t every 24h, the energy saving is about 4.5% with PSV. For the VLCC, the energy saving effect by fuel consumption is about 9.6%. For the energy saving effect of these two ships with PSV, the full scale results show the same trend as the model tests.

Table 28 Energy saving effect of PSV at design draught for 1100 TEU by model test result prediction

Load Condition	Speed V_S (kn)	Delivered power with TM19226A P_{DT0} (kW)	with TM19226A&PSV-A		with TM19226A&PSV-B	
			P_{DT1} (kW)	Energy saving 1-P_{DT1}/ P_{DT0}	P_{DT2} (kW)	Energy saving 1-P_{DT2}/ P_{DT0}
Design draft	12.00	1840	1784	3.0%	1786	2.9%
	13.00	2227	2160	3.0%	2154	3.3%
	14.00	2666	2584	3.1%	2575	3.4%
	15.00	3206	3105	3.2%	3097	3.4%
	16.00	3892	3771	3.1%	3767	3.2%
	17.00	4789	4652	2.9%	4649	2.9%
	18.00	6073	5908	2.7%	5907	2.7%
	19.00	8024	7784	3.0%	7801	2.8%
	20.00	10954	10579	3.4%	10622	3.0%
	21.00	15240	14699	3.5%	14749	3.2%

Table 29 Energy saving effect of PSV at design draught for 298,000 DWT VLCC by model test result prediction

	WITHOUT PSV		WITH PSV		ENERGY SAVING EFFECT
V_S(kn)	P_{DT}(kW)	N_T(rpm)	P_{DT}(kW)	N_T(rpm)	
11.5	7530	55.9	7008	54.0	6.93%
12.0	8522	58.4	7990	56.3	6.24%
12.5	9607	60.9	9042	58.7	5.88%
13.0	10774	63.3	10177	61.0	5.54%
13.5	12059	65.6	11370	63.2	5.71%
14.0	13500	68.1	12727	65.6	5.73%
14.5	15071	70.6	14178	68.0	5.93%
15.0	16834	73.2	15790	70.5	6.20%
15.5	18808	75.8	17541	73.0	6.74%
16.0	20997	78.6	19503	75.6	7.12%
16.5	23411	81.3	21630	78.2	7.61%
17.0	26042	84.0	23963	80.7	7.98%

Table 30 Fuel consumption for 1100 TEU with and without PSV

Proj.	Average speed (kn)	24 hour AV. Fuel consumption (t/d)	Average Loading	Corrected the same loading and speed of fuel consumption (design draft/14.5kn)
Without PSV	14.2kn	29.4t/24h	4582t	31.3t/24h
With PSV	14.5kn	29.1t/24h	3959t	29.9t/24h
Diff.	+0.3kn	-0.3t/24h	-623t	-1.4t/24h

Table 31 Fuel consumption for 298,000 DWT VLCC with and without PSV

Average data	Energy Efficiency Upgrade		Remarks
	Before	After	
F. O. C(13.00kn, T=20.0m) (tons/24hour)	75.09	67.91	PSV
$Energysaving Effect = \left(1 - \frac{F.O.C_{ESDs}}{F.O.C_{NO\ ESDs}}\right) \times 100\%$	9.6%		

For the difference between the model test prediction results and the full scale sea trial results, both 325K DWT VLOC and 210K B.C give comparative results. The prediction result of ITTC method is lower than SINTEF Ocean method about 0.16kn，the sea trail result in the middle of the prediction results. The effect of input data of environments is significant，so environment parameter of the sea trail is very importance. The results of the full scale of these two ships with sea state corrections were closer to the model test prediction.

Table 32 The prediction results with different towing tank method for 325K DWT VLOC

CSR, 15%S.M		Prediction fullscale		
Condition	ESD	SINTEF Ocean method	ITTC method +prop. correc-tion	Diff.
Ballast	PSV+HVAF	16.16kn 56.7rpm	16.00kn 56.9rpm	-0.16kn +0.2rpm

Table 33 The sea trial results with different input condition of environments for 325K DWT VLOC

CSR, 15%S.M		Sea trail results		
Condition	ESD	Input data （Wave 1.0m、tide 1.5m）	Input data （Wave 0.5m、tide 0.6m）	Diff.
Ballast	PSV+HVAF	16.12kn 57.2rpm	15.89kn 57.2rpm	-0.23kn +0.0rpm

Table 34 Model test prediction results & sea trail results for 210K B.C

		Vs(kn)	N(rpm)	LRM(%)
Design draft	Model	14.59	66.0	7.5%
	Sea trail	14.62	67.0	9.1%
Scant-ling draft	Model	14.05	65.7	7.1%
	Sea trail	14.08	66.8	8.8%

57000DWT B.C has six sister vessels with PSV and HVAF, four of which have good sea trail data. The unit energy consumption is significant effected by the loading. So the full scale ship energy saving value should be compared in the same loading condition. According to the full scale ship record results, the unit consumption of heavy fuel can be calculated for different voyage actual data and plotted the figure of “loading- unit consumption of heavy fuel”. From these results, using the unit consumption heavy fuel of the same loading condition, the energy saving is significant. The fuel consumption are decrease from 8% to 20%. The full scale sea trail result indicate that 175K DWT B.C also has 15.5% energy saving effect for fuel consumption with PSV and HVAF.

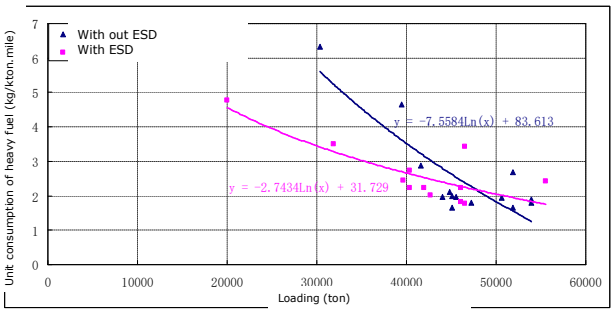

Figure 75 Loading- unit consumption of heavy fuel of “Pulan Sea”

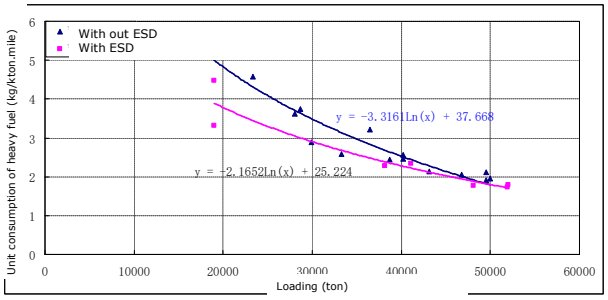

Figure 76 Loading- unit consumption of heavy fuel of “Daishan Sea”

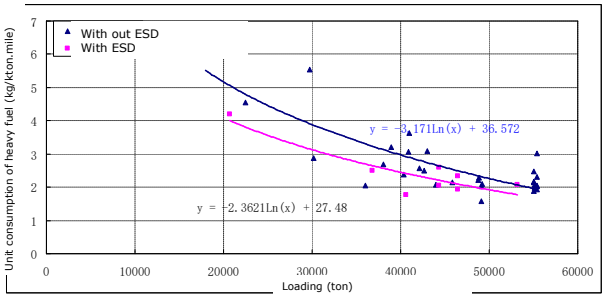

Figure 77 Loading- unit consumption of heavy fuel of “Hengshan Sea”

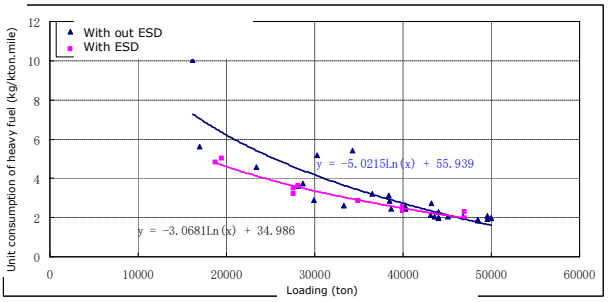

Figure 78 Loading- unit consumption of heavy fuel of “Changshan Sea”

Table 35 The fuel consumption compared with and without PSV + HVAF for 175K DWT B.C

	Without ESD	With ESD	Energy saving (%)
Total mileage recorder (mile）	46137	10834	/
Total time（h）	3834.9	796	
speed（kn）	12.03	13.61	
Total fuel consumption（T）	5467.50	1388.2	
Average day fuel consumption（T/day）	34.22	41.86	
Calculated 13kn Average day fuel consumption (T/day)	43.17	36.47	15.5%

It is common to ask whether repeated applications of energy-saving devices ahead and behind the propeller are in direct superposition energy saving effect to each other. The 180K DWT B.C could not meet the standard in the EEXI assessment, so PSV, HVAF and LR Coating were used. The model test results indicate that PSV and HVAF can increase efficiency 5.4% and 2.5%, respectively. LR Coating can saving energy 4%. Real ship data realistic combined fuel consumption assessment energy savings of 21.6%. The 230K DWT Ore Carrier used multiple energy-saving devices include PSV, Rudder Bulb and HVAF. The model test results show that the energy saving effect can obtain 9% and 10% at design and ballast condition. The full scale data give the same tendency on fuel consumption. The energy saving effect of ballast is slightly better than design draught.

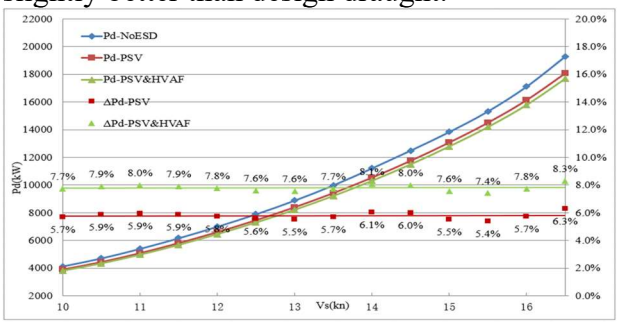

Figure 79 Model test verification the total energy saving effect of 180K DWT B.C

Table 36 The fuel consumption compared with and without ESDs for 180K DWT B.C

Average data	Energy Efficiency Upgrade		Remarks
	Before	After	
F. O. C(11.00kn, T=17.45m) (tons/24hour)	39.90	31.30	PSV+HVAF +LR Coating
$EnergysavingEffect = \left(1-\frac{F.O.C_{ESDs}}{F.O.C_{NO\ ESDs}}\right)\times 100\%$	21.6%		

Figure 80 Energy saving model test of 230K DWT Ore Carrier

Table 37 Model test results for 230K DWT Ore Carrier at design condition

without ESD			with PSV		with PSV + Rudder Bulb		with PSV + HVAF + Rudder Bulb	
Vessel Speed	Delivered Power	Rotational Speed	Power Difference	Energy Saving	Power Difference	Energy Saving	Power Difference	Energy Saving
Vs (kn)	PDT0 (KW)	N_{s0} (r/m)	P_{DT1}-P_{DT0} (KW)	ΔP_{DT1} (%)	P_{DT2}-P_{DT0} (KW)	ΔP_{DT2} (%)	P_{DT3}-P_{DT0} (KW)	ΔP_{DT3} (%)
11.0	6033	51.9	-274	4.5%	-343	5.7%	-513	8.5%
11.5	6916	54.2	-336	4.9%	-424	6.1%	-618	8.9%
12.0	7884	56.6	-404	5.1%	-511	6.5%	-732	9.3%
12.5	8940	58.9	-478	5.3%	-603	6.7%	-853	9.5%
13.0	10088	61.4	-550	5.4%	-695	6.9%	-977	9.7%
13.5	11328	63.8	-620	5.5%	-780	6.9%	-1097	9.7%
14.0	12667	66.3	-695	5.5%	-873	6.9%	-1227	9.7%
14.5	14108	68.8	-776	5.5%	-970	6.9%	-1365	9.7%
15.0	15701	71.3	-848	5.4%	-1056	6.7%	-1495	9.5%
15.5	17514	74.0	-880	5.0%	-1100	6.3%	-1592	9.1%
16.0	19582	76.7	-857	4.4%	-1081	5.5%	-1636	8.4%

Table 38 Model test results for 230K DWT Ore Carrier at ballast condition

without ESD			with PSV		with PSV + Rudder Bulb		with PSV + HVAF + Rudder Bulb	
Vessel Speed	Delivered Power	Rotational Speed	Power Difference	Energy Saving	Power Difference	Energy Saving	Power Difference	Energy Saving
Vs (kn)	PDT0 (KW)	N_{s0} (r/m)	P_{DT1}-P_{DT0} (KW)	ΔP_{DT1} (%)	P_{DT2}-P_{DT0} (KW)	ΔP_{DT2} (%)	P_{DT3}-P_{DT0} (KW)	ΔP_{DT3} (%)
11.0	4805	47.1	-324	-6.7%	-396	-8.2%	-528	-11.0%
11.5	5494	49.3	-352	-6.4%	-421	-7.7%	-573	-10.4%
12.0	6266	51.5	-390	-6.2%	-460	-7.3%	-635	-10.1%
12.5	7130	53.7	-443	-6.2%	-522	-7.3%	-720	-10.1%
13.0	8097	56.0	-515	-6.4%	-611	-7.5%	-835	-10.3%
13.5	9169	58.3	-604	-6.6%	-726	-7.9%	-980	-10.7%
14.0	10346	60.7	-695	-6.7%	-836	-8.1%	-1122	-10.8%
14.5	11627	63.2	-774	-6.7%	-920	-7.9%	-1241	-10.7%
15.0	13069	65.7	-869	-6.7%	-1024	-7.8%	-1385	-10.6%
15.5	14757	68.4	-1019	-6.9%	-1217	-8.2%	-1623	-11.0%
16.0	16633	71.1	-1164	-7.0%	-1417	-8.5%	-1874	-11.3%

Table 39 The fuel consumption compared with and without ESDs for 230K DWT Ore Carrier

Average data	Energy Efficiency Upgrade		Remarks
	Before	After	
F. O. C(13.00kn, Design draft) (tons/24hour)	65.36	55.51	Hull fouling is in good condition before Energy Efficiency Upgrade PSV+HVAF+RB+PM
$EnergysavingEffect = \left(1-\frac{F.O.C_{ESDs}}{F.O.C_{NO\ ESDs}}\right)\times 100\%$	15.1%		
F. O. C(10.50kn, Ballast draft) (tons/24hour)	33.00	27.43	
$EnergysavingEffect = \left(1-\frac{F.O.C_{ESDs}}{F.O.C_{NO\ ESDs}}\right)\times 100\%$	16.9%		

From the comparison of model test and real ship data from several ships regarding the use of

energy saving devices, the energy saving effect of the full scale is usually higher than the results of the model test.

Table 40 Summary comparison of model tests and real ship data with ESDs

No.	Ship type	ESDs and HEP	Model test results	Real ship results
1	230k Ore Carrier	PSV, HVAF, RB,PM	9.7% at design draft 10.7% at ballast draft	15.1% at design draft 16.9% at ballast draft
2	57k Bulk Carrier	PSV, HVAF,PM	5.6% at scantling draft 6.6% at ballast draft	8.3% at scantling draft 16.5% at ballast draft
3	92.5k Bulk Carrier	PSV, HVAF,PM	6.6% at scantling draft 6.7% at ballast draft	11.1% at scantling draft 12.1% at ballast draft
4	53k Bulk Carrier	PSV, HVAF	6.2% at design draft	19.8% at design draft 23.9% at scantling draft
5	3300m3-LPG	HEP, HVAF	12.5% at design draft	about 10.0% at design draft
6	298k-VLCC	PSV	5.6% at scantling draft 5.9% at design draft 7.5% at ballast draft	about 9.5% at laden draft
7	298k-VLOC	PSV, HVAF, RB, LR	12.6% at scantling draft 12.4% at ballast draft	31.9% at scantling draft 36.9% at ballast draft
8	26k Bulk Carrier	HEP, HVAF	about 6.0% at design draft	10.8~11.8% at design draft
9	82k Bulk Carrier	PSV, LR	11.4% at scantling draft	13.9~27.5% at laden condition 14.9~19.7% at ballast condition
10	180k Bulk Carrier	PSV, HVAF, LR	11.1% at scantling draft	21.6% at laden condition

17.5 Innovative Energy-saving Technology

CMES-Tech company provided some full-scale data of the benefits of ALDR about their research works. The research on ALDR technology begins with a laboratory flat plate drag study to analyse the effect of air layer structure on drag reduction. Then, some test studies of the ship model are carried out in the towing tank to consider the effect of the hull line shape. After verifying the function and energy-saving effect of the ALDR system through a large-scale prototype vessel test on the lake. Finally, the energy-saving effect under different working conditions is analysed through the test on the full scale ship.

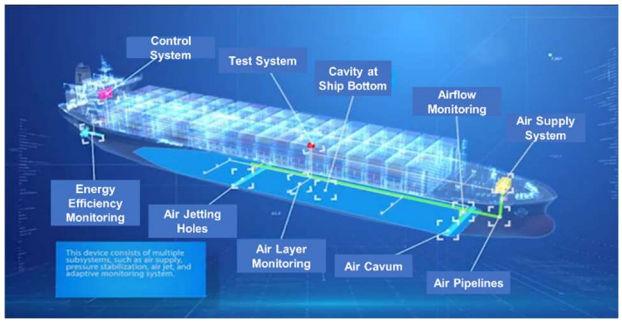

Figure 81 Air Layer Drag Reduction System (ALDR System，CMES-ALESS)

Table 41 Achieved technical index

Research Stage	Research object	Research Result
Principle Research	Flat plate model	Sigle side Friction resistance reduction was more than 60%.
Ship Model Research	Ship model	The typical drag reduction rate was about 50%.
Lake Test Research	100 ton class principle sample ship	① The typical net energy saving was about 18% within the applicable speed range; ② The net energy saving was more than 11% at designed condition.
Ship Utilization Research	Big flat plate model	The relative drag reduction rate was over 90% in the air layer covered zone.
Full Scale Ship Verification	432TEU Full scale ship	The net energy saving effect was more than 7%.
	334TEU Full scale ship	The net energy saving effect was more than 8%.

Designed and developed a 100 ton principle sample ship of the air resistance reduction principle. The application object is for 95,000 ton bulk carrier with a scaling ratio of 1:10. Within the applicable speed range, the typical energy-saving effect is 18%. Under the design draft and design speed, the energy-saving effect is more than 11%.

Figure 82 ALDR principle sample ship on lake

Table 42 Results of lake test results of ALDR

Ship Speed	Shaft Power-without ALDR	Shaft Power-with ALDR	Power of Air-jet	Net Energy Saving Effect
kn	kW	kW	kW	%
1.50	0.678	0.466	0.131	-11.95%
2.00	1.019	0.734	0.131	-15.11%
2.50	1.534	1.156	0.131	-16.10%
3.00	2.308	1.822	0.131	-15.38%
3.50	3.473	2.482	0.502	-14.08%
4.00	5.225	4.01	0.502	-13.65%
4.50	7.862	6.478	0.502	-11.22%
5.00	11.829	10.465	0.502	-7.29%
5.20	13.929	12.678	0.502	-5.38%

The ALDR system was applied to two real ships, 400 TEU and 334 TEU open container ship. The speed and shaft power obtained under the fixed engine speed N=390rpm and different air jet flow for 400TEU. The net energy-saving

effect under the best air injection flow is 12.5%. For 334 TEU ship, the energy savings were tested at different speeds with optimal ventilation and obtain above 7%.

Figure 83 ALDR applied on 400TEU container ship

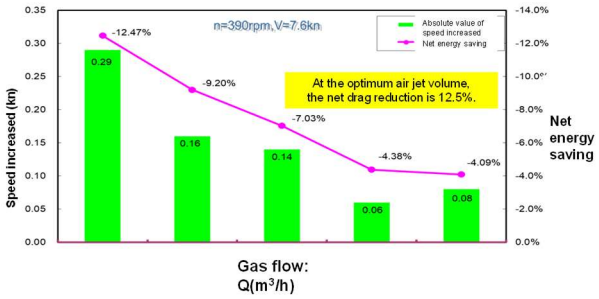

Figure 84 Speed and shaft power curve obtained under different jet volume for 400TEU

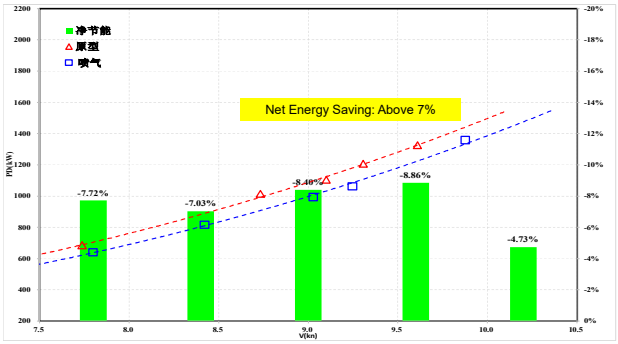

Figure 85 Full scale test result for 334TEU

Wind-assisted rotor, wind sail and seawing have been used on full scale ship. MEPC report indicate that the wind energy saving technique normally can obtain about 5%~20% energy saving. By statistical data of International Wind ship Association (IWA), there were 21 ships using the wind energy saving until third quarter of 2022. The data become to 49 ships to the end of 2023.

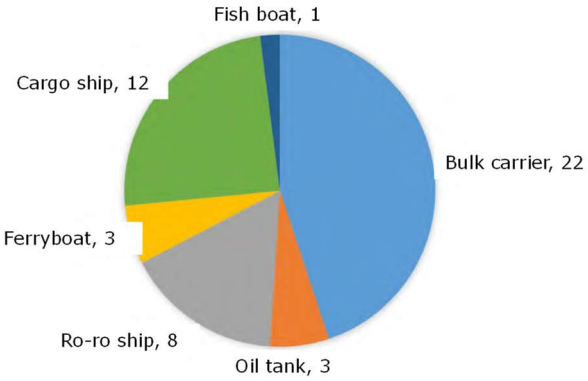

Figure 86 Using the wind energy saving ships

Figure 87 “E-Ship”-2010 and “Afros”-2018

In 2023, 45000DWT bulk carrier with four units wind-assisted rotor, the full scale sea trails have been finished at East sea of CHINA. The diameter of rotor is 2.9m and the total height is 21.6m. The max rotation speed of rotor is 280 r/min. The sea trail test content include the rotor with turn on and turn off condition. In ballast condition, wind speed is 12m/s, wind direction is 55° , the speed can be increased abt. 0.7kn. Converting into the same speed condition, the main power can be decreased more than 15%. In full load condition, wind speed is 22m/s, wind direction is 50° , the speed can be increased abt. 1.0kn. The main power can be saved abt. 30%.

Figure 88 Wind-assisted rotor of 45000 DWT B.C

Table 43 Sea trail results of 45000 DWT B.C with Wind-assisted rotor

NO.	Wind direction	Wind speed	Main Eng. Rotation speed	PD	Vs	ΔVs	Wind-assisted rotor	Rotor speed	Rotor consumed PD	Energy saving by speed increasing	Decreasing of shaft power	Consumed power	Net energy saving
	(°)	(m/s)	(r/min)	(kW)	kn	kn	ON/OFF	(r/min)	(kW)	%	%	%	%
1	56.7	11.7	95.1	3284	13.83	--	OFF	0	0.0				
	55.2	12.6	95.0	3208	14.71	0.74	ON	260	107.2	20.4%	2.3%	3.3%	19.4%
2	54.3	11.3	95.0	3261	13.97	--	OFF	0	0.0				
	52.5	11.7	95.1	3182	14.72	0.75	ON	208	62.2	17.0%	2.4%	1.9%	17.5%
3	47.7	11.3	95.0	3281	14.65	--	OFF	0	0.0				
	59.6	10.6	95.1	3178	15.36	0.70	ON	160	33.8	15.1%	3.1%	1.0%	17.2%
4	50.1	12.2	95.1	3318	14.69	--	OFF	0	0.0				
	51.6	12.3	95.1	3250	15.40	0.72	ON	160	36.2	15.2%	2.0%	1.1%	16.1%
5	53.5	11.3	95.0	3302	14.68	--	OFF	0	0.0				
	55.2	10.9	95.1	3185	14.96	0.31	ON	115	17.6	5.9%	3.5%	0.5%	8.9%

17.6 Scale Effect Research of ESDs

It is short of the model test and CFD calculation results, and compared with full scale data. Especially, it is difficult to obtain enough the full scale data when the shipyard makes the sea trial. In order to research the scale effect, the special test ship is necessary. But the full scale ship is too expensive. A mid-scale test ship can be used to do some research about the scale effect of energy saving technique. CSSRC carried out a project of "mid-scale" test ship. The "mid-scale" model tests on optimized hull lines, propeller. Model was equipped with reconfigurable ESD (pre-shroud vanes, hub vortex absorber, etc.). The particulars of the ship are L=55m, B =10m, *disp*.=1500t and speed 10knots at maximum. It can be equipped with propeller hub fins, replaceable: rudder, ESD, wind assisted rotor, air layer system. Geometry is close to VLCC under waterline. Stereo PIV measurement was carried out through the windows installed in the aft part. It is equipped with whole ship system, with the monitoring all the devices including ship route and speed optimization systems. SMART operating system was developed and ship was ready for remote control. Ship was launched 20/7/2023 and sea trials were carried out on September 2023. There were four combinations of installed ESD tested. The difference of the results between repeat tests was within the range of 1%. Turning circle tests were carried out and compared with model tests and simulation. The manoeuvring indices were compared and the influence of ESD on these indices was noticed. Further the smart operation system was tested in operation on fully remote vessel. Additional tests are planned to continue the study on the scale effect.

Figure 89 "Mid-scale" test ship

Figure 90 Carried out multiple exchange of ESDs on "Mid-scale" test ship

17.7 Conclusions

There are difficulties in comparing the effectiveness of ESD (Energy Saving Device) between model scale and full scale data due to environmental conditions during sea trials. Additionally, assessing the effectiveness of ESD in service is challenging due to uncontrolled differences in loading conditions between ships with ESD and ships without ESD.

Deep water towing tank test is the most commonly using and effective method to verify ship energy consumption. It has been verified by the actual ship operation that the hydrodynamic energy efficiency upgrade can improve the ship speed and save fuel for the main engine. It is proved that this model test is feasible.

For the operating ships, the combination of energy saving technologies such as Propeller Modification (PM), High Efficiency Propeller (HEP) and Energy Saving Devices (ESDs) can save energy consumption by more than 10%.

The energy-saving effect of real ship operation may be affected by sea conditions (such as wind, wave and current) and hull fouling conditions, and most of them are better than the results of model test.

It is necessary that more full-scale data of ALDR would be collected. Some detail influence factor should be analysed such as ship motion, wave and ship speed.

The wind-assisted rotor can obtain significant energy saving from the full scale sea trail results. It has bright future. But it is short of the model test and CFD calculation results, and compared with full scale data.

In the future, it is necessary for preparing a guideline on survey of energy saving methods for the performance of this systems in sea trials and operational conditions.

18. NEED FOR NEW PROCEDURES FOR EVALUATING SMART SHIP PERFORMANCE

18.1 Overview

Autonomous, unmanned, or smart ship technology holds promise in the commercial maritime industry due to potential improvements to safety and efficiency as well as reduced operating costs. Development of these technologies relies upon the ability to conduct tests and trials to validate predictions and demonstrate real-world performance. Existing ITTC trials procedures, notably RP 7.5-04-01-01.1, are agnostic to the method of vessel control, be it manned or unmanned. The question, therefore, is whether any gaps exist within ITTC trials procedures, unique to unmanned or autonomous ships, which are not already addressed through existing international regulatory policy.

18.2 IMO Maritime Autonomous Surface Ship (MASS) Code

In recognition of the unique safety and security issues associated with the trials of Maritime Autonomous Surface Ships (MASS), IMO issued Interim Guidelines for MASS Trials in MSC.1/Circ. 1604 (IMO, 2019). The Maritime Safety Committee (MSC) intends to adopt a non-mandatory, goal-based MASS Code to take effect in 2025. The non-compulsory code would serve as the basis for a mandatory, goal-based MASS Code expected to enter into force on 1 January 2028. The Interim Guidelines provide recommendations related to risk management, compliance, manning and qualification, human factors, infrastructure, and communications.

Regarding risk management, the Interim Guidelines address the specific risks to safety, security, and the environment. Risk identification and controls are recommended to reduce risks to acceptable levels. Contingency planning is suggested to mitigate the impacts of incidents or failures. Adequate notifications should be provided to outside parties who may be impacted by MASS trials and any associated incidents or failures. Finally, safety should be evaluated throughout trials and testing must be stopped when safety controls lose effectiveness.

Onboard or remote operation of the MASS vessel during trials should be only by qualified personnel. All personnel involved in the trials should be adequately qualified and familiar with MASS trial safety procedures. Trial planning should address the human-system interface as well the provision of adequate monitoring infrastructure to ensure that MASS trials can be conducted safely and securely.

Monitoring capabilities for all personnel should provide information regarding the performance of the vessel and the decision-making process for automated systems. Communication systems should support data and voice communications to ensure safe execution of testing and consideration of redundancy of these systems is recommended. Cyber security of the monitoring and communications systems, as well as other test infrastructure, should be considered as part of a holistic risk management process.

In summary, the Interim Guidelines for MASS Trials provide enhancements to the trial planning and execution processes to address the unique aspects of operation and testing of unmanned or autonomous vessels. The recommended guidance does not directly impact or change how S/P trials are conducted in accordance with RP 7.5-04-01-01.1.

18.3 International Network for Autonomous Ships (INAS)

The International Network for Autonomous Ships (INAS) was informally organized in 2017 as an outgrowth of the Norwegian Forum for Autonomous Ships (NFAS) (Rødseth, 2022a). The charter of the organization is to act as a forum for the retention and dissemination of information of common interest regarding unmanned, autonomous, and smart ships. SINTEF Ocean currently serves as the organization's secretariat. As of 2024, INAS is comprised of nearly 20 members or prospective members from Asia, Australia, Europe, and North America.

INAS maintains a listing of known autonomous ship test areas (Rødseth, 2022b). As of 2024, the autonomous ship test areas are in Belgium, Finland, Netherlands, Norway, the United Kingdom, and the United States. Additional test areas or research facilities that can support autonomous ship research are located in Germany and Italy.

In addition to consolidating information regarding autonomous ship test areas, INAS also maintains a repository of guidelines for MASS trials. These include various national policies, EU and IMO guidelines, as well as voluntary practices suggested by INAS itself. INAS and its progenitor, NFAS, currently serve as de facto coordinators of MASS testing guidance and policy in the absence of compulsory rules.

18.4 Conclusions

Trials of MASS vessels are typically focused on autonomous navigation and autonomous behaviours as these aspects set them apart from manned surface ships. While MASS trial procedures may incidentally coincide with the techniques utilized for S/P trials, this is expected to be the exception and rarely the purpose for MASS trials. IMO Interim Guidelines for MASS Trials do not fundamentally impact the test procedures or methodology utilized to conduct ship S/P trials. It is therefore recommended that FSSPC continue to monitor developments in IMO MASS policy, with compulsory rules expected to enter into force in 2028, as well the MASS testing guidance cultivated by INAS and NFAS.

19. CONCLUSIONS AND RECOMMENDATIONS TO THE 30TH ITTC

19.1 Main Conclusions

a) Task 1 A)
Literature survey has conducted on the application of data-driven approaches.
AI technologies can be useful and effective tools to analyze the huge volume of ship operational data and solve complicated problems such as validating the energy efficiency performance of ships, the modelling and prediction of wave added resistance of ships in the seaway, the on-line prediction of ship maneuvering behavior for collision avoidance, the monitoring of fouling and aging influence, etc.
It can be expected that there will be more and wider AI applications concerning full scale ship performance in the future.

b) Task 1 B)
Measuring techniques for waves in speed/power trials are reviewed through literature survey.

c) Task 1 C)
It is considered that MARIN's JoRes ship-scale test cases data to be published in December 2024 are most relevant to meet this

TOR task, in particular, thanks to its coverage of ship types, 3D configurations, ESDs, roughness measurements.

d) Task 1 D)
It is found that the reliability of full-scale CFD simulation results have remained quite low compared to that of model-scale results mainly due to the lack of sufficient full-scale validation data, and that performance prediction based on full-scale CFD simulation results is not practically feasible at present.

e) Task 2 A)
Survey on the requirements for changes in the light pf current practice has conducted through the questionnaire to ITTC member organizations for the revision of R.P. 7.5-01-01-01.1.

f) Task 2 B)
Needs for the new procedures for examining the full-scale effects of energy saving methods, hull/propeller surface roughness are identified.
Need for the revision of guideline for evaluating Air Lubrication System by introducing the modelling of system's parameters for air injection is identified.

g) Task 3 A)
Effect of roughness wave lengths have significant effect on added resistance due to roughness. This effect should be included in the full-scale ship performance predictions.
Non-uniformity of roughness distribution over wetter surface has significant effect on added resistance due to roughness. This effect should be included in the full-scale ship performance predictions.
Roughness height should preferably be treated in relation to the local thickness of viscous sublayer since the only part of roughness emerged from the viscous sublayer contribute in the added resistance.

h) Task 3 B)
Hydrodynamic properties of macro biofouling including newly coated surfaces have been clarified sufficiently. However, those of micro biofouling, in particular, slimes have not been fully elucidated. Since micro biofouling is most frequently encountered roughness in both speed/power trials and operations, those roughness components should be thoroughly addressed in the future.
Coating materials and ambient environmental conditions have significant influence on the growth of biofouling and resulting increase in hydrodynamic resistance. These issues should be thoroughly addressed in the future.

i) Task 3 C)
State of the art of the measurement of roughness has reviewed.
Comparison has made on the surface roughness measurements using both contact and non-contact type instruments.

j) Task 3 D)
Full-scale performance deterioration due to roughened hull and propeller surfaces have studied extensively using roughness functions derived from both CFD simulations and model experiments. However, validation of the predictions is decisively scare due to the non-availability of appropriate full-scale data.
Rigorous validations of the full-scale predictions are indispensable for the development of practically reliable procedure for evaluating roughness effects on in-service performance.

k) Task 3 E)
A prediction method developed in the Japanese cooperative research project (OCTAVIA) was reviewed. It is shown through case studies that the impact of roughness on propulsion performance can be assessed quantitatively if roughness can be expressed as an increase ratio in resistance or a deterioration rate of propulsion efficiency.

l) Task 4
The review for revision of ISO19030-2016 conducted in 2021 resulted in a major vote to leave ISO 19030:2016 unchanged. Thus, a new edition of ISO 19030 may not be published until 2029.

m) Task 5 A)
The committee members were invited to contribute to the validation of the method by conducting full-scale trials in shallow (and deep) waters. An emphasis was put on other parties than the developer of the method (MARIN), which has already provided validation within its publications. Organizing such dedicated systematic trials on commercially operated ships has proven difficult, and no new results from trials were delivered or collected.

n) Task 5 B)
The validation result of the SNNM method regarding the accuracy of its predicted mean wave added resistances in irregular waves based on a database comprised of 23 ships of various types shows that the Pearson correlation coefficient R=0.919 was achieved for all gathered data between the SNNM predictions and the benchmark data.
Further investigation based on binned wave headings shows that the SNNM method performs best in head waves (R=0.972), while its performance may be compromised in beam to following waves (R=0.713). It must be emphasized that the treatment of the extrapolation of wave added resistance QTFs in the very short-wave range plays an important role in the spectral analysis results. It is desirable to carry out further investigations concerning this issue.
Comparison of SNNM, SPAWAVE and SNU methods also reveal larger discrepancies in the short-wave period range. Moreover, the three methods have large discrepancies in stern quartering and following waves. SNU and SNNM methods are comparable except in the short waves range, while the SPAWAVE method tends to overpredict and shows larger deviations in short waves.
Another validation work using 8 ship types compared the wave added resistance QTFs obtained from the NMRI, SNNM-SNU methods and the experimental methods. The NMRI method shows very good agreement with input of more detailed hull-form data. This clearly implies that detailed hull form data is essential to improve the accuracy of added resistance predictions.

o) Task 5 C)
The resistance due to drift and rudder is small at designed speed, and influence to speed trial analysis is limited. On this stage, additional correction by the resistance due to drift and rudder is not needed.
Results of model tests with quality controlled carried showed that the tendency of added resistance in very short waves is almost constant. The effect of the tendency of added resistance in very short waves is remarkable in irregular waves. Until sufficient validation would be completed, it is recommended that the added resistance in short waves is treated as a constant value for the analysis of speed trial.
The wave height effect is difficult to be included in the conventional spectrum method. Considering the wave height at the actual speed trial, the wave height effect can be negligible.

p) Task 5 D)
From literature review, including Raven's full report, it was concluded that the total propulsion efficiency is expected to remain relatively unaffected within the application range of the correction method. Raven's study on different ships showed the thrust deduction factor t increases, but only for very shallow water (outside the method's application range). No clear trend was found within the application range. The wake fraction is more sensitive to shallow water effects within the application range, with (1-w) decreasing for shallower water.

However, no usable approximation for all ship types is found yet. The changes in thrust deduction and wake fraction combined lead to a rise in hull efficiency. On the other hand, the propeller open water efficiency is expected to drop due to the increased resistance, (and thus higher propeller loading) and a reduced inflow speed (due to the increase of the wake fraction). This counteracts the rise in hull efficiency, leading to a small overall change in propulsive efficiency ETA_D.
Based on several test cases, it was concluded by Raven that assuming an unchanged propulsive efficiency ETA_D showed better merit. For the relative rotative efficiency no clear indication is found on the effect of shallow water. While large changes to the wake field may occur at very shallow water, the effect within the trial application range is expected to be minor.
It is recommended to continue monitoring the research efforts in this field in the future.

q) Task 5 E)
Survey on new developments in measurements of wind and propeller thrust has examined has conducted.

r) Task 6
It is considered that MARIN's JoRes ship-scale test cases data to be published in December 2024 are most relevant to meet this TOR task in collecting and processing data on the ship in-service performance of interest to ITTC.
Survey to ITTC member organizations regarding the provision of their full-scale data to this TOR task was conducted. 1 organization (SVA Potsdam) has contributed full-scale speed/power trails results for 7 ships.

s) Task 7
Accuracy of CFD for shallow water applications mainly concerning the shallow-water effect on self-propulsion factors is examined by the literature. But, due to the scarcity of the published works, sufficient examination of the issue has not been conducted.

t) Task 8 A)
Based on the outcome from Task 5 C). It is decided that there is no need to update the procedure in this regard.

u) Task 8 B)
The Wind averaging method increases the uncertainty of ship's performance estimation in wind changing condition. Therefore, to directly derive wind speed and direction from each run, the utilize of Lidar or CFD pre-checking method to find proper anemometer positions could be used.

v) Task 9
The situation of ISO/TC 8/SC 6/WG 17 for revising ISO15016 has carefully followed, and some members have participated as experts in the WG so that ISO15016 can be updated in compliance with 7.5-04-01-01.1.
However, 1st DIS voting of the ISO15016 revision conducted from 25 September to 18 December 2023 resulted in the disapproval od 1st DIS.
Regarding the future schedule of the revision, it was reported that the TC 8/SC 6 Chairperson will choose from three options (2ndDIS, 2ndCD or Cancel) based on the discussions in the TC by March 12th and the Project Leader has to submit necessary materials to contribute to the TC 8/SC 6 Chairpersons ahead of the deadline of the revision.

w) Task 10
AC Working Group in principally responsible for this task and preparing the update. It is requested by AC that, after receiving proposal on the update from AC Working Group, FSSPC should prepare a new guideline on parameters for full-scale power predictions. But their work could not be conducted since AC Working Group has not provided their proposal to FSSPC. After that, AC Working Group submitted the proposal of a new guideline independently to AC

without the support of this committee due to the change of AC' policy.

x) Task 11
The guideline on CFD-based wind coefficient has revised according to the new procedure for non-dimensioning.

y) Task 12
Literature survey on the relevant techniques for ship energy saving has conducted.
A complementary metric to EEDI to represent power savings by Air Lubrication System (ALS) has examined, and issues for the future revision have clarified.

z) Task 13
Literature survey on full-scale data on the effect of energy saving methods (ESM) has conducted.
Data on the energy saving effects for a variety of ESMs have collected.

aa) Task 14 C)
State of the art of the procedures of experiments and simulations to evaluate performance of smart ship and unmanned surface vehicles has reviewed through literature survey.

19.2 Recommendations to the Full Conference

a) Adopt the revised Procedure 7.5-04-01-01: Preparation, Conduct and Analysis of Speed/Power Trials (2024)
b) Adopt the revised Guideline on the CFD-based Determination of Wind Resistance Coefficients (2024)

19.3 Recommendations for future work

1. To continue further works on update guideline for correlation factors

2. To employ outcomes from the JORES projects as benchmark data for study of full-scale performance

3. To focus on short waves issue and further investigation of QTF extrapolation method in short waves for the evaluation of added resistance

4. To conduct sensitivity study on influence of discrepancies in evaluation of added resistance on final corrections to the sea trials; study how it affects final speed-power curves

5. To carry out the comparison of validated methods on the larger set of ship types by using real ship parameters; It may be addressed to organisations not only performing model tests.

6. To consider possibility to make selection among the methods for wave correction in speed/power trials depending on the availability ship form data

7. To investigate cases when wind is sideways in head/following waves to find the necessity of correcting the issue of ship running with stable drift angles

8. To monitor and explore further measurement techniques applicable in speed/power trials and in-service monitoring: Lidar wind, thrust and wave spectra.

9. To conduct a validation of CFD based full-scale performance prediction method using full scale data

10. To perform CFD calculations for various ship types to determine the optimum anemometer position in speed/power trials.

11. To preform comparative study of influence of directional energy spreading on the wave correction in speed/power trials

12. To update database of wind resistance coefficients and validate them by using the new method included in the guideline on the use of CFD-based determination of wind resistance coefficient

13. To collect the full-scale data to evaluate the frictional resistance reduction by air lubrication system and validate correlation of actual reduction rate (ADR) and estimated reduction rate (EDR) to predict performance at full loading conditions

14. To evaluate the correlation line between the model scale and full scale friction resistance with working ALS by the CFD methods

15. To evaluate the model test procedure for flat plates (instead of method proposed in the guideline) at different Reynold numbers to find the correct α value extrapolation; standardize the injection pressure and flow rate scaling approach

16. To extend the sea trials procedure to include new metrics such as ADR and EDR, along with the methodology of measurements

17. To develop a guideline to conduct full scale performance evaluations for energy saving methods (ESM)

18. To continue monitoring the performance of energy saving devices (ESD) to collect more data to reduce the influence of weather conditions on their performances

19. To establish new committee for bio-fouling related roughness issues to cope with the fundamental issues elucidated by the committee.

20. To continue monitoring effect of roughness and analyse method for evaluating ship performance in service

21. To investigate the drift angle consideration in added wave resistance correction. And to develop definition of speed component in heading. Update procedure if necessary.

22. To develop formal definition of steady state ship's condition in speed/power trials. Update procedure if necessary.

20. REFERENCES

Air Lubrication Technology, ABS Report, April 1, 2019, https://ww2.eagle.org/content/dam/eagle/advisories-and-debriefs/Air%20Lubrication%20Technology.pdf

Cai, B. et al., 2022, "Numerical Simulation of Ship Model Self-propulsion in Shallow Water", 32th International Ocean and Polar Engineering Conference (ISOPE), Shanghai, China.

D'Agostino, D., Serani, A., Stern, F., Diez, M., 2022, "Time-series forecasting for ships manoeuvring in waves via recurrent-type neural networks", J. Ocean Eng. Mar. Energy.

Demirel, Y. K. et al., 2017, " Effect of barnacle fouling on ship resistance and powering", Biofouling, Vol.33, No.10.

Fowles, Grant R., and George L. Cassiday, 1986, Analytical Mechanics: Fifth Edition. 5th edition. Fort Worth, TX: Saunders.

Gao, N., Hu, A., Hou, L. and Chang, X., 2023, "Real-time ship motion prediction based on adaptive wavelet transform and dynamic neural network", Ocean Eng, 280, 114466.

Gong, H. and Matala, R. 2022, "A study of full-scale measurement of channel widening by IB Polaris", Proceedings of the Thirty-second International Ocean and Polar Engineering Conference Shanghai, China.

Grin, R., 2022, "SPAWAVE, an Empirical Method to Predict Wave Added Resistance in all Wave Directions", Proceedings of 14th International Marine Design Conference (IMDC 2022).

Guo, X., Zhang, X., Tian, X., Lu, W. and Li, X., 2022, "Probabilistic prediction of the heave

motions of a semi-submersible by a deep learning model", Ocean Eng. 247, 110578.

Gupta, P., Rasheed, A. and Steen, S., 2022, "Ship performance monitoring using machine-learning", Ocean Eng, 254, 111094.

Gupta, P., Kim, Y.-R., Steen, S. and Rasheed, A., 2023, "Streamlined semi-automatic data processing framework for ship performance analysis", Int. J. Nav. Archit. Ocean Eng, 15, 100550.

Himeno, Y., 1983, "A study on Frictional Resistance of Painted Rough Surface", Journal of Kansai Society of Naval Architects, Vol. 191, pp.11-15. (in Japanese)

Hunsucker, K., Z. et al., 2019, "Using Hydrodynamic Testing to Assess the Performance of Fouling Control Coatings", Ocean Engineering, Vol.194.

IMO Maritime Safety Committee, 2019, "Interim Guidelines for MASS Trials," MSC.1/Circ. 1604, London.

IMO, 2021, " 2021 guidance on treatment of innovative energy efficiency technologies for calculation and verification of the attained EEDI and EEXI", MEPC.1/Circ.896, https://wwwcdn.imo.org/localresources/en/OurWork/Environment/Documents/Air%20pollution/MEPC.1-Circ.896.pdf

IMO, 2022, "Analysing the impact of marine biofouling on the energy efficiency of ships and the GHG abatement potential of biofouling management measures", GloFouling Partnerships Project Coodination Units. https://www.glofouing.imo.org/_files/ugd/34a7be_afd9d183df9a4526bd088007436c1079.pdf

Inukai, Y., 2019, "Full Scale Measurement of The Flow Field at The Stern by Using Multi Layered Doppler Sonar (MLDS)", Sixth International Symposium on Marine Propulsors smp'19, Rome, Italy.

ITTC, 2008, "Propulsion Committee Final Report", 25th ITTC Full Conference Proceedings, Fukuoka, Japan, 2014.

ITTC, 2011, "Specialist Committee on Surface Treatment Final Report", 26th ITTC Full Conference Proceedings, Rid de Janeiro, Brazil.

ITTC, 2014, "Resistance Committee Final Report", 27th ITTC Full Conference Proceedings, Copenhagen, Denmark.

ITTC, 2017, "Resistance Committee Final Report", 28th ITTC Full Conference Proceedings, Wuxi, China.

ITTC, 2021a, "Resistance and Propulsion Committee Final Report", 29th ITTC Full Conference Proceedings, Virtual.

ITTC, 2021b, " Specialist Committee on Ships in Operation at Sea Final Report", 29th ITTC Full Conference Proceedings, Virtual.

Jabary, W., Liu, C., Sprenger, F., Kleinsorge, L., Baumfalk, H., Kaster, M. and Mewes, S., 2023, "Development of machine learning approaches to enhance ship operational performance evaluation based on an integrated data model", Proceedings of the Thirty-Third International Ocean and Polar Engineering Conference, Ottawa, Canada.

Kawashima, H. et al., 2019, "Effect of Roughness Shape Parameter of Painted Surface on Frictional Resistance", Proc. PRADS 2019, Yokohama Japan.

Ki, H.-G., Park, S.-G. and Jang, I.-H., 2015, "Full scale measurement of 14k TEU containership", 7th Inter-national Conference on hydroelasticity in marine technology, Split, Croatia.

Kijima, K., Katsuno, T., Nakiri, Y. and Furukawa, Y., 1990, "On the manoeuvring performance of a ship with parameter of loading condition", Journal of the Society of Naval Architects of Japan, Vol. 168, pages 141-148.

Kim, Y.-R., Esmailian, E. and Steen, S., 2022, "A meta-model for added resistance in waves", Ocean Eng. 266, 112749.

Kuroda, M. and Sugimoto, Y., 2022, "Development of the Evaluation Method for Life Cycle Ship Performance", Journal of JASNAOE, Vol.34, pp 19-27.

Kuroda, M., Yokota, S., Tsujimoto M. and Fukasawa, R., 2022, "Effect of Hydrodynamic Forces due to Drift Motion on Ship performance in Actual Seas at Low Speed", Proceedings of PRADS2022, pp 257-266.

Kuroda, M. and Tsujimoto, M., 2023, "The Wave Correction Method for Speed Trial Analysis: Simple-NMRI method", Report of National Maritime Research Institute, Vol.23-1, pp 73-87.

Lee, J., Kim, Y-.H., 2023, "Development of enhanced empirical-asymptotic approach for added resistance of ships in waves", Appl. Ocean Res., 280, 114762.

Leonard, S., Lübke, L., 2024, "An Investigation into the Effect on Ship Manoeuvring of a Pre-Swirl Duct", Eighth International Symposium on Marine Propulsors smp'24, Berlin, Germany.

Li, F., Goerlandt, F., Kujala, P., Lehtiranta, J. and Lensu, M, 2018, "Evaluation of selected state-of-the-art methods for ship transit simulation in various ice conditions based on full-scale measurement", Cold Regions Science and Technology, 151 94-108.

Li, F.,Lu, L., Suominen, M. and Kujala, P, 2021, "Short-term statistics of ice loads on ship bow frames in floe ice fields: Full-scale measurements in the Antarctic ocean", Marine Structures, 80, 103049.

Martić, I., Degiuli, N., Majetić, D. and Farkas, A., 2021, "Artificial Neural Network Model for the Evaluation of Added Resistance of Container Ships in Head Waves", J. Mar. Sci. Eng., 9, 826.

Mieno, H. et al., 2021, "Experimantal investigation of added frictional resistance by paint rough surface using a rotating cylinder", Journal of Marine Science and technology, Vo.26 No.1.

Mittendorf, M., Nielsen, U.D. and Bingham, H.B., 2022, "Data-driven prediction of added-wave resistance on ships in oblique waves—A comparison between tree-based ensemble methods and artificial neural networks", Appl. Ocean Res., 118.

Mittendorf, M., Nielsen, U.D. and Bingham, H.B., Dietz, J., 2023, "Assessment of added resistance estimates based on monitoring data from a fleet of container vessels", Ocean Eng., 272, 113892.

Mosaad, M., A., and Hassan, H., M., 2024, "Volumetric Image Processing for Predicting Propeller Roughness Penalties", Eighth International Symposium on Marine Propulsors smp'24, Hurghada, Egypt.

Nakamura, S., Hosoda, R. and Naito, S., 1975, "Propulsive Performance of a Container Ship in Waves (3rd Report)", Journal of the Kansai Society of Naval Architects, Japan, Vol.158, pp.37-46.

Nielsen, U., D., Johannesen, J., R., Bingham, H., B., Blanke, M. and Joncquez, S., 2019, "Indirect Measurements of Added-wave Resistance On an In-service Container Ship", PRADS 2019.

Nikolaidou, L., Laskari, A., van Terwisga, T. and Poelma, C., 2021 "On the characteristics

of air layer regimes", 11th International Symposium on Cavitation, Daejon, Korea.

Nippon Kaiji Kyokai (NK), 2010, "Guideline for the Technical Appraisal of Ship Performance in Actual Seas", Nippon Kaiji Kyokai (NK), Classification Notes, pp 1-27.

Oh., S.-M., Lee. D.-H., Kim. H.-J. and Ahn, A.-K., 2021. "Full-Scale Measurements of the Propeller Thrust during Speed Trials Using Electrical and Optical Sensors", Applied Sciences, 11(17), 8197.

Oh, S.-M., 2022. " Study on the Speed-Power Performance Assessment by Full Scale Measurements of the Propeller Thrust".

Ponkratov, D, 2023, "JoRes Joint Resraech Project – the largest global community developing benchmark for ship scale CFD", 25th Numerical Towing Tank Symposium, Ericeira, Portugal.

Seo, D.W. and Oh, J., 2021, "Uncertainty Analysis of Speed-Power Performance Based on Measured Raw Data in Sea Trials," International Journal of Naval Architecture and Ocean Engineering, Vol. 13, pp 396-404.

Rødseth, Ø.J., 2022, "Autonomous Ships Test Areas," https://www.autonomous-ship.org/testarea.html.

Rødseth, Ø.J., 2022, "International Network for Autonomous Ships," https://www.autonomous-ship.org/index.html.

Sakurada, A., Kuroda, M. and Tsujimoto, M., 2023, "Evaluation of Drift Force in Large Angles for PCC and Coastal Cargo Ship", Proceedings of 10th PAAMES and AMEC 2023.

Sasaki, N., Tsujimoto, M., Kuroda, M., Sogihara, N., Ichinose, Y., Usui, N., Ueno, M., Fujiwara, T., Hoshino, K., Kawanami, Y., Ohmatsu, S. and Shibata, K., 2009, "Development of Ship Performance Index (10 mode at Sea)", Report of NMRI, Vol.9-4, pp.219-264.

Schirmann, M.L., Collette, M.D. and Gose, J.W., 2022, "Data-driven models for vessel motion prediction and the benefits of physics-based information", Appl. Ocean Res., 120, 102916.

Schlichting, H. 1979. Boundary Layer Theory (7th ed.). McGraw-Hill.

Schultz, M., P,, 2007, "Effects of coating roughness and biofouling on ship resistance and powering", Biofouling, Vol. 23, pp.331-341.

Silva, K.M. and Maki, K.J., 2022, "Data-Driven system identification of 6-DoF ship motion in waves with neural networks", Appl. Ocean Res., 125, 103222.

Simanto, R. I. A., Hong, J. W., Ahn, B. K., and Jeong, S. W., 2023. "Experimental investigation on tip vortex cavity deformation and flow dynamics using high-speed imaging and laser Doppler velocimetry measurements". Physics of Fluids, 35(10).

Sogihara, N., Tsujimoto, M., Ichinose, Y., Minami, Y., Sasaki, N. and Takagi, K., 2010, "Performance Prediction of a Blunt Ship in Oblique Waves", Journal of Japan Society of Naval Architects and Ocean Engineers, Vol. 12, pages 9-15.

Sogihara, N., Yonezawa, T., Ishiguro T., Sugimoto, Y., Masuyama S., Mieno H., Shimada, M. and Matsubara, Y., 2019, "Introduction of OCTARVIA Project: Project for Ship Performance in Actual Seas", Proceedings of HullPIC2019, pp 12-21.

Sogihara, N., Kuroda, M. and Tsujimoto, M., 2022, "Lifecycle Assessment of Fuel Oil Consumption of a Ship in Service", Proceedings of HullPIC2022, pp 36-49.

Song, S. et al., 2019, " An Investigation into the Effects of Biofouling on Full-Scale Propeller

Performance using CFD ", 38th Int. Conf. Ocean, Offshore and Arctic Eng. (OMAE), Glasgow, UK.

Stigter, R., Birvalski, M., Schouten, R., van Rijsbergen, M.,X., van Terwisga, T., Westerweel, J., 2024, "An early assessment of the effect of water quality and sea-state on propeller cavitation inception of a full-scale vessel", 12th International Symposium on Cavitation.

Tadros, M., Ventura, M., Soares, C., G., 2023, "Review of current regulations, available technologies, and future trends in the green shipping industry", Ocean Engineering, Volume 280, 114670, ISSN 0029-8018

Tamura, K., Okada, Y., Okazaki, A., 2024, "Measurement of pressure fluctuation induced by propeller on actual ship using FBG pressure sensor", 12th International Symposium on Cavitation.

Taskar, B. and Andersen, P., 2021, "Comparison of added resistance methods using digital twin and full-scale data", Ocean Eng., 229, 108710.

Tsujimoto, M., 2012, "Validation for Estimation Methods of Added Resistance in Waves and Wind Resistance, Conference proceedings", The Japan Society of Naval Architects and Ocean Engineers, Vol.15, pp.175-178.

Tsujimoto, M., Matsuzawa, T., Sogihara, N., Hirayama, K., Sugimoto, Y., Hasegawa, K. and Yokokawa, K., 2018, "Advanced Weather Routing System for Ships in Actual Seas -Development and Validation by a Ship-", Proc. of 16th IAIN World Congress.

Tsujimoto, M. and Orihara H., 2018, "Performance prediction of full-scale ship and analysis by means of on-board monitoring (Part 1 ship performance prediction in actual seas)", Journal of Marine Science and Technology, Vol. 24, pp.16-33.

Tsujimoto, M., Yasukawa, H., Yamamoto, K. and Lee, Tae-il, 2023, "Validation of Added Resistance in Waves by Tank Tests and Sea Trial Data", Ship Technology Research (Shiffstechnik), Vol. 70, No. 1, pp.14-25.

Yasukawa, H. and Tsujimoto, M., 2020, "Impact of bow shape on added resistance of a full hull ship in head waves", Ship Technology Research (Shiffstechnik), Vol. 67, No. 3, pp.136-147.

Yokota, S., Kuroda, M., Fukasawa, R., Ohba, H. and Tsujimoto, M., 2020, "Detailed Study on the Behaviour of Ships in Very Short Waves", Proceedings of OMAE 2020.

Yokota, S., Kuroda, M., Fukasawa, R. and Tsujimoto, M., 2021, "Measurement and Estimation of Added Resistance in Waves at Low-speed", Proceedings of PAAMES/ AMEC 2021.

Yokota, S., Tsujimoto, M., Sakurada, A. and Kuroda, M., 2021, "A Practical Correction Method for Added Resistance in Oblique Waves Considering the Influence of Roll Motion", Journal of JASNAOE Vol. 34.

You, Y., Kim, J. and Seo, M.-G., 2018, "Prediction of an actual RPM and engine power of an LNGC based on full-scale measurement data", Ocean Engineering, 147 496-516.

Zhang, D., Zhou, X., Wang, Z.-H., Peng, Y. and Xie, S.-R., 2023, "A data driven method for multi-step prediction of ship roll motion in high sea states", Ocean Eng., 276, 114230.